Jenny Terzic
Edin Terzic
Romesh Nagarajah
Muhammad Alamgir

Ultrasonic Fluid Quantity Measurement in Dynamic Vehicular Applications

A Support Vector Machine Approach

Springer

Ultrasonic Fluid Quantity Measurement in Dynamic Vehicular Applications

Jenny Terzic · Edin Terzic
Romesh Nagarajah · Muhammad Alamgir

Ultrasonic Fluid Quantity Measurement in Dynamic Vehicular Applications

A Support Vector Machine Approach

Springer

Jenny Terzic
Edin Terzic
Sandringham, VIC
Australia

Romesh Nagarajah
Blackburn South, VIC
Australia

Muhammad Alamgir
Wyndham Vale, VIC
Australia

ISBN 978-3-319-00632-1 ISBN 978-3-319-00633-8 (eBook)
DOI 10.1007/978-3-319-00633-8
Springer Cham Heidelberg New York Dordrecht London

Library of Congress Control Number: 2013939054

© Springer International Publishing Switzerland 2013
This work is subject to copyright. All rights are reserved by the Publisher, whether the whole or part of the material is concerned, specifically the rights of translation, reprinting, reuse of illustrations, recitation, broadcasting, reproduction on microfilms or in any other physical way, and transmission or information storage and retrieval, electronic adaptation, computer software, or by similar or dissimilar methodology now known or hereafter developed. Exempted from this legal reservation are brief excerpts in connection with reviews or scholarly analysis or material supplied specifically for the purpose of being entered and executed on a computer system, for exclusive use by the purchaser of the work. Duplication of this publication or parts thereof is permitted only under the provisions of the Copyright Law of the Publisher's location, in its current version, and permission for use must always be obtained from Springer. Permissions for use may be obtained through RightsLink at the Copyright Clearance Center. Violations are liable to prosecution under the respective Copyright Law.
The use of general descriptive names, registered names, trademarks, service marks, etc. in this publication does not imply, even in the absence of a specific statement, that such names are exempt from the relevant protective laws and regulations and therefore free for general use.
While the advice and information in this book are believed to be true and accurate at the date of publication, neither the authors nor the editors nor the publisher can accept any legal responsibility for any errors or omissions that may be made. The publisher makes no warranty, express or implied, with respect to the material contained herein.

Printed on acid-free paper

Springer is part of Springer Science+Business Media (www.springer.com)

Preface

This book describes the research and development of a fluid level measurement system for dynamic environments. The measurement system is based on a single ultrasonic sensor. A Support Vector Machines (SVM)-based signal characterization and processing system has been developed to compensate for the effects of slosh and temperature variation in fluid level measurement systems used in dynamic environments including automotive applications. It has been demonstrated that a simple ν-SVM model with Radial Basis Function (RBF) Kernel with the inclusion of a Moving Median filter could be used to achieve the high levels of accuracy required for fluid level measurement in dynamic environments.

Contents

Acronyms

DAQ	Data Acquisition
dB	Decibel (logarithmic unit)
DCT	Discrete Cosine Transform
DFT	Discrete Fourier Transform
DOE	Design of Experiments
DSP	Digital Signal Processing
DST	Discrete Sine Transform
DWT	Discrete Wavelet Transform
FFT	Fast Fourier Transform
FS	Fourier Series
FT	Fourier Transform
FTDNN	Focused Time-Delay Neural Network
FWT	Fast Wavelet Transform
IDCT	Inverse Discrete Cosine Transform
IFFT	Inverse Fast Fourier Transform
OEL	Occupational Exposure Limit
PCMCIA	Personal Computer Memory Card International Association
PLC	Programmable Logic Controller
RBF	Radial Basis Function
SVM	Support Vector Machine
US	Ultrasonic Sensor
WT	Wavelet Transform

Variables

$\hat{p}$	Amplitude of fluctuating sound pressure
ρ	Density of the Medium kg/m^3
$\acute{\omega}$	Frame size of the signal during windowing [s (Second)]
α	Absorption Factor
θ_C	Critical angle [° (Degree)]
a	Vehicle Exerted Acceleration m/s^2
C	Capacitance [F (Farad)]
d	d-Dimensions
D	Attenuation Factor dB/m
f	Linear Frequency; Slosh Frequency [Hz (Hertz)]
f_0	Fundamental Frequency [Hz (Hertz)]
f_n	Natural Frequency [Hz (Hertz)]
f_S	Sampling Frequency [Hz (Hertz)]
i	Current [A (Ampere)]
K	Bulk Modulus [Pa (Pascal)]
L	Inductance [H (Henry)]
L_0	Height of the fuel tank [m (Meter)]
L_x	Instantaneous Fluid Level [m (Meter)]
R	Electrical Resistance [Ω (Ohm)]
T	Temperature [°C (°Celsius)]
t	Time [s (Second)]
T_S	Sampling Period [s (Second)]
V	Fluid Volume [L (Liters)]
v	Potential Voltage [V (Volt)]
v,c	Speed of the Sound Wave [m/s]
Z	Impedance [Ω (Ohm)]
δ	Error between actual and measured fluid quantity [L (Liters)]
λ	Wavelength of Slosh [m (Meter)]
τ	Time of Flight (echo return time) [s (Second)]
ω	Angular Frequency Rad/s
ν	The Nu (ν) parameter of ν-SVM

γ	Gamma parameter for different kernel functions
ξ	SVM Tolerance parameter
r	Coef0 parameter for different kernel functions
d	Degree parameter for different kernel functions

Chapter 1
Introduction

1.1 Overview

This book documents a research program undertaken to design and develop an ultrasonic sensor based fluid level measurement system for dynamic environments, in particular automotive applications. This research is a subset of an overall research program titled "Smart Sensor for Fluid Level Measurement in Hazardous and Dynamic Environments." The research work presented herein is based on the use of an ultrasonic sensors coupled with a support vector machines-based signal processing system for accurately determining the fluid level in dynamic environments. The objective of this research project is to design and develop a fluid level measurement system based on a nonmechanical and contactless sensor to accurately determine the level of fluid in a dynamic environment, especially in vehicular fuel tanks. The motivation for this research is the automotive industry's requirement for a robust and accurate fuel level measurement system that would function reliably in the presence of slosh and temperature variations.

This chapter provides a background to the research project and an overview of the problems experienced in fluid level measurement. The objectives of the project and the outline of this book are also contained in this chapter.

1.2 Background

Modern automotive vehicles are equipped with digital gauges as well as with additional functionalities that inform drivers about their vehicle's fuel consumption and the remaining distance that the vehicle can travel without refueling. However, the high precision digital displays and additional utilities have to rely on the accuracy of the fuel level measurement sensor itself. The reliability and accuracy of the fluid level measurement system in the context of a dynamic environment, which primarily depends on the level sensor, is increasingly becoming a concern for automotive industries as well as everyday vehicle users.

J. Terzic et al., *Ultrasonic Fluid Quantity Measurement in Dynamic Vehicular Applications*, DOI: 10.1007/978-3-319-00633-8_1,
© Springer International Publishing Switzerland 2013

A fluid level sensor is a device that measures the level of fluid from a reference point and produces an electrical signal at the output. The existing fluid level sensor technology is mainly based on resistive type potentiometers. Such sensors determine fuel levels by considering the resistance value of the potentiometer, such that a float interconnected with the potentiometer changes the position of the terminals forming contacts with the resistive track [1]. As the fluid level rises from empty to full, the contacts on the resistive track slide from one end to the other, forming a complete swing. The resistive type level sensors are mechanical devices that are prone to wear and corrosion [2]; therefore, they have a limited functional life. The rubbing of the contacts across the resistive track creates wear, which leads to a reduction in the accuracy of the level sensing mechanism over a short period of time. Apart from the mechanical issues of the sensor, there are electrical problems with resistive potentiometers. The changes in the contact resistance generate noise and spikes at the output voltage, which can become significant with the influence of dust, humidity, and oxidation [1].

These conventional level sensor systems used in automotive applications also occupy a significant amount of space because of the mechanical design that is associated with them. The importance of level sensor reliability in hostile environments over long periods of time has lead to the investigation of various forms of motionless level sensors. The ultrasonic sensor is one such example of a compact as well as contactless displacement sensor that is investigated in this research for accurate fluid level measurements in automotive fuel tanks under dynamic conditions. Ultrasonic sensors have been used in a variety of different applications that range from process monitoring [3, 4], control systems, sonography [5], and distance measurement [6]. According to Dunn [7], ultrasonic devices can be used in containers with pressures up to 2 mega Pascal (MPa), temperatures up to 100 °C, and depths up to 30 m, with an accuracy of approximately 2 % [6]. With the advancements in ultrasonic sensor technology, specifically the improvements in electronics and new piezoelectric materials, the applications of ultrasonic sensors requiring more accurate signal analysis methods have expanded significantly [4].

An ultrasonic level sensor determines the fluid level by transmitting high frequency sound waves as echoes or pulses and then measures the return time of the reflected echoes. If the speed of sound in the medium is known, then the fluid level can be calculated using:

$$\text{level} = \text{level}_{\text{ref}} - \frac{1}{2} v \cdot \tau \tag{1.1}$$

where $\text{level}_{\text{ref}}$ is the height of the tank, v is the speed of the sound, and τ is the time-of-flight of the ultrasonic echo (Fig. 1.1).

However, in real-life situations, the speed of sound is influenced by the temperature of the medium through which the sound waves travel [8]. Therefore, because of the changes in the ambient temperature, the usage of ultrasound in fluid

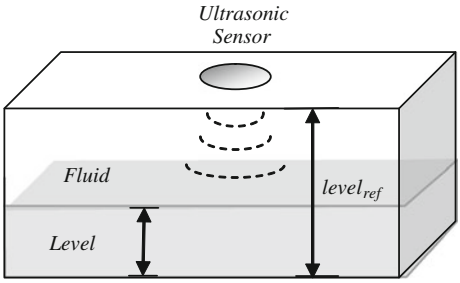

Fig. 1.1 Fluid level measurement using ultrasonic transducer

level measurement applications will lead to incorrect level readings. The speed of sound in terms of temperature can be approximated as:

$$v(T) = 331.3 + kT \text{ m/s} \tag{1.2}$$

where, T is the ambient temperature in degree Celsius, k is the rate at which the speed changes with respect to the temperature, which is approximately 0.607 m/s at every change of 1 °C in temperature [9].

Ultrasonic sensors are normally combined with a temperature sensor to compensate for the effects of temperature variations [10–13]. Apart from the accuracy of the level sensor itself, the fluid level measurement system in dynamic environments, for instance in an automotive fuel tank, is influenced by the sloshing effects caused by acceleration. In automotive fuel tanks, vehicle acceleration induces slosh waves having natural frequencies whose wave patterns are dependent on the magnitude of the acceleration, geometry of the tank, and the amount of fluid contained in the tank [14].

To compensate for the effects of sloshing in fluid level measurement systems, various mechanical dampening methods consisting of baffles, electrical dampening techniques, and statistical averaging methods have been used in the past [15, 16]. However, all these methods follow approaches that lead to higher production cost. The accuracy of these approaches under sloshing conditions is also very limited. The electrical dampening techniques and the statistical averaging methods primarily perform averaging on the raw sensor signals over some period of time. Averaging over a variable time frame has also been used in the past [17–19] to improve the level sensor accuracy under sloshing conditions by determining the running state of the vehicle using the vehicle speed data from a speed sensor. For example, fluid measurement systems described by Kobayashi et al. [18] employ a vehicle speed sensor to determine the running state of the vehicle. When the vehicle is operating at low speed (i.e., near static condition), the averaging period is reduced to small values typically in the range from 5 to 25 s, and when the vehicle is operating at a higher speed, the averaging period is prolonged up to 90 s [18]. Despite the dependence of the measurement system on the speed sensor, after analyzing the raw sensor data from a resistive type fuel level sensor in a moving vehicle, it can be observed that the averaging method still produces significant errors after averaging the raw sensor signal over a longer period of time.

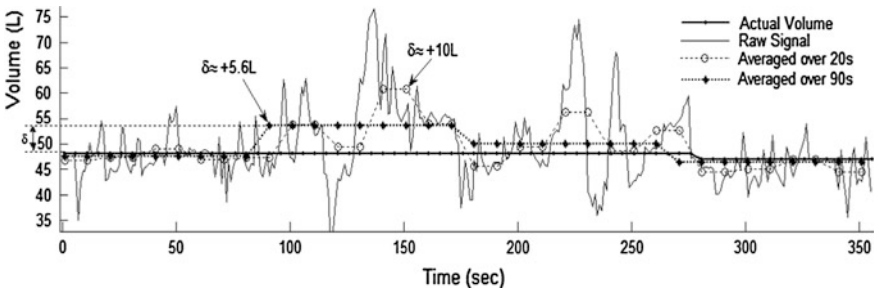

Fig. 1.2 Fuel level signal observed by the level sensor and the calculated average signal in a sample drive trial

Figure 1.2 illustrates the raw volume signal obtained from a driven vehicle, and two averaged signals calculated after averaging the raw signal over 20 s, which is the typical averaging time used in an automotive instrument cluster; and the second is an averaged signal over 90 s, which is a reasonably long period of time.

Therefore, even after performing averaging methods to reduce the effects of sloshing in level readings, the level reading error under dynamic conditions is still significant. Hence, to provide a solution to this problem, the research conducted here takes a different approach that is based on Support Vector Machines (SVM), which characterizes the slosh patterns at different tank volumes and then determines the actual fluid volume based on the prediction from the SVM. Although there are other methods, apart from SVM, such as Artificial Neural Network (ANN), K-means, and Principle Component Analysis (PCA) that could also be used to develop a system for slosh pattern characterization and recognition, after conducting the literature review (Chap. 2), it was observed that the SVM has better advantages due to its flexibility and signal processing speed; hence, it was chosen as the appropriate method for signal classification.

Support Vector Machines (SVM) is a newly developed machine learning algorithm [20]. SVM is based on Statistical Learning Theory and has the ability to recognize patterns [21]. SVM represents novel learning techniques in the framework of structural risk minimization (SRM) and in the theory of Vapnik–Chervonenkis [22] (VC) bounds [23–25]. SVM has been successfully used in various applications for solving classification, regression, time series prediction, and function estimation problems [26]. Meyer et al. [27] conducted a benchmark test in which SVM and several other types of classification techniques were benchmarked. Their findings [27] revealed that the performance of the SVM classification and regression was in general better than other investigated classification and regression techniques [27]. SVM has quickly found its place in many applications of pattern recognition requiring an artificial intelligence approach such as handwritten character recognition [28], speech recognition [29], image classification [21, 30], face detection [31], signal processing [32], and commerce [33] etc.

SVM has also the potential to be used in combination with an ultrasonic sensor to predict the fluid level in a dynamic environment, especially considering the

variations in temperature and the vehicle movement creating slosh waves. The implementation of SVM is carried out using LIBSVM [34] software, which is a popular SVM classification and regression software available [35]. The approach to sensing developed in this research is also applicable to nonacoustic sensors such as capacitive and hall-effect sensors.

Additionally, prior to classifying the sensor signals with SVM, the signals from the sensor should be clean from unwanted noise. Hence, the systems approach described in this book performs signal smoothing on raw sensor signals to filter out unnecessary range of noise frequencies. Three commonly used signal smoothing filters have been investigated through experimentation. The investigated filters consist of Moving Mean, Moving Median, and Wavelet filters. These filters provide the following enhancements [36]:

- Remove impulse noise,
- Smooth the signal,
- They can be taken over a wider interval so that the filter removes transients longer than a time instant in duration, and
- Preserve sharp edges of the signal curve.

In this research, various configurations of ultrasonic sensors have been investigated to determine the most appropriate, yet cost effective setup of the ultrasonic type level measurement system. Various limitations of ultrasonic sensors when operating in dynamic environments have been identified to develop a robust system that will perform to an acceptable level of accuracy. The experimental program for this research has been designed and conducted using the Design of Experiments (DOE) methodology. The DOE consists of creating different scenarios of combinations of input factors to test the effects of those combinations on the outcome (response factor) [37]. DOE is the most appropriate way to measure 'main effects and interactions' of the factors that influence the accuracy of a fluid level measurement system [37]. To determine the most appropriate configuration of the support vector machines (SVM), experiments have been performed to compare the performance of various commonly used SVM kernel functions, namely, linear, polynomial, radial basis function (RBF), and Sigmoid type kernel functions. The SVM training technique uses the one-against-all technique that provides a better performance while considering the trade-off of classification error, speed, and memory usage [38]. Further experiments have been conducted to compare the performance of the three investigated signal smoothing filters, namely, moving mean, moving median, and wavelet filter. Finally, based on the experimental results, a robust fluid level measurement system with high accuracy is developed and analyzed using an extensive field trial program. To investigate the performance of the proposed system, several field trials are carried out by actually driving a vehicle on suburban roads. This book also includes details of comparisons of the developed fuel level measurement system with that used currently. The results indicate that the proposed system is able to determine fluid levels in dynamic environments with high accuracy and is superior in performance to existing systems.

1.3 Aims and Objectives

The purpose of this research is to investigate the use of artificial intelligence techniques in combination with acoustic type ultrasonic sensor technology to achieve accurate fluid level measurement in dynamic environments. The research involves the design, development, and validation of a fluid level measurement methodology and system that is applicable in the context of potentially hazardous fluids and dynamic environments.

The research aims to develop a robust fluid level sensor that maintains its performance and preserves its accuracy over a long period of time. The sensor system is required to accurately determine the fluid level under dynamic operating conditions especially, temperature variation, and slosh. To validate the artificial intelligence based fluid level measurement system under dynamic environments; several field trials are carried out experimentally on a running vehicle, where the goal is to accurately determine the fuel level in the vehicle fuel tank under dynamic and sloshing conditions. It is aimed that the harshness of ambient environments would not adversely affect the accuracy of the final sensor system.

In summary, the research addresses the following aims:

- To obtain an understanding of the possible weaknesses and drawbacks of using an ultrasonic sensor as a fluid level measurement sensor,
- To understand the effects of liquid sloshing, and temperature variations on the sensor response,
- To understand the effectiveness of using support vector machines as a signal processing technique to overcome the effects that sloshing and other environmental changes consisting of temperature variation might have on the level sensor readings, and
- To understand the enhancement of the accuracy of the measurement system by using different preprocessing filters on the sensor signal.

It is intended that the knowledge gained through this project will have the broadest possible application in intelligent sensor design.

1.4 Methodology and Approach

To achieve the aforementioned research objectives, an approach is undertaken that consists of the following steps:

- Examining the relationship between the ultrasonic sensor output and the influential factors such as temperature, slosh, and contamination that may cause false echoes to occur, by adopting the DOE methodology,
- Understanding the characteristics of slosh waves at different levels of the fluid in a storage tank,
- Understanding the patterns of the ultrasonic sensor output under dynamic conditions in both time and frequency domains,

- Determining the effectiveness of the support vector machines (SVM)-based signal processing technique in improving the accuracy of the ultrasonic sensor based measurement system,
- Determining the most suitable SVM configuration by developing and validating different types of SVM kernel functions using slosh and temperature data sets,
- Developing and training the selected SVM configuration with sample data obtained from field trials experiments and investigating the accuracy of the ultrasonic sensor based measuring system in a real-life application, and
- Investigating the influence of different signal filtration methods in improving the performance of the SVM based signal processing system under dynamic conditions.

1.5 Outline of the Book

The outline of the book provides an overview layout of the different topics covered in this research. The book is comprised of eight chapters that are briefly introduced below:

Chapter 1—*Introduction* provides an introduction to the background problem and the project. An overview of the research program, covering the objectives of this research, and the methodology, are detailed in this chapter.

Chapter 2—*Ultrasonic Sensing Technology* provides a review of ultrasonic sensor technology, details of ultrasonic type measurement sensors and their application in industrial environments, and describes limitations of ultrasonic sensors in the context of industrial applications.

Chapter 3—*Support Vector Machine-Based Intelligent Level Sensing* focuses on signal processing and classification aspects of Support Vector Machines in the level sensing application. A background to various signal classification approaches is also provided in this chapter. Furthermore, Chap. 3 particularly focuses on Support Vector Machines basics and its variants, kernel functions, and its use in industrial applications.

Chapter 4—*Methodology* introduces the innovative concept of having an ultrasonic sensor combined with Support Vector Machines based signal processing for accurate and reliable fluid level measurement in dynamic environments. The methodology underpinning the proposed system is detailed in this chapter.

Chapter 5—*Experimental Program* describes the experimental setup for the research work. The Design of Experiments approach and the equipment used for the experiments are described in Chap. 5. In brief, it covers all major experiments that were performed:

1. To analyze the sensor response under dynamic conditions;
2. To determine the performance of different SVM configurations on the ultrasonic sensor signals under dynamic conditions;
3. To understand the improvements provided by the three signal smoothing functions (moving mean, moving median, and wavelet filter).

Chapter 6—*Results* presents the experimental results for the three major sets of experiments performed using the proposed system. It details experimentation results of the three experiments in the presentation of main effects plots, interaction plot, observed sensors signals, frequency coefficients plot, SVM Validation, and validation error plot.

Chapter 7—*Discussion* provides detailed discussion of the experimental results. The influence of two main factors (temperature, and slosh) on the response of the ultrasonic sensor is discussed. The performance of different SVM configurations is also analyzed. The influence of signal filtration on the performance of the SVM based signal classifier is described and the results are compared with existing methods.

Chapter 8—*Conclusions and Future Work* provides the final conclusions of the research investigation. The summary of the findings of this research and details of possible future improvements to the proposed system presented here.

References

1. Pallas-Areny R, Webster JG (2001) Resistive sensors. Sensors and signal conditioning. Wiley. New York, pp 73–131
2. Fischer-Cripps AC (2002) Force, pressure and flow. Newnes interfacing companion. Newnes, Oxford, pp 54–70
3. Astashev VK, Babitsky VI (2007) Ultrasonic processes and machines: dynamics, control and applications. In: Babitsky VI, Wittenburg J (eds). Springer, Berlin
4. Hauptmann P, Lucklum R, Püttmer A, Henning B (1998) Ultrasonic sensors for process monitoring and chemical analysis: state-of-the-art and trends. Sens Actuator A: Phys 67(1–3):32–48
5. Jan J (2006) Medical image processing, reconstruction, and restoration: concepts and methods. Taylor & Francis, Boca Raton
6. Dunn WC (2005) Level measurement. Introduction to instrumentation, sensors and process control. Artech House, Boston, pp 115–126
7. Dunn WC (2005) Introduction to instrumentation, sensors and process control. Artech House, Boston
8. Kuttruff H (1991) Ultrasonics—fundamentals and applications. Elsevier Applied Science, London
9. Serway RA, Jewett JW (2004) Sound waves. Physics for scientists and engineers, 6th edn. Thomson-Brooks/Cole, Belmont, pp 512–542
10. Song Z-Y, Liu C-Y, Song X-L (2004) Application research of information fusion technology of multi-sensor in level measurement. In: International conference on machine learning and cybernetics, vol 6, pp 3511–3514
11. Song Z, Liu C, Song X, Zhao Y, Wang J (2007) A virtual level temperature compensation system based on information fusion technology. In: IEEE international conference on robotics and biomimetics, pp 1529–1533
12. Gazis DC, Kane WF, von Gutfeld RJ (inventors), International Business Machines Corporation, (assignee) (1996) Ultrasonic liquid level gauge for tanks subject to movement and vibration. Patent no. 5,793,705
13. Combs CM, Goodwin PH Jr, (inventors), Robertshaw Controls Company, (assignee) (1978) Adjustable ultrasonic level measurement device. Patent no. 4221004

14. Ibrahim RA (2005) Liquid sloshing dynamics: theory and applications. Cambridge University Press, Cambridge
15. Kim H-S, Lee Y-S (2008) Optimization design technique for reduction of sloshing by evolutionary methods. J Mech Sci Technol 22:25–33
16. aus der Wiesche S (2003) Computational slosh dynamics: theory and industrial application. Comput Mech 30(5–6):374–387
17. Kobayashi H, Obayashi H (inventors), Nissan Motor Company, Limited, (assignee) (1983) Fuel volume measuring system for automotive vehicle. Patent no. 4611287
18. Kobayashi H, Kita T (inventors), Nissan Motor Company, Limited (assignee) (1982) Fuel gauge for an automotive vehicle. Patent no. 4470296
19. Guertler T, Hartmann M, Land K, Weinschenk A (inventors); Daimler Benz AG (DE) (assignee) (1997) Process for determining a liquid quantity, particularly an engine oil quantity in a motor vehicle. Patent no. 5831154
20. Zhao S (2004) Remote sensing data fusion using support vector machine. In: IEEE international geoscience and remote sensing symposium proceedings, vol 4, pp 2575–2578
21. Reyna RA, Esteve D, Houzet D, Albenge M-F (2000) Implementation of the SVM neural network generalization function for image processing. In: IEEE International workshop on computer architectures for machine perception (CAMP'00)
22. Vapnik VN (1998) Statistical learning theory. Wiley, New York
23. Vapnik VN (1995) The nature of statistical learning theory. Springer, New York
24. Hu YH, Hwang J-N (2002) Handbook of neural network signal processing. CRC Press, Boca Raton
25. Kecman V (2001) Learning and soft computing: support vector machines, neural networks, and fuzzy logic models. MIT Press, Cambridge
26. Zhang J, Liu X, Liu J, Peng F, Tian J, Wang Y, Zhang W, Xie M (2001) SVM-based ultrasonic medicine image diagnosis. Med Image Acquis Process 4549:92–95
27. Meyer D, Leischa F, Hornikb K (2003) The support vector machine under test. Neurocomputing 55(1–2):169–186
28. Ahmad AR, Viard-Gaudin C, Khalid M, Poisson E (2004) Online handwriting recognition using support vector machine. In: IEEE Region 10 international conference (TENCON'04)
29. Ganapathiraju A, Hamaker J, Picone J (2004) Applications of support vector machines to speech recognition. IEEE Trans Signal Process 52(8):2348–2355
30. Rajpoot KM, Rajpoot NM (2004) Wavelets and support vector machines for texture classification. In: Proceedings of international multitopic conference (INMIC), pp 328–333
31. Huang J, Shao X, Wechsler H (1998) Face pose discrimination using support vector machines (SVM). In: International conference on pattern recognition, vol 1, pp 154–156
32. Boni A, Gasparini L, Pianegiani R, Petri D (2005) Low-power and low-cost implementation of SVMs for smart sensors. In: IEEE instrumentation and measurement technology conference proceedings, vol 1, pp 603–607
33. Wang J, Wu X, Zhang C (2005) Support vector machines based on K-means clustering for real-time business intelligence systems. Int J Bus Intell Data Min 1(1):54–64
34. Chang C-C, Lin C-J (2001) LIBSVM: a library for support vector machines. Software available at http://www.csie.ntu.edu.tw/~cjlin/libsvm
35. Ahmad AR, Khalid M, Yusof R, Viard-Gaudin C (2009) The comparative study of SVM tools for data classification. Journal [serial on the Internet]. http://metalab.uniten.edu.my/~abdrahim/p4.pdf
36. Allen RL, Mills DW (2004) Time-domain signal analysis. Signal analysis: time, frequency, scale, and structure. IEEE Press; Wiley-Interscience. Piscataway, p 322
37. Bass I, Lawton B (2009) Improve. Lean six sigma using SigmaXL and Minitab. McGraw-Hill, New York, pp 213–282
38. Yom-Tov E (2004) An introduction to pattern classification. In: Bousquet O, von Luxburg U, Rätsch G, School, Machine Learning Summer, (eds) Advanced lectures on machine learning: ML Summer Schools 2003, Canberra, Australia, 2–14 Feb 2003, Tübingen, Germany, Springer, Berlin, pp 1–20 (4–16 Aug 2003: revised lectures)

Chapter 2
Ultrasonic Sensing Technology

2.1 Overview

This chapter describes the basic properties of ultrasonic technologies and their associated use in various ranges of sensors in industrial applications. Physical properties as well as the limitations of the piezoelectric devices used in ultrasonic sensors are described here. Particularly, the usage of ultrasonic sensors in fluid level measurement systems is discussed. Various configurations of ultrasonic sensors used with hazardous fluids, particularly gasoline-based fuels, in the application of level measurement have also been described in this section. In summary, this chapter provides the detailed background to ultrasonic type sensors and their application in dynamic environments.

2.2 Principles of Ultrasonic Sensing

2.2.1 Overview

Fundamentals of ultrasonic transducers are discussed in this section. The nature of the ultrasound waves and their associated parameters such as ultrasound velocity and range are described.

2.2.2 Ultrasound Waves

Ultrasound waves are similar to sound waves, where both travel through a medium. Ultrasound waves consist of high-frequency sound waves that are inaudible to human beings. The frequency of the ultrasound waves is normally above 20 kHz. However, some creatures such as bats can hear as well as generate the high-frequency ultrasound waves [1, 2].

J. Terzic et al., *Ultrasonic Fluid Quantity Measurement in Dynamic Vehicular Applications*, DOI: 10.1007/978-3-319-00633-8_2,
© Springer International Publishing Switzerland 2013

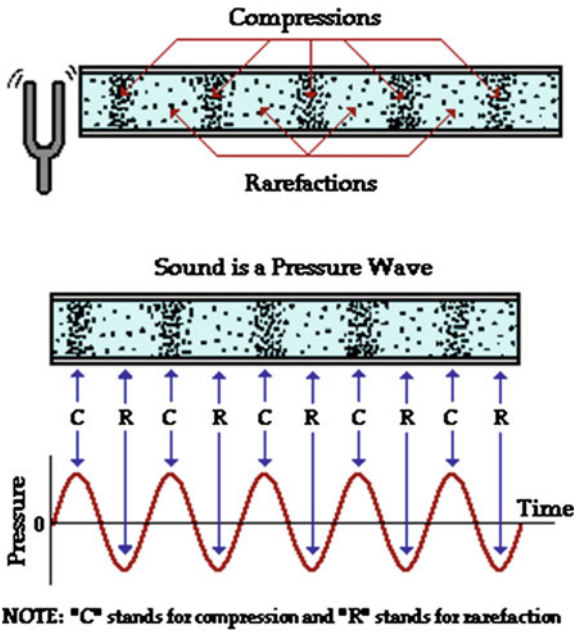

Fig. 2.1 Sound waves produced by a fork [3]

As the sound waves travel through the air, they produce vibration in the air particles which changes the density and pressure of the air particles along the direction of motion of the wave. If a sound wave is moving from left to right through air, particles of air will be displaced both rightward and leftward as the energy of the sound wave passes through it. If the source of the sound waves vibrates sinusoidally, the pressure variations are also sinusoidal. Figure 2.1 illustrates the propagation of the sound waves produced by a fork. Patterns of high and low pressure points will be created in the air by the vibration of the fork. These patterns of varying pressure points can be observed using a sound wave detector [3].

Ultrasound can be thought of as analogous to ultraviolet light in that it characterizes that region of acoustical phenomena which is not accessible to human perception [4]. Some creatures such as bats, dolphins, and whales are able to hear and generate ultrasonic waves. Figure 2.2 shows a graph of different hearing ranges in animals and humans.

2.2.3 Sound Velocity

The sound velocity is defined by the rate of change of particle displacement with respect to time. Sound or ultrasound waves can only be propagated in a material medium. Different characteristics of different materials will influence the velocity

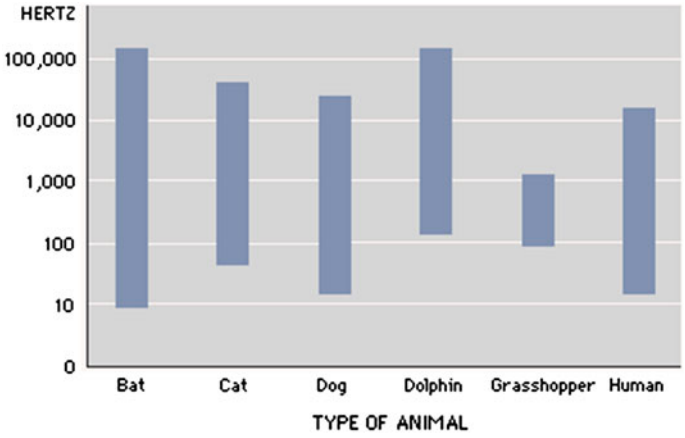

Fig. 2.2 Hearing range threshold in different living beings, *courtesy* Microsoft Encarta 2008

of the sound differently. The characteristics of the material medium have effects on the velocity and the attenuation of ultrasound waves. The speed of sound waves in a medium depends on the compressibility and density of the medium [5]. If the medium is a liquid or a gas and has a bulk modulus K and density ρ, the speed of sound waves in that medium or fluid is given by Cheeke and David [6]:

$$c_{\text{fluid}} = \sqrt{\frac{K}{\rho}} \tag{2.1}$$

The general expression of the speed of all mechanical waves in a given material is expressed as [5]:

$$v = \sqrt{\frac{\text{elastic\_properties}}{\text{inertial\_properties}}} \tag{2.2}$$

The speed of sound changes according to the surrounding temperature. The speed of sound in atmosphere reaches 331.45 m/s at 0 °C. The speed of sound in terms of temperature can be determined with the following equation:

$$c_{\text{air}}(t) = C_0 + kt \tag{2.3}$$

where, c_{air} is the speed (m/s) of the sound in air,

t is the air temperature in degree Celsius, and

k is the rate at which the speed changes with respect to the temperature, which is approximately 0.607 m/s at every change of 1 °C in temperature.

Table 2.1 lists some materials and their characteristics that relate to the speed of ultrasonic waves. The characteristic impedance factor (Ns/m^3) represents the resistance to propagation of ultrasonic sound in a given material.

Table 2.1 Sound velocity and characteristic impedance of gases and liquids [4]

Material	Temperature (°C)	Density (kg/m^3)	Sound velocity (m/s)	Characteristic impedance (Ns/m^3)
Gases				
Air	0	1.293	331.45	429
Argon	0	1.783	319	569
Helium	0	0.178	965	172
Oxygen	0	1.429	316	452
Nitrogen	0	1.251	334	418
Ammonia	0	0.771	415	320
Liquids				($106\ Ns/m^3$)
Water	20	998	1483	1.48
Diesel oil	20	800	1250	1.0
Mercury	20	13500	1451	19.6
Methyl alcohol	20	720	1120	0.89
Ethyl alcohol	20	790	1159	0.92
Ethyl ether	20	714	1006	0.72
Glycerine	20	1228	1895	2.33
Acetone	20	794	1189	0.94
Transformer oil	20	890	1425	1.27

2.2.4 Ultrasonic Wave Generation

The generation of ultrasonic waves is similar to the generation of an audible sound wave using a speaker. The diaphragm of the speaker is electronically driven to move back and forth, which produces low pressure and high pressure points in the air. For ultrasonic wave generation, the diaphragm needs to move back and forth at a much greater rate than for an audible sound wave.

The frequency and amplitude of sound waves can be measured by measuring the fluctuations and the pressure difference in air particles propagating sound waves through air. The diaphragm of the microphone, shown in Fig. 2.3, produces electrical signals which are a replica of the sound pressure experienced by the diaphragm. The vibration of the diaphragm and the pressure on it reflects the frequency and amplitude of the sound waves.

2.2.5 Piezoelectric Effect

Since ultrasonic waves are high-frequency waves, sensitivity of a device to detect high-frequency waves plays an important role in ultrasonic wave detection. The piezoelectric effect can be used to detect as well as generate ultrasonic waves.

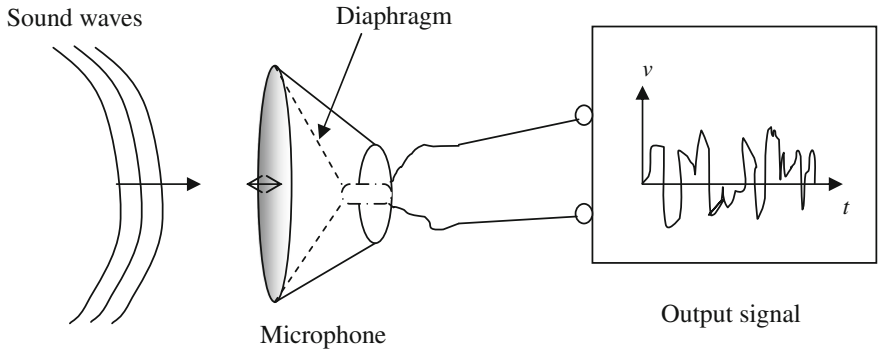

Fig. 2.3 Sound detection using microphone

These days, most practical ultrasound sources are based on the piezoelectric principle of transconduction [4]. Piezoelectric sources have the advantage of simple construction and operation, which makes them suitable for a variety of applications.

A piezoelectric ultrasound generator consists of a layer of piezoelectric material with thin metal electrodes on both its sides. If an alternating electrical voltage is applied to these electrodes, the thickness of the layer will vary according to the variations of the electrical field [4], thus fluctuations in the air or a medium will be produced. Alternatively, the piezoelectric effect can be reversed to detect ultrasonic waves and to transform waves into an electrical signal. Figure 2.4 illustrates the piezoelectric effect, where the induced voltage is increased as the applied pressure increases.

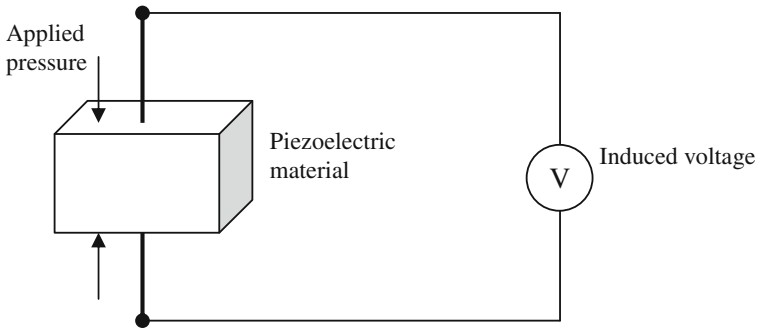

Fig. 2.4 Piezoelectric effects

2.2.6 Characteristics of Ultrasonic Waves

2.2.6.1 Overview

This section discusses some characteristics and physical factors that influence the propagation of ultrasonic waves. Phenomena such Reflection, Refraction, Diffraction, and Absorption of the ultrasonic wave during its propagation are described in the following subsections.

2.2.6.2 Reflection

When a wave is traveling through one material and impinges on a boundary between it and a second medium, part of the energy travels forward as one wave through the second medium while a part is reflected back into the first medium, usually with a phase change [7]. Specific acoustic impedance is the characteristic that determines the amount of reflection and it is the product of the density and velocity. The amplitude of the reflected wave is given as:

$$A_r = \frac{R_1 - R_2}{R_1 + R_2} \tag{2.4}$$

where, $R_1 = \rho_1 c_1$,
$R_2 = \rho_2 c_2$,
ρ is the density of each material,
c is the speed of the source, and
A_r is the ratio between reflected and incident amplitudes.

2.2.6.3 Refraction

A wave traveling from one material into another material can experience a change in its course. A wave at θ_1 in medium A can end up traveling at θ_2, as illustrated below (Fig. 2.5).

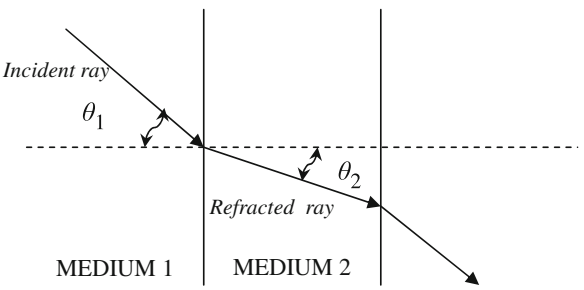

Fig. 2.5 Refraction of mechanical waves in different media

The ratio of the two angles is proportional to the ratio of the speed in both media, and it is given by:

$$\frac{\sin(\theta_1)}{\sin(\theta_2)} = \frac{c_1}{c_2} \tag{2.5}$$

The principles of refraction can cause a ray traveling at a critical angle to disappear as total refraction. The critical angle θ_c can be determined by the following equation. For liquids and solids, θ_c is about 15° [7].

$$\theta_c = \theta_1 = \sin^{-1}\frac{c_1}{c_2} \tag{2.6}$$

2.2.6.4 Diffraction

Ultrasonic waves do not always propagate in a rectilinear manner. For example, a wave passing near the edge of an object has a tendency to become bent toward and around it. This bending of the wave, as shown in Fig. 2.6, is called diffraction.

Ultrasonic signals that would normally be received at a certain point may be diverted by diffraction and received at some other position [7]. If the object is small compared to the wavelength there will be no noticeable shadow behind it at all since the sound is strongly deflected by the object [4].

2.2.6.5 Absorption

The existence of sound waves is always restricted to a material medium, the nature and the structure of which determines the particular parameters of their propagation. Ultrasonic waves may lose energy and get absorbed depending on the type of material and distance it traveled. The loss of sound energy is caused by the fact that any kind of matter consists of small but finite components such as atoms,

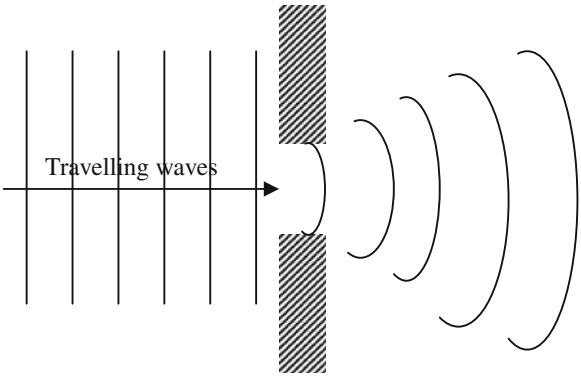

Fig. 2.6 Diffraction phenomenon in mechanical waves

molecules, and ions, which interact with each other [4]. Sound absorption in a plane harmonic sound wave is characterized by an exponential decrease of amplitude with traveling distance as [4]:

$$\hat{p}(x) = \hat{p}_0 e^{-\alpha x} \tag{2.7}$$

where $\hat{p}$ is the amplitude of the fluctuating sound pressure at distance x, $\hat{p}_0$ is the initial pressure, and the quantity α is the absorption constant. Its magnitude depends on the kind of wave medium and on the sound frequency and is the reciprocal of the distance along which the amplitude falls by $\frac{1}{e}$ of its initial value [4]. The attenuation constant D may be derived from the absorption constant α.

$$D = 20\alpha \cdot \log_{10} e \approx 8.69\alpha \text{ dB/m} \tag{2.8}$$

2.2.7 Ultrasonic Measurement Principles

The ultrasonic wave detection and measurement principle is primarily the reverse operation of ultrasonic wave generation. During ultrasonic wave generation, the transducer element (i.e., piezoelectric) is excited by applying an electrical signal across it. But during ultrasonic wave detection, an electrical voltage signal across the piezoelectric element is monitored. As soon as an ultrasonic wave strikes the transducer, the piezoelectric element vibrates accordingly; thus it generates a voltage signal across its terminals.

Figure 2.7 shows a simple configuration of an ultrasonic sensor in a level sensing application. An ultrasonic wave reflector (obstacle) floats on the liquid surface. A transducer is mounted at the bottom of the tank and transmits a signal. It determines the fluid level by detecting and measuring the time-of-flight of the reflected ultrasonic wave.

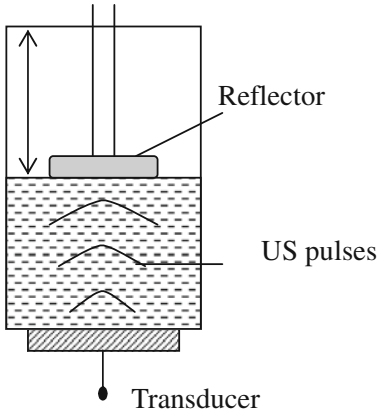

Fig. 2.7 A simple configuration of an ultrasonic level sensor system

A technique known as *Interferometry* can be used with an ultrasonic sensor to determine fluid level. Interferometry consists of diagnosing the properties of two or more waves by studying the pattern of interference created by their superposition. In interferometry, a wave of some specific shape is transmitted and then incoming waves that have the same pattern (i.e., frequencies) are detected. The difference between the two waves (transmitted wave and received wave) is identified. In ultrasonic level sensing systems, the same principle of interferometry can be applied. Figure 2.8a shows a simple circuit that can be used to generate a pulse of an ultrasonic wave signal (shown in Fig. 2.8b). After transmitting a pulse signal, the circuit listens for any incoming reflected echo pulse that has similar features (i.e., frequency) as the transmitted echo. The time difference or time-of-flight is calculated based on the times of transmission and reception of the pulse wave.

Paulsen [8] has used the same method for detecting fluid levels as described above, in which an ultrasonic transducer driver generates a voltage proportional to the resonant frequency of the ultrasonic transducer. A reference voltage is then generated and the reference voltage and the first voltage are monitored and compared, and a surface detect signal is generated when the first voltage drops below the reference voltage [8].

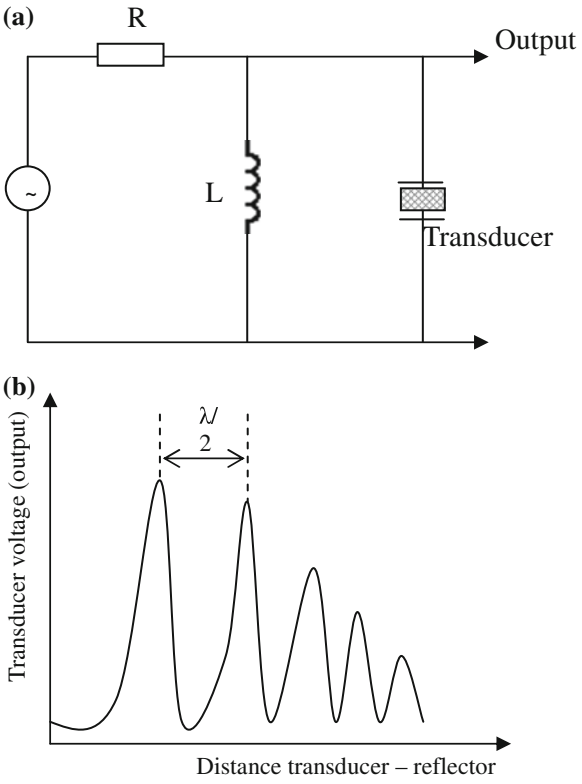

Fig. 2.8 Example of an ultrasound interferometer

Wang [9] also developed a system based on the principle described above. But instead of a simple pulse, a switch-mode ultrasonic Radio Frequency (RF) burst emission circuit was used, which is based on the optimum transient response formed between a series resonance network of a piezoelectric crystal oscillator of an ultrasonic transducer and an active switch device (transistor). Wang [9] has claimed that the circuit produces a highly efficient emission of an ultrasonic RF burst. Figure 2.9 illustrates a basic setup of the ultrasonic RF burst emission generator designed by Wang [9]. The circuit consists of a transistor T, two diodes D1, D2, and a load network of piezoelectric oscillator TD. The function of diodes D1 and D2 is to form an isolating stage between the switch transistor and receiver amplifier.

Suzuki [10] described a method of generating and receiving ultrasonic waves using a single ultrasonic transducer. Suzuki [10] has used a negative immittance converter in the circuitry in order to cancel components which impede the damping characteristics of the ultrasonic transducer. This provides the benefits of receiving an ultrasonic wave having good receiving response and sensitivity without using any mechanical damping method [10].

2.3 Level Measurement Using Ultrasonic Sensors

Ultrasonic transducers transmit ultrasonic waves and then receive those ultrasonic waves reflected from an object. The time delay between transmission and reception of the ultrasonic waves is used to detect the position of the object. This technique can be used to determine the height or vertical distance of an object from the ultrasonic sensor. Thus ultrasonic transducers can be used to determine the height or level of fluid in a container (Fig. 2.10).

Durkee [11] described an aircraft fuel gauging and battle damage detection system that comprises an ultrasonic transducer incorporable in the fuel tank of the aircraft. An electrical circuit excites the ultrasonic transducer to transmit an acoustic pulse toward the surface of fuel in the tank. Then the ultrasonic transducer receives the ultrasonic echo pulses reflected from the fuel surface, which is then

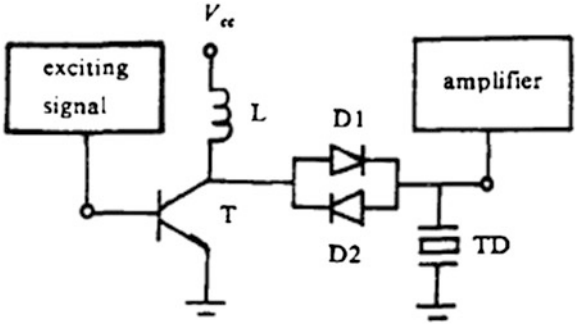

Fig. 2.9 A typical switch-mode ultrasonic RF burst emission circuit [9]

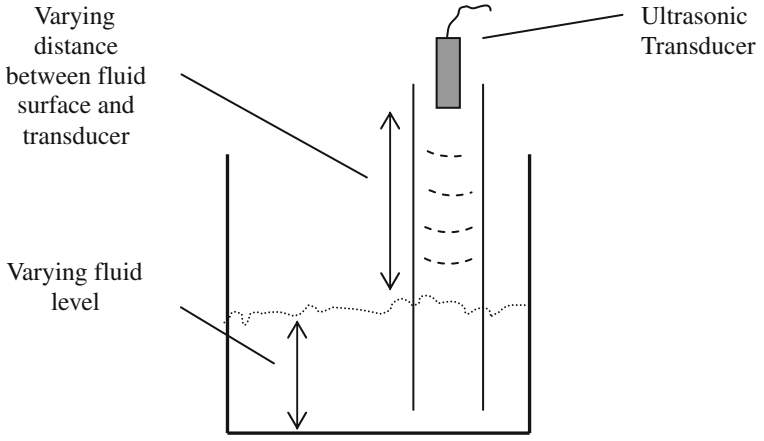

Fig. 2.10 Fluid level measurement using ultrasonic transducer

converted from ultrasonic echo pulses to electrical echo pulses. The system uses another electrical circuit to receive and process the electrical echo pulses from the ultrasonic transducer. The second circuit performs fuel quantity measurements using the electrical echo pulses and also performs battle damage detection using the electrical compression wavefront pulses.

Koblasz et al. [12] described an ultrasound liquid level detection system for automatically controlling the dispensing of a post-mix beverage. The design uses microprocessor-controlled circuitry for monitoring and implementing the automatic dispensing process. The microprocessor is interfaced with an ultrasonic transducer that transmits ultrasonic waves toward the target container that needs to be filled. It receives the reflected ultrasonic wave and then analyzes the characteristics of the received wave. Then, when required, it uses the microprocessor to implement control functions of the automatic dispensing process. The system also has additional safeguards programmed into the microprocessor to preclude operator errors such as triggering of the dispenser system by devices other than the container to be filled [12].

Ellinger et al. [13] described a method that determines the quantity and density of fuels stored in aircraft fuel containers using an ultrasonic transducer. Multiple ultrasonic sensors were used for the application. The ultrasonic sensors, including an altitude sensor, were controlled by a computer. Each ultrasonic transducer was supported within the stillwell by the container. Sensors in the fuel tanks were multiplexed by two redundant synchronized processors; so that failure of a sensor interface of one processor will not affect input to the other processor. An ultrasonic signal was transmitted and received from the transducer within the stillwell. The round-trip time period from sending to receiving the signal is measured. The quantity of fuel in the container is determined from the round-trip time period and data stored on the container volume in the central processing unit. The electrical wiring and sensor are mounted outside of the tank, which not only makes it

intrinsically safe but also avoids the possibility of performance degradation due to the contamination in the liquid [13].

Palmer et al. [14] described an ultrasonic sensor based liquid level sensor system that comprises a tubular probe having a peripheral wall and suspended in a liquid container. An ultrasonic signal is transmitted around the wall from a transmitting transducer that is embedded in a block, which is bonded to the inner surface of the wall, to a receiving transducer that is also embedded in the same block. A detector circuit discriminates between the signal levels when the ultrasonic probe is immersed outside of liquid and when the probe is immersed in liquid, hence it provides a corresponding switched output [14].

Getman et al. [15] described a liquid level sensing system that uses the pulse transit time technique to sense the level of liquid in a vessel. An ultrasonic transducer is mounted above the highest permissible level in the vessel, where it emits ultrasonic transmission pulses to the surface of the liquid and receives the ultrasonic echo pulses reflected from the liquid surface. The level in the vessel is established from the transit time of the ultrasonic pulses. To detect an overfill when the ultrasonic transducer is immersed in the liquid, the decaying output signal of the ultrasonic transducer generated by the ringing of the ultrasonic transducer following the end of the each ultrasonic transmission pulse is analyzed. With this arrangement, Getman et al. [15] claim that due to the better coupling of the ultrasonic transducer to the liquid than to air, the ringing duration is shorter when the ultrasonic transducer is covered by the liquid.

Lichte [16] described a fluid volume measurement system, where an ultrasonic sensor is mounted at the bottom of the tank. Echo pulses are transmitted from the sensor and travel through the fluid and reflect back, as shown in Fig. 2.11.

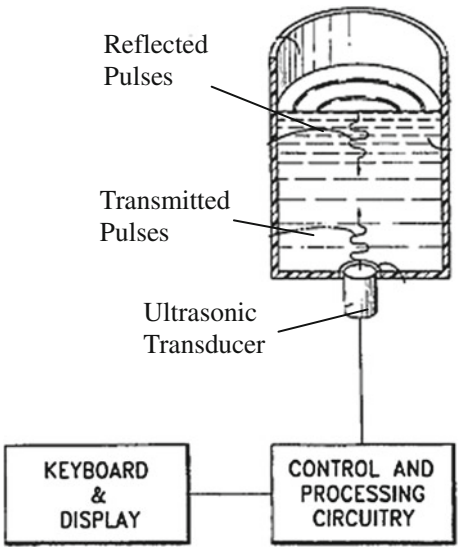

Fig. 2.11 An ultrasonic sensor based volume sensing system [16]

Marini et al. [17] described a method that determines the ratio of the volume of the gas present in an enclosure containing a diphase liquid–gas mixture to the total volume of the enclosure. The undissolved gas in the liquid is assumed to be in the form of a layer surmounting the liquid. This method requires an extremely rapid determination of the void coefficient. The time delay between the first frequency and the second frequency is used to determine the form of gas in the enclosure. Thereafter, the void coefficient is determined from the propagation velocities of the ultrasound in the gas and the liquid and from the measured propagation time of the ultrasonic waves. Ultrasonic waves at different frequencies are propagated through the fluid filling the enclosure. The propagation times of the waves are measured and the difference between these propagation times is calculated. If the propagation times are identical, it is deduced that all the gas is in the form of a layer surmounting the liquid. The void coefficient is determined from the propagation velocities of the ultrasound in the gas and the liquid and from the measured propagation time. If the propagation times are different, a part of the gas is in the form of bubbles in the liquid, the void coefficient due to the gas surmounting the liquid and the void coefficient due to the gas bubbles in the liquid are determined separately. The total void coefficient is determined by adding the two values obtained. The void coefficient due to the gas surmounting the liquid may be determined by virtue of the waves reflected by the gas–liquid interface. The void coefficient due to the gas bubbles is determined by virtue of the relationships existing between the velocity of the ultrasound and the frequency of the waves, according to the pressure and the void coefficient. This invention was used in the measurement of the void coefficient in a pressurized water nuclear reactor after an accident [17].

2.4 Ultrasonic Sensor Based Level Measurement in Dynamic Environments

2.4.1 Overview

Any kind of sound—in contrast to electromagnetic waves—can only be propagated in a material medium, and is strongly influenced by that medium, the velocity of sound, as well as its attenuation, depend in a characteristic way on the nature of the medium [4]. As described in Sect. 2.2.3, any change in temperature will alter the velocity of the ultrasonic wave. Since the velocity of sound varies with temperature, if the measurement system assumes the sound velocity to be constant, such a system will produce unreliable results and measurement accuracy will deteriorate. Apart from the temperature factor affecting fluid level measurement systems, contamination could be another factor that acts as a barrier, by reflecting the echo pulse back sooner than it should normally do, thus deceiving the system and creating errors. This section discusses the issues of ultrasonic level sensing in dynamic environments.

2.4.2 Effects of Temperature Variations

As discussed earlier, the variation in the ambient temperature influences the speed of sound. Since the variation in ambient temperature is continuous, the speed of the ultrasonic wave should not be considered constant. In vehicular fuel tanks, the temperature can vary from −40 to 110 °C. To improve the reliability of ultrasonic sensing systems, generally a temperature sensor is included in the system design to adjust the speed of ultrasonic waves used in the level calculation by using Eq. (1.1), which describes the relationship between the speed of the ultrasonic wave and temperature.

Crayton et al. [18] described a way to determine the fuel level in a storage tank using an ultrasonic sensor by controlling a Motorola's 68HC05 type microcontroller. This system is designed to perform calculations and produce fuel level output signals. The microprocessor is programmed to consider the effects of temperature variations on the speed of sound. For this, a temperature sensor is implanted in the tank that feeds temperature values into the microprocessor, which then compensates for the effects of temperature and reduces the output error. Crayton et al. [18] have claimed that the performance of the level sensing system is not degraded by the effects of temperature and rugged terrain that may cause the storage tank to tilt up to 45° in any direction [18].

Forgue [19] described a fluid level sensor that is able determine the ultrasonic velocity for the purpose of calibration of the fluid level measurement that is compensated for temperature, fluid composition, and other velocity affecting factors. It generally consists of a single ultrasonic transceiver and a housing component. The ultrasonic transceiver has a measurement section and a reference section that are separated by an insulating section, while the housing component has a reference element and an aperture that are located at the axial end. The measurement section transmits ultrasonic measurement signals that pass through the aperture and reflect off a fluid surface. The ultrasonic transceiver includes a disk-shaped measurement section and a ring-shaped reference section. An impedance layer is located adjacent to the ultrasonic transceiver such that ultrasonic signals pass through the impedance layer. The sensors signals are fed into an electronic controller to determine a signal velocity calibrated measurement of the fluid level that is compensated for temperature, fluid composition, and other velocity affecting factors [19].

Combs et al. [20] described an ultrasonic liquid level measurement device used to measure the depth of a flowing liquid in a channel using an ultrasonic transducer. An ultrasonic burst is directed toward the channel and the reflected echo from the surface of the liquid is returned and sensed by the transducer. The transit time of ultrasonic transmission and echo return is indicative of the liquid level. An adjustable discriminator is provided to specify a maximum liquid level in the channel and a minimum liquid level, which, typically is the floor of the channel. The maximum and minimum levels are adjustable to accommodate variable channel configurations and transducer mounting arrangements. Automatic adjustment is

provided to compensate for different cable lengths which may be used to connect the ultrasonic transducer to the transducer driver and receiving section. Temperature compensation is provided to accommodate changes in ultrasonic transmission propagation through ambient air with temperature, and time variable gain amplification is provided to compensate for geometric spreading of reflected ultrasonic energy echo pulses and for air path absorption [20].

Durkee [21] described an ultrasonic based fluid quantity measurement system that takes the effects of liquid temperature into consideration. The method does this by measuring the temperature of the liquid at at least two different heights. The method then determines the velocity of sound in the liquid at at least two different predetermined heights. It then establishes an approximation of a velocity of sound versus temperature profile for the liquid and determining an approximation of a velocity of sound versus height profile for each of at least two height regions based on the temperature measurements [21].

Crayton et al. [18] described a measuring system that determines the height of liquid contained in a storage tank. A tube is placed inside the tank which contains a float that is buoyed on the surface of the liquid. An ultrasonic transducer is placed inside the tube. The ultrasonic transducer emits ultrasonic pulses directed at the float, receives the reflected ultrasonic pulses, and responsively produces an echo signal. The float has a top portion and a bottom portion separated by a cylindrical portion. The bottom portion including a spherical surface which receives the ultrasonic pulses. The spherical surface has a predetermined radius which is a function of the inside diameter of the tube, the height of the cylindrical portion of the float, and the outside diameter of the cylindrical portion of the float. A temperature sensor monitors the temperature of the liquid and produces a thermometric signal in response to the liquid temperature. A microprocessor receives the echo and thermometric signals, determines the speed of the ultrasonic pulse traveling in the liquid, and responsively determines the liquid height [18].

2.4.3 Electromagnetic Interference

Birkett [22] has described a method of fluid level measurement that reduces the effects of electromagnetic interference (EMI) that can adversely affect the measurements obtained by the device. For providing better shielding from EMI, the piezoelectric crystal and other electrical components are enclosed in a tube. The piezoelectric device is positioned at the end of the tube so as to direct the ultrasonic pulse along the axis of the stillwell. The interior walls of the enclosure are provided with a metallic layer to block electromagnetic interference from the interior space [22].

2.4.4 *Effects of Contaminants and Obstacles*

Puttmer et al. [23] introduced a low noise ultrasonic density sensor configuration with high accuracy, long-term stability, and robustness by taking into account significant effects such as: drift of the piezoceramic transducer and electronic system; chemical, geometric, and acoustic properties of the reference material; reduction of signal amplitude or signal-to-noise-ratio (SNR) by the acoustic reference path; and the acoustic field. The sensor consists of a transducer with a piezoceramic disk mounted between two reference rods of quartz glass. Additionally, a second transducer is used as an ultrasound receiver. The density is obtained from the reflection coefficient of ultrasound at the interface between the quartz glass rod and the liquid and the transit time of sound between this interface and the second transducer. The reference signal is generated using the sound radiated from the rear side of the piezoceramic disk [23].

Borenstein et al. [24] categorized different types of noise and discussed methods for eliminating effects of each type of noise. Borenstein et al. [24] introduced a method called error eliminating rapid ultrasonic firing (EERUF), which combines different noise rejection techniques and optimizes them for rapid firing. EERUF almost completely eliminates crosstalk. Its unique noise rejection capability allows multiple mobile robots to collaborate in the same environment, even if their ultrasonic sensors operate at the same frequencies. For each noise category, methods are described to identify and reject the resulting errors. These individual rejection measures were combined into one error rejection method which was then combined with a fast firing algorithm. The resulting combination was EERUF. The EERUF method was implemented on a mobile robot; as a result, a mobile robot was able to traverse an obstacle course of densely spaced, pencil-thin poles at speeds of up to 1 m/s.

Soltz [25] described an ultrasonic liquid level measurement gauge that can determine true ultrasonic echo pulses from false parasitic pulses originating from reflecting wall surfaces and other obstacles in the vicinity of the tank. The parasitic pulses may be confused with the main echo pulses and can result in an erroneous reading [25].

Durkee [26] described an ultrasonic liquid gauging systems that is generally related to improving the detection of valid echoes under low liquid level and echo drop out conditions to improve the accuracy of the measured liquid quantity. A particular problem that can arise at low liquid levels is the detection of secondary and tertiary echoes from multiple or harmonic reflections at the liquid surface of the transmitted ultrasonic energy. The effects can cause echoes to be lost or missed, including echoes from the surface as well as from the target.

Kumar [27] has described an ultrasonic liquid level gauging system that can discriminate true echoes from false echoes. The device uses echo energy as a factor to distinguish a true echo from a false echo [27].

2.5 Effects of Liquid Sloshing

2.5.1 Overview

In mobile fluid tanks such as automotive fuel tanks, acceleration will induce waves in the storage tank. This phenomenon of fluid fluctuation is called *sloshing*. The magnitude of sloshing is dependent on the value of the acceleration or deceleration that may be caused by braking, speeding, and irregular terrain. A level measurement device observing the fluid level under sloshing conditions will produce erroneous level readings.

The sloshing phenomenon in moving rectangular tanks (e.g., automotive fuel tanks) can be usually described by considering only two-dimensional fluid flow, if the width of the tank is much less than its breadth [28]. The main factors contributing to the sloshing phenomenon are the acceleration exerted on the tank, amount of existing fluid, internal baffles, and the geometry of the tank [29, 31]. A detailed analysis of liquid sloshing using the numerical approach for various tank configurations has been provided in the literature [29–39].

Different designs of fluid level measurement systems have used different techniques to compensate for the erroneous reading of liquid level due to the effects of sloshing. This section of the literature review focuses on some level sensing devices that attempt to operate effectively in both static and dynamic environments.

2.5.2 Slosh Compensation by Dampening Methods

Fluid sloshing can be physically and electrically dampened to compensate for the sloshing effects. The following diagram shows a basic geometrical dampening method. The sensor is placed inside a vessel, where fluid can enter from the bottom of the vessel. The fluid stored in the vessel will experience less slosh than the fluid outside the vessel. Therefore, the fluid inside the vessel will be stable relative to the outside level. Various methods have been investigated that generally follow a similar principle (Fig. 2.12).

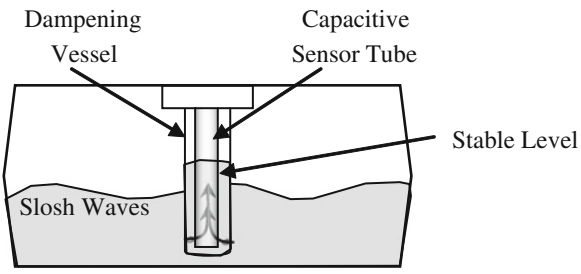

Fig. 2.12 Geometrically dampening the slosh waves

Kikuta et al. [40] described an ultrasonic level gauge that measures the level of a test surface inside a tank. It can measure the level of a test surface even when the distance between the test surface and the ultrasonic transceiver is very small. The level gauge includes a guiding pipe that guides the ultrasonic wave transmitted by an ultrasonic transceiver to the test surface, and guides the ultrasonic wave reflected by the test surface back to the ultrasonic transceiver. The gauge is capable of having an extended portion at the base of the guiding pipe that extends the propagation distance of the ultrasonic wave guided by this guiding pipe. A helical portion or a slanting portion may be provided in the guiding pipe to make the ultrasonic wave transmitted by the ultrasonic transceiver enter the test surface in a slanting direction. Since the ultrasonic wave making a round trip between ultrasonic transceiver and the liquid surface is guided by the guiding pipe, reflection of the ultrasonic wave by any of the inner walls of the tank does not occur. As a result, any measurement error due to the reflection by the inner walls of the tank, other than the liquid surface, can be prevented. It can also minimize the measurement error of the liquid level of the test surface even when the liquid is shaken, as in a fuel tank inside a car, while the car is moving.

2.5.3 Use of Tilt Sensors

Tiltmeters or inclinometers can be used in situations where the fluid tank can experience sloppy surfaces such as rough roads in hilly areas. Nawrocki [41] described a method that incorporates an inclinometer into a fuel gauging device. The level signal from the fuel level sensor can be transmitted to the fuel gauge only when the vehicle is tilted less than a predetermined degree. To accomplish this, a signal from the fuel sensor is passed through to the display by a microprocessor only when the vehicle is substantially level and not accelerating or decelerating. When the level condition is met, the signal indicative of the amount of fuel left in the tank is stored in the microprocessor memory and displayed on the fuel gauge, and is updated again when the vehicle reaches the next level condition. Alternatively, a correction factor matrix stored in the memory can be applied to the signal received from the fuel sensor to calculate a corrected signal indicative of the amount of fuel remaining in the fuel tank. Figure 2.13 shows an overview of the method described by Nawrocki [41].

Breed et al. [42] described a fuel level measurement system that measures the quantity of fuel in a tank using one or more load cells or fuel level measuring devices and other sensors to measure the pitch or roll angle of the vehicle. A processor and algorithm, which may be a look-up table or formulae, are combined to correct for the inaccuracies arising from the pitch and roll angles of the vehicle, other external forces, or from variations in fuel density. This method supports a variety of different fuel measuring transducers which by themselves give an inaccurate measurement of the quantity of fuel in the tank, but when combined with an empirically derived algorithm results in a highly accurate fuel quantity

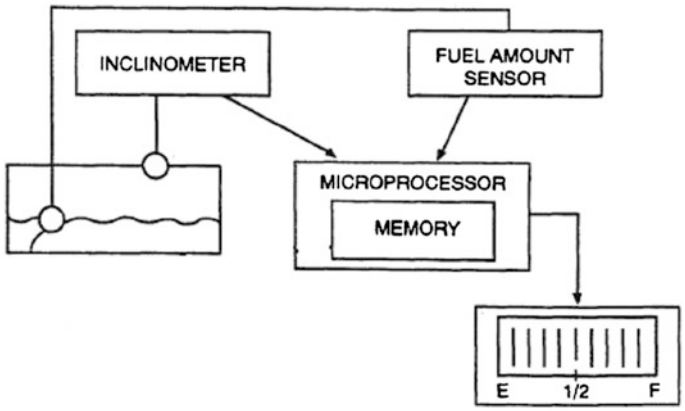

Fig. 2.13 Fuel level measurement system having an inclinometer [41]

measurement system. These transducers can be weight measuring load cells, vehicle angle measuring transducers, or fuel level measuring devices based on either float, ultrasonic, or capacitive measurement devices.

The method described by Breed et al. [42] comprises steps of: generating an algorithm for use on the vehicle by placing a known quantity of fuel into the tank. It then collects reflected wave patterns from ultrasonic transducers arranged on the bottom of the tank at discrete locations. It then compares the wave patterns from the ultrasonic transducers reflected under various conditions from an at rest position to a driving state over a variety of road surfaces. The wave patterns are inputted into a neural network generating program to classify different wave patterns [42].

Figure 2.14 shows an ultrasonic filling level sensor described by Voss [43], which has an elongated measuring chamber that is provided with an opening at each of its two ends. The sensor includes an ultrasonic transceiver, which is associated with one end of the measuring chamber and the emitted sound signals which are reflected at the surface of the liquid and at a calibrating reflector and received by the ultrasonic transceiver, in order to determine the filling level from the relationship between the transit times of the two signals. It is ensured that the cross-section of the measuring chamber and the nature of a wall of the measuring chamber are made to suit the properties of the liquid in such a way that, even in a tilted position of the measuring chamber, the surface of the liquid forms a meniscus which forms a reflection portion directed toward the ultrasonic transceiver. When elongated measuring chambers are used, the sound waves are emitted by a transceiver disposed at the bottom of the measuring chamber. They pass through the elongated measuring chamber substantially without being reflected at the walls of the measuring chamber, to be reflected at the surface of the liquid. Only the portion of the reflected sound signals that is reflected precisely in its direction reaches the transceiver. Such a filling level sensor only functions when the reflection area is directed toward the ultrasonic transceiver, that is to say

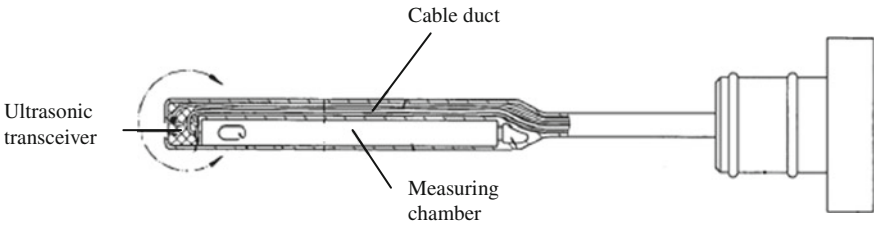

Fig. 2.14 Oil pump dipstick used in motorcycle engines [43]

extends substantially transversely to the longitudinal direction of the measuring chamber. For this reason, the known ultrasonic filling level sensors can only be used in a vertical position. This invention is therefore based on the object of developing an ultrasonic filling level sensor of the generic type which is simpler in terms of production engineering and advantageous in use [43].

2.5.4 Averaging Methods

Averaging method is another method besides the mechanical dampening that can compensate for the sloshing effects and produce better level readings. This statistical method generally collects the past sample values and determines the future level reading by using different calculation techniques. There have been a few different averaging techniques applied in the past that include a simple Arithmetic Mean, Weighted Average, and Variable Averaging Interval.

2.5.4.1 Arithmetic Mean

Arithmetic mean or simply mean is the traditional method of averaging the level sensor readings. The mean value of the sampled signal $x = [x_1, x_2, x_3, \ldots, x_n]$ for n number of samples is calculated using:

$$\text{mean}(x) = \bar{x} = \frac{1}{n}\sum_{i=1}^{n} x_i \tag{2.9}$$

The downside of averaging is that it produces a significant error for a momentarily large spike or an abnormal data entry in the elements of x. For example, if a sampled signal is given as:

$$x = [1.21, 1.30, 1.25, 1.27, 1.23, 1.91] \tag{2.10}$$

$$\bar{x} = \frac{1.21 + 1.30 + 1.25 + 1.27 + 1.23 + 1.91}{6} = 1.36 \tag{2.11}$$

$$\bar{x} = \frac{1.21 + 1.30 + 1.25 + 1.27 + 1.23}{5} = 1.25 \tag{2.12}$$

The average value obtained in the presence of an abnormal entry '1.91' in signal x is given in (2.11), which is significantly larger than the average value when obtained without '1.91' element in x (2.12).

Gazis et al. [44] described an ultrasonic liquid level gauge design, in which one or more high-frequency ultrasonic transducers are used to measure the liquid level of tanks containing any type of fluid. The invention relates specifically to tanks that are subject to movement and vibration which generally makes the use of ultrasonic echoes unreliable for obtaining accurate level measurements. A special algorithm is used to obtain the temporal center of the distribution of echo arrival times over a preset time interval. From this temporal center of an echo distribution, the liquid level is readily obtained through the acoustic velocity, time, and distance relationship. An annular piezoelectric plate, independently driven at low ultrasonic frequencies (kHz range), mounted on the tank bottom surrounds the high-frequency ultrasonic transducer. The function of the piezoelectric plate is to send out propagating ultrasonic waves (essentially longitudinal) to maintain the tank area in the immediate region of the high-frequency transducer free from debris and sediment deposits at the bottom of the tank thereby avoiding the uncertainty in the measurement that is introduced by debris on the tank bottom. The device uses a continuous or quasi-continuous signal averaging technique to present a distribution of echo signals as a function of time from which liquid levels can be accurately determined and monitored on a continuous or quasi-continuous basis. Several averaging methods are described from which the temporal center of the distribution can be determined. One or more ultrasonic transducers are firmly mounted on the bottom of a fuel tank to transmit and receive acoustic pulses. The received echo pulses are rectified and filtered before a channel analyzer processes it. Signal processing is used to determine the center of the echo time. This time is then used by a computer to obtain the level of the fluid in the tank [44].

An improved version of averaging is described by Tsuchida et al. [45]. Their method determines the center value of the past sensor readings. The center value is assumed to be the accurate level reading. The method repeatedly reads the amount of fuel remaining in the fuel tank of a vehicle and then it determines a center value from the past fuel quantity readings. A microcontroller is used to determine limit values for the center value by a predetermined margin. A subsequent value that exceeds the limit values is set as a new limit value. The method then determines an average value out of the predetermined number of detected sampling values. The method also performs the function of discriminating and eliminating any sudden changes or abnormal values that may be caused by the sudden changes in the attitude of the vehicle or by the acceleration to provided stable values of the remaining fuel quantity [45].

2.5.4.2 Weighted Average

Weighted average is similar to the simple averaging method, except that there are additional weights (w) assigned to each element in the sample signal $x = [x_1, x_2, x_3,\ldots,x_n]$. In the absence of the weights, all data elements in x contribute equally to the final average value. But, with the usage of the additional weights (w), the final average can be controlled. If all the weights are equal, then the weighted mean is the same as the arithmetic mean. The weighted average of a signal $x = [x_1, x_2, x_3,\ldots,x_n]$ and the weights $w = [w_1,w_2,w_3, \ldots,w_n]$ for n number of sampled points can be calculated using:

$$W_{\text{mean}}(x) = \bar{x} = \frac{\sum_{i=1}^{n} w_i x_i}{\sum_{i=1}^{n} w_i},\ w_i > 0 \tag{2.13}$$

2.5.4.3 Variable Averaging Interval

In the variable averaging method, raw sensor readings are averaged at different time intervals depending on the state or motion of the vehicle. During static conditions, when the vehicle is stationary or when the vehicle is operating at a low speed, the averaging time is reduced to a small interval to quickly update the sensor readings by assuming that there will be negligible slosh. During the dynamic conditions, the averaging period is increased for averaging the sensor readings over a longer period of time. Normally, a speed sensor is used to determine the running state of the vehicle.

Kobayashi et al. [46] described a sensor that uses digital signals as opposed to analog signals to determine the fluid volume in a fuel storage tank. The digital fuel volume measuring system can indicate the amount of fuel within a fuel tank precisely in the unit of 1.0 or 0.1 l. The volume detection signals are simply averaged during a relatively short averaging time period at regular measuring cycles when the vehicle is being refueled, and further weight-averaged or moving-averaged at regular measuring cycles when the vehicle is running. Therefore, fuel volume can be indicated quickly at a short response speed when the vehicle is being refueled and additionally fluctuations in the fuel volume reading can be minimized when the vehicle is running. Further, the system discloses the method of detecting the state where the vehicle is being refueled on the basis of the fact that the difference between at least one of the current data signal indicative of fuel volume and at least one of the preceding data signal indicative of fuel volume exceeds a predetermined value [46].

Guertler et al. [47] described a process that determines the quantity of a liquid contained in a largely closed system. The liquid fluctuations in a dynamic or a moving vehicle can produce erroneous results. These fluctuations can be calculated out as the result of the predetermined dependence of the liquid level and therefore of the amount of fluid from the driving condition and, in addition, can be

statistically averaged out because of the continuous obtaining of measuring values. This permits the reliable determination of the fluid quantity whose level fluctuates as a function of the driving condition by way of level measurements not only when the vehicle is stopped and the engine is switched-off, but also in the continuous driving operation.

Kobayashi et al. [48] utilize the information about the various different states of the vehicle, such as ignition ON–OFF, idle state, and up and down speeding. The fuel level readings are averaged over time intervals which vary according to whether the liquid level of the fuel in the tank is stable or unstable. A fuel quantity is calculated and displayed according to the averaged value. The stable or unstable condition of the fuel level is discriminated in accordance with vehicle speed, the "on" or "off" position of an ignition switch. Accordingly, when the fuel level is unstable, the signal value is averaged over a time interval which is longer than that used when the fuel level is stable so that the response of display to variation of the fuel level is improved [48].

2.6 Summary

A detailed investigation of ultrasonic sensing technology described in this chapter reveals the fact that ultrasonic technology is increasingly being used in a broad range of applications due to its nonmechanical and contactless nature; robustness in harsh environments; its ability to work with a wide range of chemical substances; compact and flexible size; longer functional life; and lower manufacturing cost.

Even though the uses of ultrasonic sensing technology in fluid level measurement systems has produced satisfactory outcomes in a broad range of applications, the literature review has highlighted some of the weaknesses of ultrasonic sensing technology in relation to its accuracy in level measurement particularly in dynamic environments. Level sensing in dynamic environments is characterized by three factors:

- Slosh
- Temperature variation
- Contamination (obstacles and dust)

Solutions to each of these three above mentioned factors have been reviewed in this chapter. However, all these solutions entail either higher production cost because of the requirement for additional sensors, or they provide only marginal improvement in terms of accuracy compared to current systems [46–48].

To provide a practical and compact solution to the above mentioned problems pertaining to the inaccuracy of ultrasonic level sensing systems in dynamic environments, an intelligent ultrasonic sensor system is to be developed for fluid level sensing with the incorporation of a Support Vector Machine (SMV) based signal characterization and classification methodology.

References

1. Everest FA (2001) The master handbook of acoustics, 4th edn. McGraw-Hill, New York
2. Bruneau M, Scelo T (2006) Fundamentals of acoustics. ISTE Ltd, London
3. The Nature of a Sound Wave. www.physicsclassroom.com/Class/sound/U11L1c.html
4. Kuttruff H (1991) Ultrasonics—fundamentals and applications. London, Elsevier Applied Science
5. Jewett JW, Serway RA (2004) Physics for scientists and engineers, 6th edn. Thomson, Toronto
6. Cheeke J, David N (2002) Bulk waves in fluids. Principles and applications of ultrasonics. CRC, Boca Raton, pp 39–58
7. Carlin B (1960) Ultrasonics, 2nd edn. McGraw-Hill, New York
8. Paulsen MT, (inventors), Pasteur S (Diagnostics assignee) (1992) Diagnostics assignee. Method of and device for fluid surface detection using an ultrasonic transducer
9. Wang Y (1993) Switch-mode ultrasonic wave RF burst emission circuit. In: International conference on acoustic sensing and imaging, pp 172–177
10. Suzuki H (inventor) (1978) Method for damping an ultrasonic transducer
11. Durkee, SR (inventor), Simmonds Precision Products, Inc. (assignee) (2004) Ultrasonic system and method of gauging aircraft fuel and detecting battle damage Patent no. 6957582
12. Koblasz A, Hollister J, Alexander D (inventors), The Coca-Cola Company (assignee) (1983) Ultrasound level detector. Patent no. 4559979
13. Ellinger SM, Jones HP (inventors), Simmonds Precision Products, Inc.; Edo Corporation (assignee) (1987) Ultrasonic fuel quantity gauging system. Patent no. 4815323
14. Palmer SB, Primavesi GJ (inventors), Bestobell Mobrey Limited (assignee) (1980) Liquid level sensor. Patent no. 4316183
15. Getman I, Lopatin S, Muller R (inventors), Endress Hauser GmbH Co. (assignee) (1998) Method and assembly for overfill detection in liquid level sensing in a vessel by the pulse transit time technique. Patent no. 6142015
16. Lichte LJ (inventor) (1994) Container and adaptor for use with fluid volume sensor. Patent no. 5586085
17. Marini J, Roi ML, Heinrich J-P, Champs-sur-Marne (inventor), Framatone & Cie, Courbevoie, France (assignee) (1985) Method of ultrasonic measurement of the ratio of the volume of gas present in an enclosure. Patent no. 4,491,008
18. Betts JWC, Timothy AB, David A (inventor), Caterpillar Inc., Peoria (assignee) (1994) Ultrasonic fuel level sensing device. Patent no. 5,319,973
19. Forgue JR (inventor), TI Group Automotive Systems, L.L.C. (Warren, MI, US) (assignee) (2003) Fluid level sensor. Patent no. 6993967
20. Combs CM, Goodwin Jr, Perry H (inventors), Robertshaw Controls Company (assignee) (1978) Adjustable ultrasonic level measurement device. Patent no. 4221004
21. Durkee SR (inventor), Simmonds Precision Products, Inc. (assignee) (2000) Ultrasonic liquid gauging system. Patent no. 6236142
22. Birkett RE (inventor), Simmonds Precision Product, Inc. Akron, Ohio (assignee) (1993) Ultrasonic transducer assembly for measuring liquid level. Patent no. 5410518
23. Puttmer A, Hauptmann P, Henning B (2000) Ultrasonic density sensor for liquids. IEEE Trans Ultrason Ferroelectr Freq Control 47(1):8
24. Borenstein J, Koren Y (1992) Noise rejection for ultrasonic sensors in mobile robot applications. In: IEEE international conference on robotics and automation proceedings, vol 2, pp 1727–1732
25. Soltz DJ (inventor), Fischer & Porter Co. (assignee) (1987) Parasitic echo pulse rejector for ultrasonic liquid level meter. Patent no. 4821569
26. Durkee SR (inventor), Simmonds Precision Products, Inc., Akron, Ohio (assignee) (1999) Processing echoes in ultrasonic liquid gauging systems. Patent no. 5856953

27. Kumar L (inventor), Simmonds Precision Products, Inc. (assignee) (1993) Apparatus and method for discriminating true and false ultrasonic echoes. Patent no. 6046960
28. Ibrahim RA (2005) Introduction. Liquid sloshing dynamics: theory and applications. Cambridge University Press, Cambridge, p xvii
29. Ibrahim RA (2005) Liquid sloshing dynamics: theory and applications. Cambridge: Cambridge University Press
30. Kim H-S, Lee Y-S (2008) Optimization design technique for reduction of sloshing by evolutionary methods. J Mech Sci Technol 22:25–33
31. aus der Wiesche S (2003) Computational slosh dynamics: theory and industrial application. Comput Mech 30(5–6):374–387
32. Dai L, Xu L (2006) A numerical scheme for dynamic liquid sloshing in horizontal cylindrical containers. Proc Inst Mech Eng Part D J Automob Eng 220(7):901–918
33. Modaressi-Tehrani K, Rakheja S, Sedaghati R (2006) Analysis of the overturning moment caused by transient liquid slosh inside a partly filled moving tank. Proc Inst Mech Eng Part D J Automob Eng 220(3):289–301
34. Sinha NC, Pal SK, Bhattacharyya RK (2001) Experimental investigation of slosh dynamics of liquid-filled containers. Exp Mech 41:63–69
35. Liu D, Lin P (2008) A numerical study of three-dimensional liquid sloshing in tanks. J Comput Phys 227(8):3921–3939
36. Kita KE, Katsuragawa J, Kamiya N (2004) Application of Trefftz-type boundary element method to simulation of two-dimensional sloshing phenomenon. Eng Anal Boundary Elements 28(2004):677–683
37. Pal NC, Bhattacharyya SK, Sinha PK (2001) Experimental investigation of slosh dynamics of liquid-filled containers. Exp Mech 41(1):63–69
38. Arafa M (2006) Finite element analysis of sloshing in rectangular liquid-filled tanks. J Vib Control 13(7):883–903
39. aus der Wiesche S (2003) Computational slosh dynamics: theory and industrial application. Comput Mech 30(5):374–387
40. Kikuta M, Takahashi T, Terayama T, Hasegawa K, Hayashi C (inventors), Toyoda Gosei Co., Ltd. (assignee) (1988) Ultrasonic level gauge. Patent no. 4909080
41. Nawrocki R (inventor), FORD MOTOR CO (US) (assignee) (1990) Apparatus and method for gauging the amount of fuel in a vehicle fuel tank subject to tilt. Patent no. 5072615
42. Breed DS, Wilbur E, Johnson WC (inventors), Automotive Technologies International Inc. (assignee) (2003) Method and apparatus for measuring the quantity of a liquid in a vehicle container. Patent no. 6892572
43. Voss W, Iserlohn (DE) (inventor) Werner Turck GmbH & Co. KG, Halver (DE) (assignee) (2004) Ultrasonic filling level sensor. Patent no 7168314
44. Gazis DC, KW Francis, von Gutfeld RJ (inventors), International Business Machines Corporation (assignee) (1996) Ultrasonic liquid level gauge for tanks subject to movement and vibration. Patent no. 5,793,705
45. Tsuchida T, Okada K, Okuda Y, Kondo N, Shinohara T (inventors), Toyota Jidosha Kogyo Kabushiki Kaisha (assignee) (1981) Method of and apparatus for indicating remaining fuel quantity for vehicles. Patent no. 4402048
46. Kobayashi H, Obayashi H (inventors), Nissan Motor Company, Limited (assignee) (1983) Fuel volume measuring system for automotive vehicle. Patent no. 4611287
47. Guertler T, Hartmann M, Land K, Weinschenk A (inventors), Daimler Benz AG (DE) (assignee) (1997) Process for determining a liquid quantity, particularly an engine oil quantity in a motor vehicle. Patent no. 5831154
48. Kobayashi H, Kita T (inventors), Nissan Motor Company, Limited (assignee) (1982) Fuel gauge for an automotive vehicle. Patent no. 4470296

Chapter 3
Ultrasonic Sensor Based Fluid Level Sensing Using Support Vector Machines

3.1 Overview

The characteristics, principles, and applications of ultrasonic type sensors, including some issues of the ultrasonic type level sensing applications in dynamic environments, were discussed in Chap. 2. In this chapter, first, the fundamental principles of signal classification and processing are discussed. Then the background and application of Support Vector Machines (SVM) in the context of this research are described. Finally, the use of SVM in providing solutions to the problems encountered in fluid-level measurement in dynamic environments is described.

3.2 Signal Processing and Classification

3.2.1 Overview

Signal processing and signal classification plays a crucial role in the improvement of the accuracy of any fluid-level measurement system, particularly, in dynamic environments. This section broadly focuses on various aspects of signal processing and classification. Various components of signal preprocessing such as *Data collection methods, Feature extraction methods, and Signal filtration methods* are discussed. Thereafter, a diverse range of signal classification techniques are described in this section (Fig. 3.1).

3.2.2 Data Collection

Typically, the output from a fluid level sensor is in the form of a continuous voltage over time. However, to digitally process the sensor's analog signal, the signal needs to be converted into a discrete signal by sampling it at some constant

J. Terzic et al., *Ultrasonic Fluid Quantity Measurement in Dynamic Vehicular Applications*, DOI: 10.1007/978-3-319-00633-8_3,
© Springer International Publishing Switzerland 2013

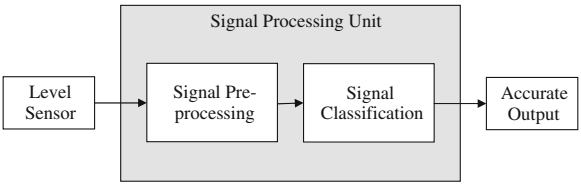

Fig. 3.1 Overview of sensor signal processing

sampling frequency f_s [1]. The sampling interval T_s is the time between two sampled points, which is simply equal to:

$$T_s = \frac{1}{f_s} \tag{3.1}$$

Figure 3.2 shows a continuous analog signal and its sampled version when sampled at a sampling frequency of 20 Hz. If $x(t)$ is the analog sensor output signal, the discrete sampled signal $x[n]$ at sampling frequency f_s can be described as [2]:

$$x[n] = x(nT_s) = x\left(\frac{n}{f_s}\right), \quad \text{where } n = 0,\ 1,\ 2,\ 3, \ldots \tag{3.2}$$

3.2.3 Signal Filtration

The signal values obtained from the level sensor are processed with different signal filtration functions to enhance the performance of the signal classification system before the signal is interpreted [3]. The signal feature coefficients from a noisy signal can weaken the performance of signal classification [3, 4]. Noisy signals can be filtered using different approaches, such as low-pass filter, high-pass filter, or band-pass filter. A low-pass filter can be used to eliminate high-frequency noise,

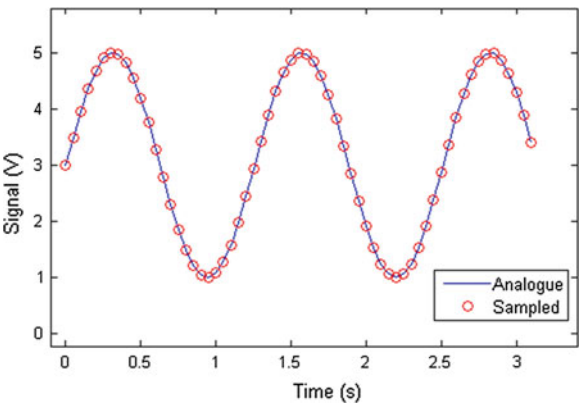

Fig. 3.2 Illustration of an analog waveform and its sampled digital signal

especially when the level sensor signal consists of low-frequency content (i.e., slosh waves). Band-pass filters can be very useful if the range of effective frequency of interest is known.

Variable filters such as *adaptive filter* can be very useful for the reduction of white-noise [5].

3.2.4 Feature Extraction

Apart from signal filtration, another operation performed in signal preprocessing is the selection of features and reduction of the size of the input signal, while at the same time trying to preserve the information contained in the input signal. The reduction in the signal size will reduce the input size of the classification network, if one is used, as well as increase the network performance [4]. Trunk [6] has demonstrated that use of large quantities of data may be detrimental to classification, especially if the additional data is highly correlated with previous data [4]. The following methods are commonly used to extract and reduce the number of feature from the input signal [4]:

- Fast Fourier Transform (FFT)
- Discrete Cosine Transform (DCT) [7]
- Wavelet Transform (WT)
- Principle Component Analysis (PCA)
- Fisher Discriminant Analysis (FDA)
- Independent Component Analysis (ICA).

3.2.4.1 Fast Fourier Transform

The Fast Fourier Transform (FFT) algorithm is widely used to transform a time domain signal into the frequency domain [8]. The Fourier transform of a signal involves decomposing the waveform into a sum of sinusoids of various frequencies. A time domain signal $y(t)$ can be transformed into the frequency domain as $Y(\omega)$ [9]:

$$Y(\omega) = \int_{-\infty}^{\infty} y(t) e^{-j\omega t} \mathrm{d}t \tag{3.3}$$

Discrete Fourier Transform (DFT) is used where the input signal is discrete or sampled at fixed intervals. The DFT rule is described by the following equation, where $Y(k)$ is the transformed function of y(t) for frequency k [10].

$$Y(k) = \frac{1}{N} \sum_{n=1}^{N} y(n) e^{-j2\pi(k-1)\left(\frac{n-1}{N}\right)}, \quad 1 \le k \le N \tag{3.4}$$

Once a signal has been transformed into a form that contains discrete frequency coefficients using the FFT function, feature selection can be applied by selecting only the desired range of frequency components. In fuel level sensing systems, the slosh waves produced in the tank consist of low-frequency components. Therefore, only the lower frequency range (0–10 Hz) can be selected and fed into the signal classification unit (i.e., neural network).

3.2.4.2 Discrete Cosine and Sine Transforms

A sequence of finite data points can be expressed in terms of a sum of cosine functions oscillating at different frequencies using the Discrete Cosine Transform (DCT) function. The DCT has been used in numerous applications in the fields of science and engineering, from digital compression of images and audio, to spectral methods for the numerical solution of partial differential equations. DCT plays a vital role in JPEG [11] and MPEG [12] type still images and multimedia compression.

In principle, the Discrete Cosine Transform (DCT) is related to Fourier Transformation (FT), however, DCT only operates on the real data with even symmetry. Discrete Cosine Transform (DCT) of a sample signal $x(0)$, $x(1)$,..., $x(N-1)$ consisting of N number of samples is defined as [13]:

$$y(k) = \alpha(k) \sum_{n=0}^{N-1} x(n) \cos\left(\frac{\pi(2n+1)k}{2N}\right), \quad k = 0,\ 1,\ \ldots,\ N-1 \tag{3.5}$$

The Inverse Discrete Cosine Transform (IDCT) function can be given as:

$$x(n) = \sum_{k=0}^{N-1} \alpha(k) y(k) \cos\left(\frac{\pi(2n+1)k}{2N}\right), \quad n = 0,\ 1, \ldots, N-1 \tag{3.6}$$

where,

$$\alpha(k) = \begin{cases} \sqrt{\frac{1}{N}}, k = 0 \\ \sqrt{\frac{2}{N}}, k \neq 0 \end{cases}$$

The transformation in vector form is written as [13]:

$$y = C^T x, \tag{3.7}$$

where, the elements of the matrix C are given by:

$$C(n,k) = \frac{1}{\sqrt{N}}, \quad k = 0, \quad 0 \leq n \leq N-1 \tag{3.8}$$

$$C(n,k) = \sqrt{\frac{2}{N}}\cos\left(\frac{\pi(2n+1)k}{2N}\right), \quad 1 \le k \le N-1, \quad 0 \le n \le N-1 \tag{3.9}$$

The Discrete Sine Transform (DST) is similar to DCT, however, it operates on the real-odd portions of the DFT. Discrete Sine Transform (DST) is defined via the transform matrix [13]:

$$S(k,\ n) = \sqrt{\frac{2}{N+1}}\sin\left(\frac{\pi(k+1)(n+1)}{N+1}\right), \quad k,\ n = 0,\ 1, \ldots, N-1 \tag{3.10}$$

The DCT and DST belong to the family of transforms that can be computed via a fast logarithmic method in [14]. The Discrete Cosine Transform (DCT) [7] is a real transform that has great advantages in energy compaction [15]. The use of DCT rather than DST is critical in data compression applications, since the cosine functions (used in DCT) are much more efficient in transformation and require fewer data points to approximate a typical signal.

3.2.4.3 Wavelet Transform

The *Wavelet Transform* is similar in concept to FFT, however, with the exception that WT not only provides the frequency representation of the signal but also retains the time information [16]. It uses the windowing technique with variable sized regions to provide a time–frequency representation of the input signal. It is useful for analyzing nonstationary signals, where the frequency varies over time [16]. Therefore, local analysis can be performed using the WT method. Wavelet Transform of a continuous signal $y(t)$ can be defined as:

$$C(s,\ p) = \int_{-\infty}^{\infty} y(t)\,\psi(s,\ p,\ t)\mathrm{d}t \tag{3.11}$$

where $\psi(s,p,t)$ is the mother wavelet with s as the scale and p the position at time t.

To transform signals that are discontinuous (sampled signals), Discrete Wavelet Transform (DWT) algorithm is used to analyze signals at different frequency bands by decomposing them into coarse information and detail information sets [17]. The coarse information set contains the low frequencies, whereas, the detailed information contains the high-frequency components of the input signal. To decompose an input signal into high-frequency and low-frequency components, DWT employs two sets of functions known as the scaling functions and wavelet functions, where the functions can be viewed as low-pass and high-pass filters, respectively [17].

Figure 3.3 shows the input signal *S,* consisting of 1,000 sample points, being decomposed and down-sampled into high-frequency (*cD*) and low-frequency (*cA*) components. Down-sampling is useful in compressing the signal by discarding the higher frequency component, which is usually the noise [17]. The coefficients *cA*

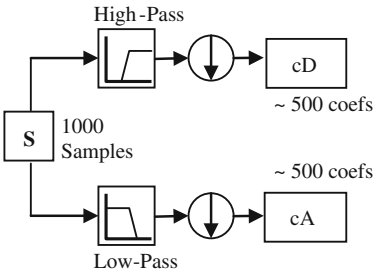

Fig. 3.3 Decomposition of signal *S* into high- and low-frequency portions [17]

and *cD* represent the features of the original signal. After performing DWT on the input signal, the *cA* coefficients can be fed into the signal classification unit.

3.2.5 Signal Classification Techniques

Pattern classification methods are divided into two classes [18]:

- Supervised Classification
- Data Clustering (unsupervised classification).

Supervised classification methods require both the *input* and the *target* output data. It consists of the assignment of labels to the test pattern based on the training patterns. There are two phases in supervised classification methods: learning and classification. The pattern classifier system learns the system based on the training data, and after training, it can be used to classify the test patterns. There are several different data classification methods, each method has different advantages and disadvantages. Table 3.1 lists common classification methods and provides a comparison of their performance, computational cost, and other factors [4].

In data clustering (unsupervised classification), the target value is not used while training. The clustering method clusters the sample data points according to their correlation with different cluster centers so as to attain a good partition of the data. There are many different types of data clustering methods available, some famous methods are listed below [4]:

- K-means [19]
- Fuzzy k-means [20]
- Kohonen maps [21]
- Competitive learning [22].

Supervised classification methods such as SVM and Neural Networks are more flexible and can yield much better results when compared with the data clustering methods such as K-means [23].

Table 3.1 Comparison of various classification algorithms [4]

Algorithm	Classification error	Computational cost	Memory requirements	Difficult to implement	On-line	Insight from the classifier
Expectation maximization (EM)	Low	Medium	Small	Low	No	Yes
Nearest neighbor	Med–Low	High	High	Low	No	No
Decision trees	Medium	Medium	Medium	Low	No	Yes
Parzen windows	Low	High	High	Low	No	No
Linear least squares (LS)	High	Low	Low	Low	Yes	Yes
Genetic programming	Med–Low	Medium	Low	Low	No	Some
Neural networks	Low	Medium	Low	High	Yes	No
Ada-Boost	Low	Medium	Medium	Medium	No	No
Support vector machines (SVM)	Low	Medium	Low	Medium	Yes	Some

3.3 Support Vector Machines

3.3.1 Overview

Support Vector Machines (SVM) is a learning method used for data classification and regression purposes. SVM is related to supervised learning methods, where sample data or training points are used by the SVM system for training and regression analysis purposes. The advantage of SVM to classify linearly separable and nonlinearly separable data has quickly introduced SVM in many scientific and engineering applications [24]. This section describes the theory of SVM and its various configurations and applications in dynamic environments.

3.3.2 Two-Class Support Vector Machines

The basic idea behind the SVM is to create a distinction between two or more data classes. The explanation of the SVM theory is best described using a binary (two)-class solution that is provided in this section. For a given set of training samples, SVM constructs a system model to predict the output based on the training samples and a set of given input samples. In principle, SVM constructs a hyperplane between two classes of data and then optimizes the separation distance between the two classes to provided optimal classification for a given set of data points D containing N number of data points such that:

$$\mathbf{D} = \left\{ (\mathbf{x}_1,\ y_1),\ (\mathbf{x}_2,\ y_2),\ \ldots,\ (\mathbf{x}_N,\ y_N) \,\middle|\, \mathbf{x}_i \in \Re^d,\ y_i \in \{-1,\ +1\} \right\}_{i=1}^{N} \quad (3.12)$$

where, $\mathbf{x}_i$ is the feature vector containing d number of features (d-dimensional), y_i is the corresponding class of $\mathbf{x}_\mathrm{i}$ or expected output value. For example, Class A can be assigned the value of y_i as '−1' and Class B as '+1'. SVM classifies the above mentioned data points for the two-class solution (Class A and B) by first plotting the data points **D** into the feature space. Then, SVM constructs a hyperplane that separates the data points of one class (i.e., Class A) from other class (i.e., Class B).

Figure 3.4 shows an illustration of SVM-based pattern classification between two classes of data using three hyperplanes (H_1, H_2, and H_3). It shows that there are infinite number of ways to create a hyperplane. However, in SVM the goal is to create an optimal hyperplane that creates the best distinction line between the two classes of data. In Fig. 3.4, H_1 does not separate the two classes of data in any way, whereas, H_2 and H_3 do separate the two groups of data. However, H_3 provides the best separation between the two classes when compared with H_2. Any hyperplane can be described as set of points **x** satisfying:

$$\mathbf{w} \cdot \mathbf{x} - b = 0 \quad (3.13)$$

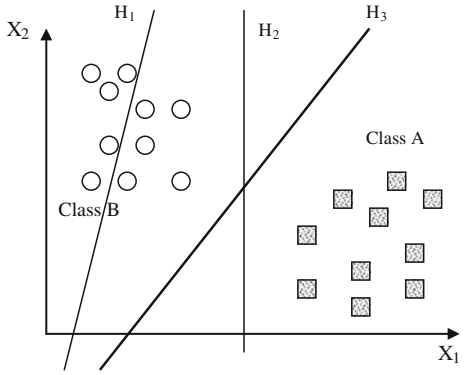

Fig. 3.4 Classification of a set of two class data using hyperplanes

where, vector **w** is a normal vector perpendicular to the hyperplane and b is the bias value of the hyperplane. The offset of the hyperplane from the origin along the normal vector **w** can be described by parameter $\frac{b}{\|\mathbf{w}\|}$.

The goal in SVM is to maximize the margin or separation between the two classes of data as far apart as possible while still separating the two groups of data. Maximum-margin hyperplanes can be described by the follow equations:

$$\mathbf{w} \cdot \mathbf{x} - b = -1 \quad \text{(Class A)} \tag{3.14}$$

$$\mathbf{w} \cdot \mathbf{x} - b = +1 \quad \text{(Class B)} \tag{3.15}$$

Hence, each data point in both classes has to satisfy the following conditions:

$$\mathbf{w} \cdot \mathbf{x}_i - b \leq -1 \quad \text{for Class A} \tag{3.16}$$

or,

$$\mathbf{w} \cdot \mathbf{x} - b \geq +1 \quad \text{for Class B} \tag{3.17}$$

Figure 3.5 For an optimal classification solution, a maximum-margin hyperplane is solved using the mathematical programming solution by minimizing the $\|\mathbf{w}\|$ and b parameters. In the case of a basic two-class SVM, the optimization can be written as:

$$\min_{\mathbf{w},\, b} \|\mathbf{w}\| \tag{3.18}$$

$$\text{subject to:} \quad y_i(\mathbf{w} \cdot \mathbf{x}_i - b) \geq +1\,, \quad \text{for any } i = 1,\ 2,\ \ldots,\ N$$

The above optimization problem depends on $\|\mathbf{w}\|$, which involves a square root; hence, this solution is difficult to solve. However, if the term $\|\mathbf{w}\|$ is replaced with $\frac{1}{2}\|\mathbf{w}\|^2$, then the problem could be simplified and solved using the quadratic mathematical programming (QP) method. The above problem can now be rewritten as:

$$\min_{\mathbf{w},b} \frac{1}{2} \|\mathbf{w}\|^2 \tag{3.19}$$

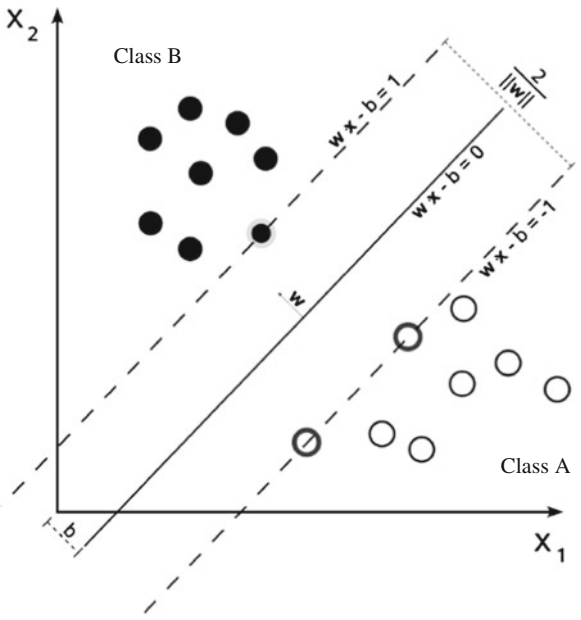

Fig. 3.5 Maximum-margin hyperplane between two classes of data

$$\text{subject to:} \quad y_i(\mathbf{w} \cdot \mathbf{x}_i - b) \geq +1, \quad \text{for any } i = 1, 2, \ldots, N$$

The above optimization can be expressed in terms of Lagrange multipliers α_i as [25]:

$$\min_{\mathbf{w},b,\boldsymbol{\alpha}} \left\{ \frac{1}{2} \|\mathbf{w}\|^2 - \sum_{i=1}^{N} \alpha_i [y_i(\mathbf{w} \cdot \mathbf{x}_i - b) - 1] \right\} \tag{3.20}$$

This problem can now be solved using any standard quadratic programming method. The solutions for **w** and b can be expressed in the following forms [25]:

$$\mathbf{w} = \sum_{i=1}^{N} \alpha_i y_i \mathbf{x_i} \tag{3.21}$$

$$b = \frac{1}{N_{SV}} \sum_{i=1}^{N_{SV}} (\mathbf{w} \cdot \mathbf{x_i} - y_i) \tag{3.22}$$

where, vector $\mathbf{x_i}$ is the *support vector points* that lie exactly on the margin hyperplanes, and N_{SV} is the total number of *support vectors*.

The above optimization problem can be further simplified by expressing it in the Dual form. The classification rule in the unconstrained dual form reveals that the maximum-margin hyperplane is only a function of the support vectors (training points that lie on the two margins of the hyperplane). By substituting the normal vector $\mathbf{w} = \sum_{i=1}^{N} \alpha_i y_i \mathbf{x_i}$ into $\|\mathbf{w}\|^2 = w \cdot w$, the above SVM optimization problem can be expressed in dual form as [26, 27]:

$$\max_{\alpha_i} L(\alpha) = \sum_{i=1}^{N} \alpha_i - \frac{1}{2} \sum_{i,j} \alpha_i \alpha_j y_i y_j \mathbf{x}_i^{\mathrm{T}} \mathbf{x}_j \tag{3.23}$$

$$\text{subject to: } \alpha_i \geq 0, \quad \text{and} \quad \sum_{i=1}^{N} \alpha_i y_i = 0 \tag{3.24}$$
$$\text{for any } i = 1, 2, \ldots, n$$

3.3.3 Soft-Margin Support Vector Machines

The SVM optimization solution presented in the previous section can be applied to classify only linearly separable data consisting of two classes. However, in real-life situations, due to the influence of noise, a training data set can often be inseparable. To classify the inseparable data set with good accuracy, in 1995, Vladimir Vapnik and Corinna Cortes [28] suggested a modified maximum-margin idea that allows an inseparable data set to be classified with a good accuracy. The improved form of the SVM optimization problem includes a non-negative tolerance (slack) variable ξ_i:

$$y_i(\mathbf{w} \cdot \mathbf{x}_i - b) \geq 1 - \xi_i, \quad \text{for } i = 1, 2, \ldots, N \tag{3.25}$$

With the inclusion of the slack variable, a feasible solution always exists [29]. If the value of the slack variable ξ_i is between 0 and 1, for any training data $\mathbf{x_i}$, the data is said to be correctly classified [29] (see Fig. 3.6). However, any data for which the value of $\xi_i \geq 1$, the data is said to be unclassified by the optimal hyperplane [29].

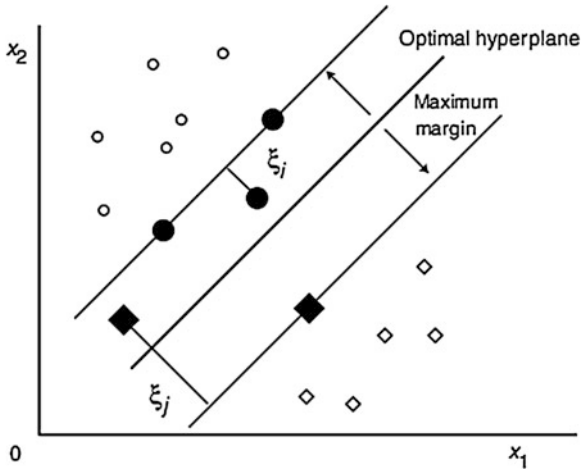

Fig. 3.6 Improved SVM classification using soft-margin method [29]

To obtain an optimal hyperplane, while reducing the number of unclassified points is the goal of a feasible SVM-based optimization approach. This optimization can be described as [27]:

$$\min_{\mathbf{w},\, b,\, \boldsymbol{\xi}} L(\mathbf{w},\ b,\ \boldsymbol{\xi}) = \frac{1}{2}\|\mathbf{w}\|^2 + C\sum_{i=1}^{N} \xi_i^p \tag{3.26}$$

$$\text{subject to:} \quad y_i(\mathbf{w}^{\mathbf{T}}\mathbf{x_i} + b) \geq 1 - \xi_i \text{ for } i = 1,\ 2, \ldots, N,$$

Where, $\boldsymbol{\xi} = (\xi_1, \ldots, \xi_N)^{\mathrm{T}}$ and C are margin parameters used as trade-off between the maximization of the separation margin and minimization of the classification error [29]. There are two variants of *soft-margin* SVM, namely *L1 soft-margin support vector machine* and *L2 soft-margin support vector machine* [29]. The L1 SVM uses $p = 1$ and L2 SVM uses $p = 2$ for the above mentioned SVM optimization problem [29]. This soft-margin SVM optimization problem can also be expressed in terms of non-negative *Lagrange* multipliers α_i and β_i as [29]:

$$L(\mathbf{w},\ b,\ \boldsymbol{\xi},\ \alpha,\ \beta) = \frac{1}{2}\|\mathbf{w}\|^2 + C\sum_{i=1}^{N} \xi_i - \sum_{i=1}^{N} \alpha_i(y_i(\mathbf{w}^{\mathbf{T}}\mathbf{x_i} + b) - 1 + \xi_i) - \sum_{i=1}^{N} \beta_i \xi_i \tag{3.27}$$

3.3.4 v-Support Vector Machines

The *v*-Support Vector Machine [30] is an improved form of the soft-margin SVM described in the previous section [26]. The soft-margin SVM described previously are also called *C*-SVM [31]. The *v*-SVM [30] includes two additional cost factors v and ρ [29]. The role of these two additional parameters is to improve the classification accuracy. The optimization problem for *v*-SVM can be expressed as [30, 32]:

$$\min_{\mathbf{w},\, b,\, \boldsymbol{\xi},\, \rho} \frac{1}{2}\|\mathbf{w}\|^2 - v\rho + \frac{1}{m}\sum_{i=1}^{m} \xi_i \tag{3.28}$$

$$\text{subject to:} \quad \mathrm{y_i}((\mathbf{w} \cdot \mathbf{x_i}) + b) \geq \rho - \xi_\mathrm{i}, \quad i = 1,\ 2, \ldots, m;$$
$$\xi_i \geq 0;\ \text{and}\ \rho \geq 0$$

The above optimization problem can be expressed in the dual form using the Lagrange multipliers as [32]:

$$L(\mathbf{w},\ \boldsymbol{\xi},\ b,\ \rho,\ \boldsymbol{\alpha},\ \boldsymbol{\beta},\ \delta) = \frac{1}{2}\|\mathbf{w}\|^2 - v\rho + \frac{1}{m}\sum_{i=1}^{m}\xi_i - \sum_{i=1}^{m}\left(\alpha_i(y_i(\mathbf{w}\cdot\mathbf{x_i}+b) - \rho + \xi_i) + \beta_i\xi_i - \delta\rho\right) \tag{3.29}$$

Some variants of v-SVM have been described in [31, 33, 34].

3.3.5 Nonlinear Support Vector Machines

The various forms of SVM classification and optimization methods presented so far in this chapter are related to *linearly separable or non-separable* data sets. In many real-life applications, the data set may not be linearly separable, especially due to the effects of measurement errors and noise [35]. To accurately classify data sets that are nonlinear, the training data sets are mapped onto higher (or infinite) dimensional space called *feature space* (Hilbert Space or Inner Product Space). The intuition of mapping data sets into higher dimensional space is that data can be clearly separated and hence better classified in higher dimensional space as illustrated in Fig. 3.7.

SVM optimization for the data sets that are not linearly separable can be carried out simply by mapping each feature vector $\mathbf{x}$ with a mapping function such that $\mathbf{x} \mapsto \varphi(\mathbf{x})$ and then carrying out the SVM optimization described in the previous sections [36]. For a set of training samples $T = \{(\mathbf{x}_1, \mathrm{y}_1), (\mathbf{x}_2, \mathrm{y}_2), \ldots, (\mathbf{x}_\mathrm{n}, \mathrm{y}_\mathrm{n})\}$, where $\mathbf{x}$ is an d-dimensional feature vector, the mapping of the training data set T is expressed in the feature space as:

$$\varphi(T) = \{(\varphi(\mathbf{x_1}), y_1), (\varphi(\mathbf{x_2}), y_2), \ldots, (\varphi(\mathbf{x_n}), y_n)\} \tag{3.30}$$

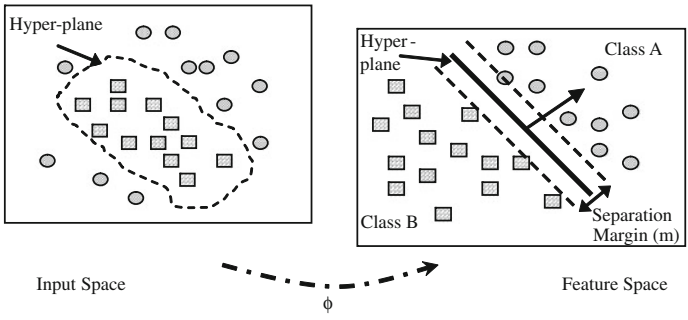

Fig. 3.7 Mapping of nonlinearly separable data sets into higher dimensional feature space

Hence, the decision function $D(\mathbf{x_k})$ for the prediction of the output can be given as [35]:

$$D(\mathbf{x_k}) = \text{sign}[\mathbf{w} \cdot \varphi(\mathbf{x_k}) + b] = \text{sign}\left(\sum_{i=1}^{n} \alpha_i y_i \varphi(\mathbf{x_i}) \cdot \varphi(\mathbf{x_k}) + b\right) \tag{3.31}$$

3.3.6 Kernel Trick

Kernel Trick involves the use of a kernel function to map input features into higher dimensional feature space. A kernel function can be expressed as [35]:

$$\kappa(\mathbf{x_i}, \mathbf{x_j}) = \varphi(\mathbf{x_i}) \cdot \varphi(\mathbf{x_j}) \tag{3.32}$$

Any kernel function following Mercer's conditions [25] represents an inner product in feature space [35].

$$\kappa(\mathbf{x_i}, \mathbf{x_j}) = \sum_{k}^{\infty} a_k \varphi_k(\mathbf{x_i}) \varphi_k(\mathbf{x_j}) \quad \text{for, } a_k \geq 0 \tag{3.33}$$

and

$$\iint \kappa(\mathbf{x_i}, \mathbf{x_j}) g(\mathbf{x_i}) g(\mathbf{x_j}) d\mathbf{x_i} d\mathbf{x_j} > 0 \tag{3.34}$$

There are numerous kernel functions available to map data points from input space into feature space. The four most popular kernel functions are listed below [35, 37].

Linear Kernel [35]:

$$\kappa(\mathbf{x_i}, \mathbf{x_j}) = \mathbf{x_i} \cdot \mathbf{x_j} \tag{3.35}$$

Polynomial Kernel [35, 38]:

$$\kappa(\mathbf{x_i}, \mathbf{x_j}) = (\gamma(\mathbf{x_i} \cdot \mathbf{x_j}) + r)^d, \quad \gamma > 0 \tag{3.36}$$

Radial Basis Function (RBF) Kernel [38]:

$$\kappa(\mathbf{x_i}, \mathbf{x_j}) = \exp(-\gamma \left\| \mathbf{x_i} - \mathbf{x_j} \right\|^2), \quad \gamma > 0 \tag{3.37}$$

Sigmoid Kernel [38]:

$$\kappa(\mathbf{x_i}, \mathbf{x_j}) = \tanh(\gamma(\mathbf{x_i} \cdot \mathbf{x_j}) + r), \quad \gamma > 0 \tag{3.38}$$

where, γ, r, and d are kernel parameters.

The selection process for a kernel function suitable for a particular application has been described in [39].

References

1. Pharr M, Humphreys G (2004) Sampling and reconstruction. Physically based rendering: from theory to implementation. Elsevier/Morgan Kaufmann, Amsterdam, pp 279–367
2. Hayes MH (1999) Sampling. Schaum's outline of theory and problems of digital signal processing. McGraw Hill, New York, pp 101–141
3. Blum A, Langley P (1997) Selection of relevant features and examples in machine learning. Artif Intell 97:245–271
4. Bousquet O, von Luxburg U, Rätsch G (2004) Machine learning summer school. In: O. Bousquet, U. von Luxburg, G. Rätsch (eds) Advanced lectures on machine learning: ML summer schools 2003, Canberra, Australia, February 2–14, 2003, Tübingen, Germany, August 4–16, 2003: revised lectures. Springer, Berlin
5. Diniz PSR (2006) Adaptive filtering: algorithms and practical implementation. Springer, New York
6. Trunk GV (1979) A problem of dimensionality: a simple example. Pattern Anal Mach Intell PAMI-1(3):306–307
7. Ahmed N, Natarajan T, Rao KR (1974) Discrete cosine transform, IEEE Trans Comput 23(1):90–93
8. Brigham EO (1988) The fast Fourier transform and its applications. Prentice Hall, Englewood Cliffs
9. Zonst AE (1995) Understanding the FFT: a tutorial on the algorithm and software for laymen, students, technicians and working engineers. Citrus Press, Titusville
10. Oklobdzija VG (2002) The computer engineering handbook. CRC Press, Boca Raton
11. Pennebaker WB, Mitchell JL (1992) JPEG still image data compression standard. Van Nostrand Reinhold, New York
12. Salomon D, Bryant D, Motta G (2007) Data compression: the complete reference. Springer, London
13. Theodoridis S, Koutroumbas K (2003) The discrete cosine and sine transforms. Pattern recognition, 2nd edn. Elsevier Academic Press, San Diego, pp 230–231
14. Jain AK (1989) Fundamentals of digital image processing. Prentice Hall, Englewood Cliffs
15. Nixon MS, Aguado AS (2002) Discrete cosine transform. Feature extraction and image processing. Newnes, Oxford, pp 57–58
16. Mallat SG (1999) A wavelet tour of signal processing. Academic Press, San Diego
17. Misiti M, Misiti Y, Oppenheim G, Poggi J-M (2009) Discrete wavelet transform. Wavelet toolbox 4—users guide. MathWorks 1:24–28
18. Demuth H, Beale M, Hagan M (2008) Neural network toolbox 6—users guide. MathWorks 9(4):259–265
19. Lloyd S (1982) Least squares quantization in PCM. IEEE Trans on Inf Theory 28(2):129–137
20. Bezdek JC (1973) Fuzzy mathematics in pattern classification. Applied Mathematics Center, Cornell University, Ithaca
21. Kohonen T (1989) Self-organization and associative memory. Springer, New York
22. Rumelhart DE, Zipser D (1986) Feature discovery by competitive learning. Parallel distributed processing. MIT Press, Cambridge, pp 151–193
23. Hruschka H, Natter M (1999) Comparing performance of feed forward neural nets and K-means for cluster-based market segmentation. Eur J Oper Res 114(2):346–353
24. Shavers C, Li R, Lebby G (2006) An SVM-based approach to face detection. In: Proceeding of the thirty-eighth southeastern symposium on system theory
25. Vapnik VN (1995) The nature of statistical learning theory. Springer, New York
26. Hu YH, Hwang J-N (2002) Handbook of neural network signal processing. CRC Press, Boca Raton
27. Vapnik V (1999) An overview of statistical learning theory. IEEE Trans Neural Netw 10(5):988–1000
28. Cortes C, Vapnik V (2005) Support-vector networks. Mach Learn 20(3):273–297

29. Abe S (2005) Two-class support vector machines. Support vector machines for pattern classification. Springer, London, pp 15–82
30. Schölkopf B, Smola A, Williamson R, Bartlett, P (2000) New support vector algorithms. Neural Comput 12(5):1207–1245
31. Chang C-C, Lin C-J (2001) Training v-support vector classifiers: theory and algorithms. Neural Comput 13(9):2119–2147
32. Chen P, Lin C-J, Schölkopf B (2005) A tutorial on v-support vector machines. Appl Stoch Models Bus Ind 21(2):111–136
33. Davenport MA (2005) The 2nu-SVM: a cost-sensitive extension of the nu-SVM. Journal [serial on the Internet]. http://dspace.rice.edu/handle/1911/19831
34. Jia Y-S, Jia C-Y, Qi, H-W (eds) (2005) A new nu-support vector machine for training sets with duplicate samples. In: 2005 international conference on machine learning and cybernetics, Guangzhou, 18–21 Aug
35. Ivanciuc O (2007) Applications of support vector machines in chemistry. Rev Comput Chem 23:291–400
36. Schölkopf B, Smola AJ (2002) Learning with kernels: support vector machines, regularization, optimization, and beyond. MIT Press, Cambridge
37. Abe S (2005) Support vector machines for pattern classification. In: Singh S (ed) Springer, London
38. Hsu C-W, Chang C-C, Lin C-J (2008) A practical guide to support vector classification
39. Ikeda K (2006) Effects of kernel function on Nu support vector machines in extreme cases. IEEE Trans Neural Netw (a publication of the IEEE Neural Networks Council) 17(1):1–9

Chapter 4
Methodology and Experimental Program

4.1 Overview

This chapter discusses the characteristics of the ultrasonic sensor signal obtained from a fuel level sensor under dynamic conditions and describes a methodology to be used to develop a fluid level measurement system that compensates for the effects of a dynamic environment. This involves using an intelligent signal classification approach based on support vector machines. This chapter also describes the signal filtration functions that will be implemented to enhance the performance of the SVM-based signal classification system.

4.2 Ultrasonics-Based Level Sensing

The output of ultrasonic sensors is normally a continuous voltage signal over time. The voltage signal is the representation of the fluid level measured by the sensor. The range, resolution, and the linearity of the output signal could be different from one type of ultrasonic sensor to another. The sensor signal representing the fluid level is illustrated in Fig. 4.1.

If L is the height of the tank, where the ultrasonic sensor has been mounted at the top of the tank, and v is its represented level in voltage, assuming the sensor response to be linear, the resolution can be given as:

$$\text{Resolution} = \frac{\Delta L}{\Delta v} \text{ metre per volt} \tag{4.1}$$

The ultrasonic sensor mounted at the top of the tank will detect the maximum level when the time-of-flight of the ultrasonic echo will be least. At the maximum level, the voltage output from the ultrasonic sensor will also be at maximum. Likewise, the minimum level will be detected when the time-of-flight of the ultrasonic echo will be the most.

J. Terzic et al., *Ultrasonic Fluid Quantity Measurement in Dynamic Vehicular Applications*, DOI: 10.1007/978-3-319-00633-8_4,
© Springer International Publishing Switzerland 2013

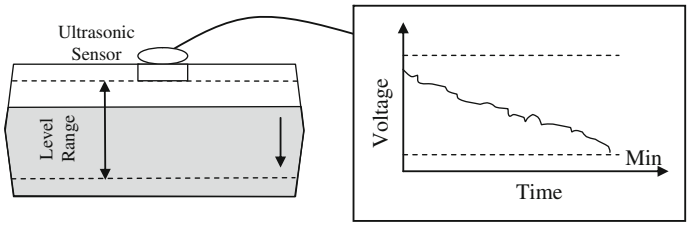

Fig. 4.1 Ultrasonic sensor signal representing fluid level in voltage

4.3 Sensor Response Under Slosh Conditions

Slosh waves will be produced in a tank filled with liquid when an external force is applied to it. The ultrasonic sensor with short response time will produce a corresponding signal at the output, which will reflect the same waveform that was exhibited in the tank. If the ultrasonic sensor can produce instantaneous readings of the fluid level in the form of electrical voltage, a replica of these slosh waves will be observed on the oscilloscope attached to the ultrasonic sensor. Figure 4.2 shows the output of the ultrasonic sensor reading that might be seen on an oscilloscope under both static and dynamic conditions. Figure 4.2a shows that the sensor response is fairly constant under static condition; Fig. 4.2b shows that the sensor response produces a replica of the actual slosh waves.

As the fluid fluctuates (see Fig. 4.3), the sensor output produces a replica of the slosh waves that contains the following two components:

- Oscillating wave, and
- Bias shift

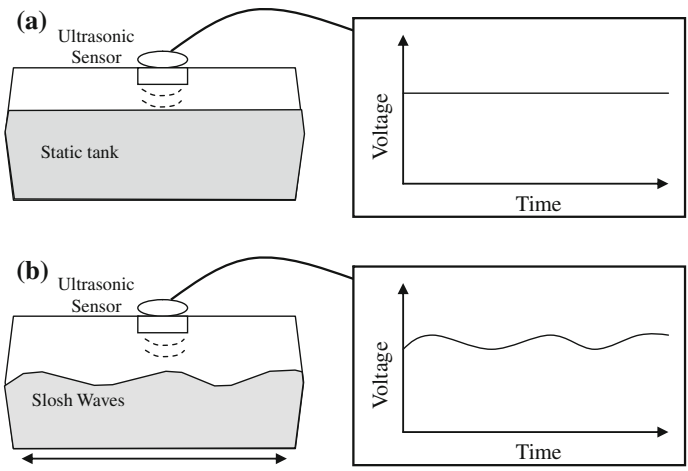

Fig. 4.2 Sensor response under static and dynamic conditions. **a** Tank remains static. **b** Tank movement is produced

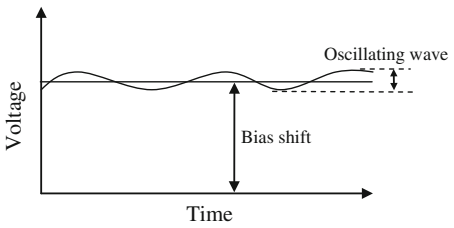

Fig. 4.3 Two components of the slosh wave

The frequency response of the oscillating slosh waves can be observed by transforming the ultrasonic signal into the frequency domain. Fast Fourier Transform (FFT) function can be used to obtain the frequency coefficients. The magnitude of these frequency coefficients and the median value (bias shift) can be used to describe the slosh pattern that exists in the fluid container. These signal characteristics can be processed through a support vector machine (SVM)-based classification system to eliminate the effects of dynamic slosh. Additionally, along with the frequency coefficients and bias shift, temperature values could also be processed through the SVM to eliminate their effects on signal measurement accuracy.

4.4 Design of Methodology

The observation and analysis of the slosh pattern produced under the effects of acceleration in a closed container, instigated an approach that can eliminate the sloshing effects, whereby accurate fluid level measurements would be possible in dynamic environments. If the fluid quantity in a storage container remains constant, the instantaneous fluid level in a dynamic environment can be defined as:

$$L(t) = L_0 \cdot f \tag{4.2}$$

where L_0 is the tank level under static conditions, and f is the unknown sloshing function that depends on the acceleration effects exhibited on the tank, the existing fluid level, and the tank geometry. The goal is focused on determining the existing fluid level L_0 using the sensor output $L(t)$ and the function f.

The output of the fluid level sensor is observed to have a direct relationship with the vehicle acceleration when observed in a running vehicle, as shown in Fig. 4.4. The knowledge of the relationship between acceleration and the output $L(t)$ can eliminate the sloshing effects, however, with the knowledge of the sloshing function f.

$$L_0 = \frac{L(t)}{f} = \text{constant} \tag{4.3}$$

The unknown function f is solved by experimentation with the aid of an SVM-based approach. An SVM model is constructed and trained with the actual driving data obtained through several field trials. Figure 4.5 demonstrates the method to be adopted to develop the accurate fluid level measurement system.

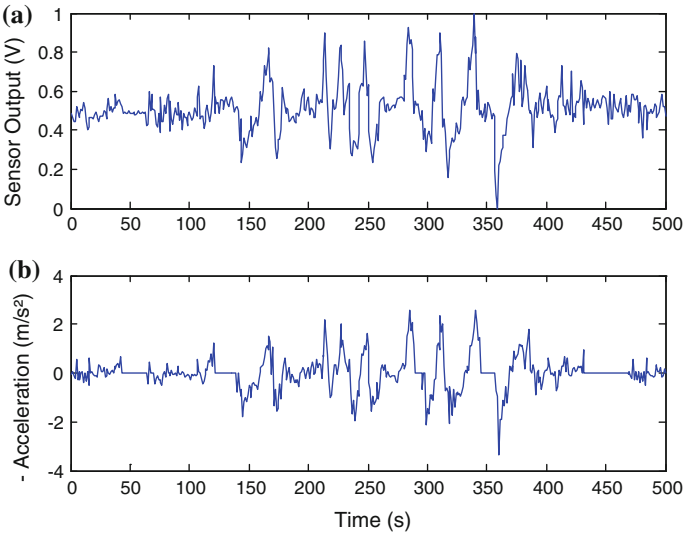

Fig. 4.4 Vehicle acceleration and the raw sensor signal. **a** Raw Sensor Signal **b** Inverted Vehicle Acceleration

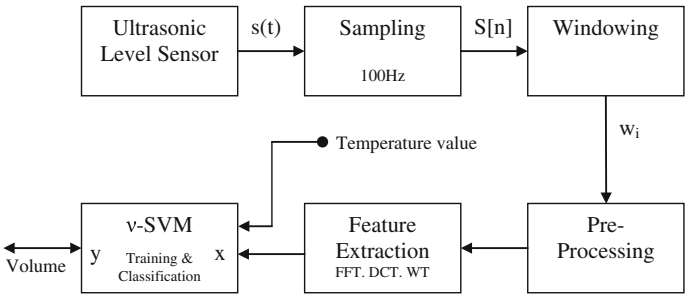

Fig. 4.5 Block diagram of the proposed system

For the ultrasonic transducer mounted at height $\text{level}_{\text{ref}}$ on top of the tank, the instantaneous output of the ultrasonic level sensor at time t and temperature T can be given as [1]:

$$\text{Level}(t, T) = \text{level}_{\text{ref}} - \frac{\tau(t)}{2} v(T) \tag{4.4}$$

where $\tau(t)$ is the time-of-flight at instant t of the ultrasonic echo, and $v(T)$ is the speed of ultrasonic echo at temperature T. The expression $v(T)$ can be obtained using Eq. (1.2).

In a dynamic environment, the term $\tau(t)$ will exhibit variation that reflects an inverted image of the slosh wave produced in the liquid tank. The term $\tau(t)$ will be

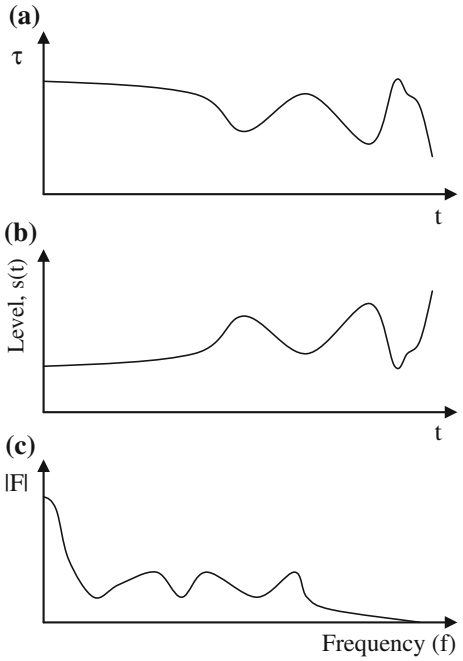

Fig. 4.6 Illustration of **a** the time-of-flight signal, **b** the exhibited slosh wave, and **c** the frequency spectrum of the level signal

inverted since the ultrasonic sensor is facing down measuring time-of-flight of the ultrasonic echo from the top of the tank. The expression $\frac{\Delta\tau}{\Delta t}$ will vary over time in a dynamic environment; however, under static conditions, the expression $\frac{\Delta\tau}{\Delta t}$ will be equal to zero. Figure 4.6 shows the variation in $\tau(t)$ and the actual slosh wave produced in the liquid tank.

The ultrasonic level sensor signal, denoted as $s(t)$, is typically a voltage signal in the range of 0.5–4.5 V, which represents the minimum and maximum of the level range, respectively. A more detailed description of the methodology is provided in Chap. 5. The sensor signal $s(t)$ is sampled at 100 Hz. The sampled signal is accumulated in a $\acute{\omega}$ second window frame (w_i). The optimal value of $\acute{\omega}$ will be determined by experimentation as described in Chap. 5. After collecting the sensor data over $\acute{\omega}$ seconds, the $\acute{\omega}$ second data is filtered using the investigated filters. Then the signal features are extracted using the three feature extraction methods FFT, DCT, and WT. The performance and influence of these three feature extraction functions will be investigated to determine the optimal feature extraction method for the SVM-based fuel level measurement system. The coefficients (coef) obtained from the feature extraction functions, the median value (med) of the $\acute{\omega}$–second ultrasonic sensor signal, and the temperature readings T are all contained in a vector forming *input features* for the SVM model. The SVM input vector $\mathbf{x_i}$ can be represented as:

$$\mathbf{x_i} = \{\text{coef}_1, \text{coef}_2, \ldots, \text{coef}_n, \text{med}, T\} \tag{4.5}$$

4.5 Feature Selection and Reduction

Signal feature extraction, selection, and reduction play an important role in signal classification systems. An introduction to feature extraction was given in Sect. 3.2.4. Improper format of input signals to the classifier can result in a poorly constructed classification problem. Trunk [2] has demonstrated that some training data can be detrimental to classification, especially if the data is highly correlated [3]. Apart from the correlation of data, the size of input feature data is also important in signal classification systems. An increase of the input feature dimension ultimately causes a decrease in performance [4]. Hence, the correlation of the input data and the number of input features will be investigated during the development of the SVM-based classification system.

The process of choosing a subset of the features is referred as 'feature selection', and the process of finding a good combination of the features is known as 'feature reduction' [5]. The goal of feature selection and reduction in signal preprocessing is to choose a subset of features or some combination of the input features that will best represent the data [5]. According to Yom-Tov [5], finding the best subset of features by testing all possible combinations is practically impossible even when the number of input features is modest. For example, to test all possible combinations of the input data with 100 input features will require testing 10^{30} combinations [5].

According to Richards et al. [6], feature reduction can be effectively performed by transforming the data to a new set of axes in which separability is higher in a subset of the transformed features than in any subset of the original data [6]. Therefore, in the ultrasonic type fluid level system, the raw time-based level signals will be converted into the frequency domain using the Fast Fourier Transform (FFT) function described in Sect. 3.2.4. By carrying out the Fourier Transformation, the raw signal contents that will be used as inputs will be represented by frequency coefficients. Figure 4.7 shows the example of the raw time-domain signal from the ultrasonic sensor over 60 s, and the frequency response of the same signal obtained using the FFT function. The frequency spectrum of the raw sensor signal under the influence of slosh describes the fluctuations or slosh frequencies in the fuel tank. Here in Fig. 4.7, the fuel tank was sliding linearly back and forth at a fixed cycle of 0.8 Hz. The frequency spectrum shown in Fig. 4.7 displays two large spikes at 0.4 and 0.8 Hz, which represent two harmonics waves of the slosh.

According to Richards et al. [6], features which do not aid discrimination, by contributing little to the separability of spectral classes, should be discarded. Richards et al. [6] describe feature selection as the process in which the least effective features are removed. Feature selection methods can be divided into three main types [2]:

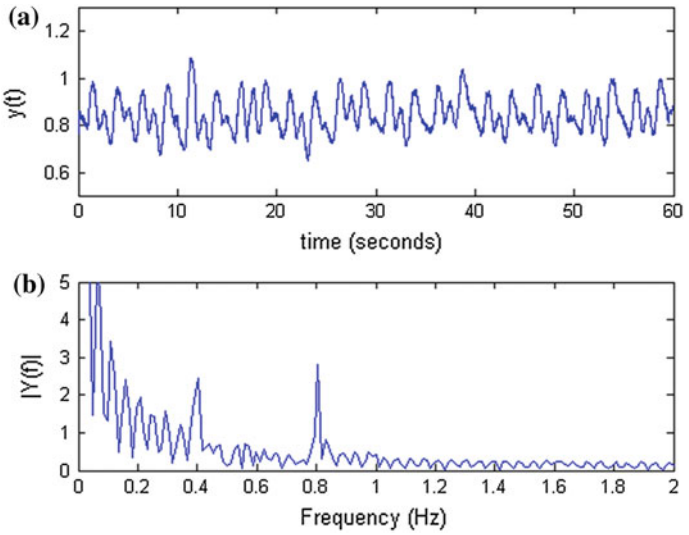

Fig. 4.7 Feature extraction using FFT function **a** Raw signal at various Slosh. **b** FFT of the raw sensor signal y(t)

1. *Wrapper methods:* The feature selection is performed around (and with) a given classification algorithm. The classification algorithm is used for ranking possible feature combinations.
2. *Embedded methods:* The feature selection is embedded within the classification algorithm.
3. *Filter methods:* Features are selected for classification independently of the classification algorithm.

In the proposed ultrasonic type fluid level measurement system, the filtration method is used to perform feature selection because this is the method that is independent of the classification algorithm.

After transforming the time-based sensor signal into the frequency spectrum, the less relevant portion of frequencies mainly consisting of low-amplitude noise is omitted. To determine the range of frequencies that may be exhibited in the fuel tank, a 60 km test drive was carried out in a suburban area, where occasional stops were made. Figure 4.8a shows the typical range of slosh frequencies observed in the vehicular fuel tank using the ultrasonic type level sensor during a 60 km test drive. A close view of the 0–2 Hz slosh frequency range is shown in Fig. 4.8b. By using a low-pass filter, frequencies higher than the normal range of slosh frequency (especially noise) can be removed.

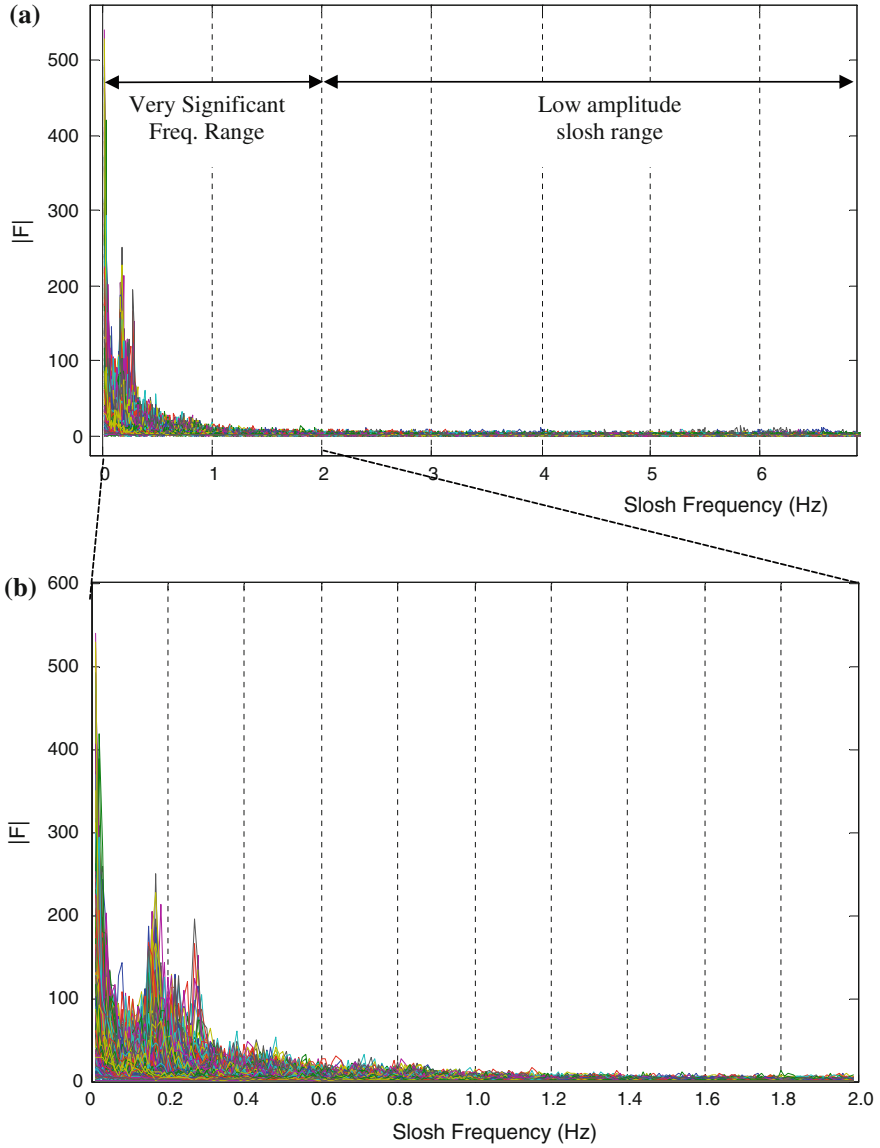

Fig. 4.8 Typical range of slosh frequency in the fuel tank during normal driving

4.6 Signal Smoothing

In the signal smoothing process, the raw signal is filtered to remove the signal noise by smoothening it with the three investigated methods: moving mean, moving median, and wavelet transform. A raw signal over $\acute{\omega}$-second is passed

through the investigated filters, where $\acute{\omega}$ is the length of time in second of the collected raw signal. The moving mean and moving median filters slide across the raw signal and calculate the mean/median values in the neighboring sampled points. If **x** is the sampled raw signal of N length, and w is size of the moving window, then the filtered output y using mean and median can be obtained using Eqs. (4.6) and (4.7), respectively. The width of the moving window w will be determined by experimentation (Chap. 5). The sliding window (moving window) function takes w samples of the raw signal and produces a *mean* or *median* value at the output.

$$\begin{aligned} y[i] &= \text{mean}(x[i-1], x[i-2], \ldots, x[i-w]),\ w \le i \le N \\ y[i] &= \text{mean}(x[1], x[2], \ldots, x[i]),\ \text{ for } 1 \le i < w \end{aligned} \tag{4.6}$$

$$\begin{aligned} y[i] &= \text{median}(x[i-1], x[i-2], \ldots, x[i-w]),\ w \le i \le N \\ y[i] &= \text{median}(x[1], x[2], \ldots, x[i]),\ \text{ for } 1 \le i < w \end{aligned} \tag{4.7}$$

The value of N for a signal frame of $\acute{\omega}$–second at 100 Hz is calculated as:

$$N = 100 \text{ samples/s } \times \breve{\omega}\, s = 100\, \breve{\omega} \text{ samples} \tag{4.8}$$

Figure 4.9 illustrates the *moving mean* and *moving median* filters when applied to the raw signal data. As the moving window slides across the 20 second ($\breve{\omega} = 20$) long raw signal, mean/median functions are applied to the raw signal values within the window range and a smooth signal is produced. The filtered versions of the raw signal using both filters do not contain high-frequency noise.

Another filter investigated is the Wavelet Transform (WT) filter that analyzes signals at different frequency bands by decomposing them into coarse information and detailed information sets. The coarse information set contains the low frequencies, whereas, the detailed information set contains the high frequencies of the input signal. Only the low-frequency components, which reflect a smoothened version of the raw signal are used, and the high-frequency components of the raw signal, which usually contain noise, are eliminated. Hence, a smooth signal is produced using the wavelet transform function, as shown in Fig. 4.10. The wavelet transformation is processed through MATLAB using *dwt* [7] function with Daubechies [8] Wavelet (*db1*).

Figure 4.10 shows the high-frequency signal (b) and the low-pass filtered signal (c) when the raw sensor signal (a) is processed with the discrete wavelet transform (DWT) function.

All filtered signals using the investigated filtration methods are transformed into the frequency domain and the frequency coefficients are obtained, which are then fed into the SVM-based signal processing system.

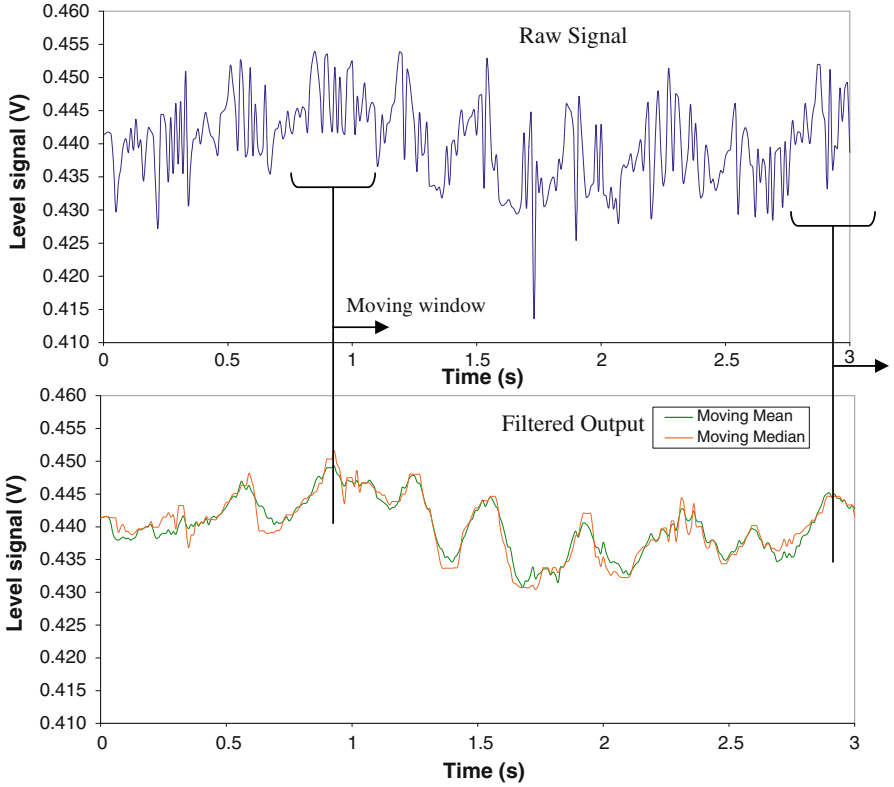

Fig. 4.9 Illustration of the moving mean and moving median filters

4.7 Influential Factors Analysis

An analysis of the influential factors will be carried out before the development of the SVM-based ultrasonic signal processing system. In the influential factors analysis, the effects and interaction between the influential factors will be studied by observing the response of the ultrasonic sensor. It was proposed in Chap. 2 that the main factors influencing the accuracy of the measurement system are: slosh, temperature, and contamination. Therefore, the results from the factors analysis experiment will provide better measures of the magnitude of the effects that these three influential factors may contribute to the response of the ultrasonic sensor output. According to Dean et al. [9], it is more efficient to examine all possible causes of variation simultaneously rather than one at a time. Therefore, all three influential factors will be simultaneously analyzed by developing a two-level (2^n) factorial design experiment. Factorial experiments include all possible combinations of factor–level in the experimental design [10]. Detailed information on the factorial design is given in Sect. 5.5.2.

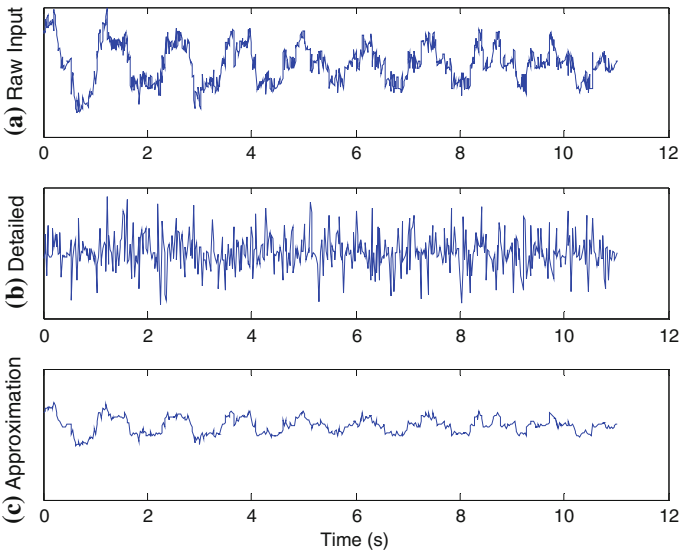

Fig. 4.10 Wavelet filter applied on the raw signal

Factorial experiments provide an opportunity to study not only the individual effects of each factor but also their interactions [11]. The results obtained from the factorial analysis experiment will be used to generate main effects plots and interaction plots of the three main influential factors. Main effects plot provides detailed information on the influence of each influential factor on the response of the ultrasonic sensor output. The interaction plots provide details of interaction that may be found between the influential factors. The main effects plots and interaction plots will provide a better understanding of the impact the three influential factors have on the ultrasonic sensor output. These plots will be generated with Minitab software [12]. According to Bass et al. [13], The Minitab software suit is widely used in many corporations and universities [13]. Minitab is a very sophisticated and easy to use software, which has also been adopted by most Six Sigma practitioners as a preferred tool [14].

References

1. Pedersen TO, Karlsson N (1999) Time-of-flight ultrasonic displacement sensors. In: Webster JG (ed) The measurement, instrumentation, and sensors handbook. CRC Press LLC, Boca Raton, pp 6, 92–98
2. Blum A, Langley P (1997) Selection of relevant features and examples in machine learning. Artif Intell 97:245–271
3. Bousquet O, von Luxburg U, Rätsch G Machine Learning Summer School (2004) Advanced lectures on machine learning: ML Summer Schools 2003, Canberra, Australia, 2–14 Feb

2003, Tübingen, Germany, 4–16 Aug 2003: revised lectures/Olivier Bousquet, Ulrike von Luxburg, Gunnar Rätsch (eds). Springer Berlin; New York
4. van der Heijden F, Duin RPW, de Ridder D, Tax DMJ (2004) Feature extraction and selection. classification, parameter estimation, and state estimation: an engineering approach using MATLAB. Wiley, Chichester, pp 183–214
5. Yom-Tov E (2004) An introduction to pattern classification. In: Bousquet O, von Luxburg U, Rätsch G, School, Machine Learning Summer (eds) Advanced lectures on machine learning: ML Summer Schools 2003, Canberra, Australia, 2–14 Feb 2003, Tübingen, Germany, 4–16 August 2003: revised lectures: Springer Berlin, New York, pp 1–20
6. Richards JA, Jia X (2006) Feature reduction. Remote sensing digital image analysis: an introduction, 4th edn. Springer, Berlin, pp 267–294
7. Misiti M, Misiti Y, Oppenheim G, Poggi J-M (2009) Wavelet toolbox 4—users guide. MathWorks
8. Daubechies I (ed) (1992) Ten lectures on wavelets. Society for Industrial and Applied Mathematics, Philadelphia
9. Dean A, Voss D (1999) Principles and techniques. Design and analysis of experiments. Springer, New York, pp 1–5
10. Mason RL, Gunst RF, Hess JL (2003) Factorial experiments in completely randomized designs. Statistical design and analysis of experiments: with applications to engineering and science. Wiley-Interscience, Hoboken, pp 140–160
11. Das MN, Giri NC (1987) Factorial experiments. Design and analysis of experiments. Halsted Press, New York, pp 98–159
12. MINITAB user's guide 2: data analysis and quality tools. Minitab Inc., State College
13. Bass I, Lawton B, NetLibrary, Inc. (2009) Lean six sigma using SigmaXL and Minitab. McGraw-Hill, New York
14. Bass I (2007) An overview of Minitab and Microsoft Excel. Six sigma statistics with Excel and Minitab. McGraw-Hill, New York, pp 23–40

Chapter 5
Experimentation

5.1 Overview

The implementation of the Support Vector Machine (SVM)-based ultrasonic signal classification system requires training samples of the system with actual data under various dynamic conditions. A detailed discussion of the experimental setup used for the research is provided in this section. There are three major experiments performed in this research. All experiments are carried out using a regular standard automobile fuel tank. The first experiment determines the influence of temperature, contamination, and sloshing factors. The second experiment determines the suitability and performance of different SVM kernel functions. Finally, extensive experimentation is carried out at a variety of different fuel levels in the tank. The data obtained from the third experiment will be used to train the SVM model having the Radial Basis Function (RBF), a widely used kernel function, while also applying the various signal filtration methods, namely, moving mean, moving median, and wavelet filters.

5.2 Methodology

These sets of experiments are performed in this research to study the effects of the influential factors, in order to develop and enhance the performance of the SVM-based fluid level measurement approach. The methodology used to run the experiments and validation plan is shown in Table 5.1 (Fig. 5.1).

Table 5.1 shows the overview of the experimental setup for the development and validation of the SVM-based fluid level measurement system. The experiments are configured into three discrete sections, which are labeled as *Experiment Set A*, *Experiment Set B*, and *Experiment Set C*. The overview and purpose of the three parts of the experimental program are given below. The detailed description of these three experiments will be provided later in this chapter.

J. Terzic et al., *Ultrasonic Fluid Quantity Measurement in Dynamic Vehicular Applications*, DOI: 10.1007/978-3-319-00633-8_5,
© Springer International Publishing Switzerland 2013

Table 5.1 Methodology of experiments with test conditions, constants, and output parameters

	Fluid levels tested	Test conditions	Test output parameters
Experiment Set A	40, 45, 50, 55 L	• Slosh • Temperature • Contamination	Ultrasonic sensor response without SVM
Experiment Set B	40, 45, 50, 55 L	• Slosh • Temperature • Kernel functions (Linear, Polynomial, RBF, Sigmoid)	Ultrasonic sensor response to slosh and temperature with different SVM kernels
Experiment Set C	5–9 L, 15, 20, 25, 30 L, 35–40 L, 45–50 L	• Slosh • RBF kernel • Signal filters (Moving mean, Moving Median, Wavelet)	Ultrasonic sensor response to slosh with RBF kernel and different filtration functions

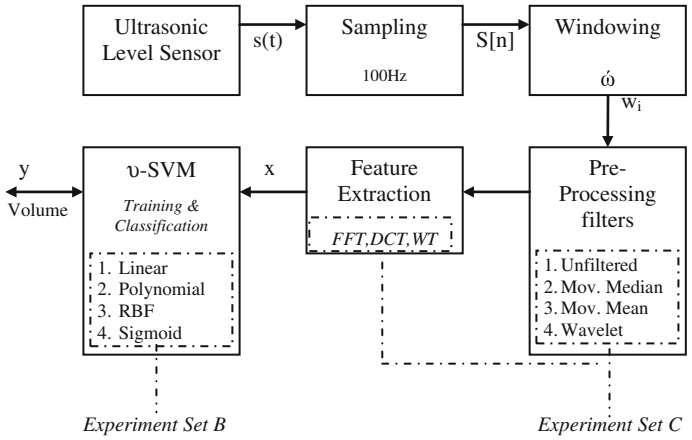

Fig. 5.1 Overview of the experimental methodology

Experiment Set A is performed to study the interaction and effects of the influential factors, which were perceived in Chap. 2 to be: *Slosh frequency, Temperature, and Contamination.* In order to fully comprehend the behavior of the ultrasonic sensor in a dynamic environment, it is important to determine the magnitude of the influence that the environmental factors contribute to the response of the ultrasonic sensor in a dynamic environment. Experiment Set A is designed with the Design of Experiments (DOE) methodology to observe main effects plots and interaction plots of the influential factors. To set the slosh factor, Experiment Set A is conducted on-site using a linear actuator (see Sect. 5.4.3).

The fuel tank filled with fluid is mounted on the linear actuator. The linear actuator is controlled with a digital timer, which could be configured to generate a particular slosh frequency in the liquid container. A heater is used to set the temperature factor. To observe the sensor response under contamination, Arizona dust sample of varying quantities are mixed in the fluid. The detailed description of Experiment Set A is given in Sect. 5.5.

Experiment Set B is performed to determine the most suitable SVM kernel function from a set of commonly used kernels. To compare the performance of different kernel functions under the influence of slosh, Experiment B is conducted in similar fashion to the Experiment Set A. However, the influence of contamination is ignored during Experiment Set B as the results from Experiment Set A did not show any influence of contamination on the sensor output (discussed Chap. 6). The slosh and temperature factors as demonstrated in Experiment Set A results (see Sect. 6.2) are observed to be the prominent factors affecting the accuracy of the measurement system. The primary focus of Experiment Set B is to examine the performance of the SVM-based signal classification system under sloshing and temperature varying conditions. The data obtained from Experiment Set B is used to develop and validate four SVM models, each with a different kernel function. The detailed description of Experiment Set B is given in Sect. 5.6.

Experiment Set C is carried out to understand the effectiveness of the SVM-based signal classification system using the slosh test data obtained from a running vehicle. The selection of the optimal parameters for the SVM-based system was performed in this experiment. The influence of signal filtration operations on the performance of the SVM-based system is also investigated. Signal filtration is performed on the raw sensor signals to enhance the performance of the SVM signal classification system. In contrast to Experiment Set A and Experiment Set B, which are both performed onsite on an experimental rig containing a linear actuator, the Experiment Set C is performed on the road during field trials to examine the performance of the SVM-based fluid level measurement system under actual driving conditions (i.e., dynamic environment). Extensive field trials are carried out for over 20 different tank levels in the automotive fuel tank. The fluid temperature and the slosh waves are generated within the fuel tank and recorded during the experiment. The data obtained from the field trials are used to train four SVM models incorporating a RBF kernel function but each using a different signal processing filter. The detailed description of Experiment Set C is given in Sect. 5.7.

5.3 Data Collection and Processing Methodology

The raw data obtained using experimentation from the ultrasonic type level sensor is processed using the methodology illustrated in Fig. 5.2.

The output from the ultrasonic type fluid level sensor is in the form of an analogous voltage signal. The amplitude of the sensor voltage signal denotes the

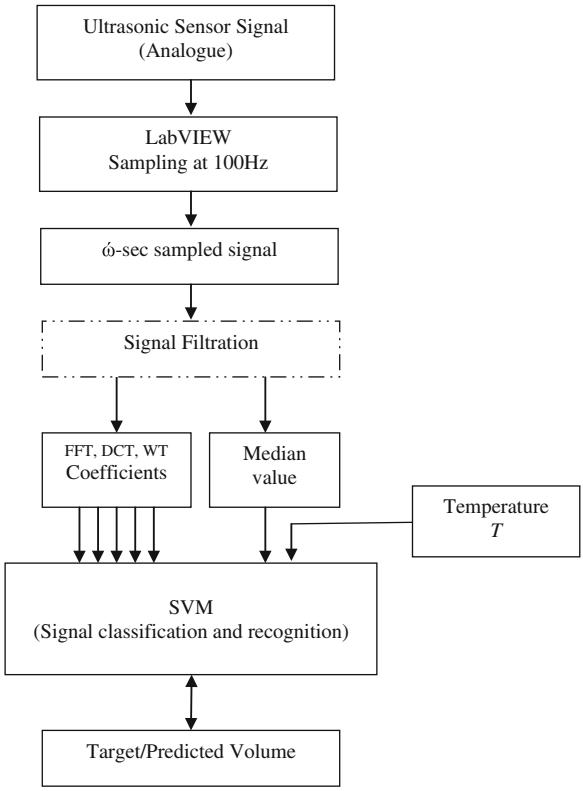

Fig. 5.2 Measurement system's signal processing block diagram

level of fluid contained in the tank. The sensor signal voltage linearly ranges from 0 V (empty) to 5 V (full). A detailed description of the ultrasonic level sensor used in the experiments is provided in Sect. 5.4.1. The level signal from the ultrasonic sensor is sampled at 100 Hz using the Data Acquisition Card in conjunction with the LabVIEW software program. The sampled signal is accumulated over $\acute{\omega}$ seconds, where $\acute{\omega}$ is the length of time of the sampled signal, and then the sampled signal is processed through the SVM classifier. In Experiment Set C, where the influence of signal filtration is examined, the accumulated sensor signal over $\acute{\omega}$ seconds is processed through a signal filtration function before processing the signal data through the SVM-based signal processing system. Feature extraction is performed on the signals prior to processing them through the SVM.

Statistical median function is used to calculate the middle value of the raw sampled signals. The median function provides the middle value as opposed to the mean function that provides average value. In Sect. 2.5.4, it was discussed that the downside of averaging is that it produces significant error for a momentarily large spike an abnormal data entry. Therefore, median value is used as the middle value or the bias value (refer Sect. 4.3) of the fluctuating fluid level (slosh wave).

The frequency coefficients, the median value of the sampled signal, and the temperature value from the temperature sensor are incorporated in the feature vector. The signal feature vector is then used as input to the SVM-based signal processing system for training and validation of the network. Signal processing and signal classification are both carried out using MATLAB and LIBSVM [1] software.

5.4 Apparatus and Equipment Used in the Experimental Program

The equipments used along with the assumptions made during the experiments are described in this section.

5.4.1 Ultrasonic Level Sensor

All experiments are performed using the SSI Technologies Fluid-Trac 3-Wire Level Sensor, which is shown in Fig. 5.3. Fluid-Trac 3 Wire Level Sensor is suitable of use in a variety of different liquids including gasoline and diesel (Table 5.2)

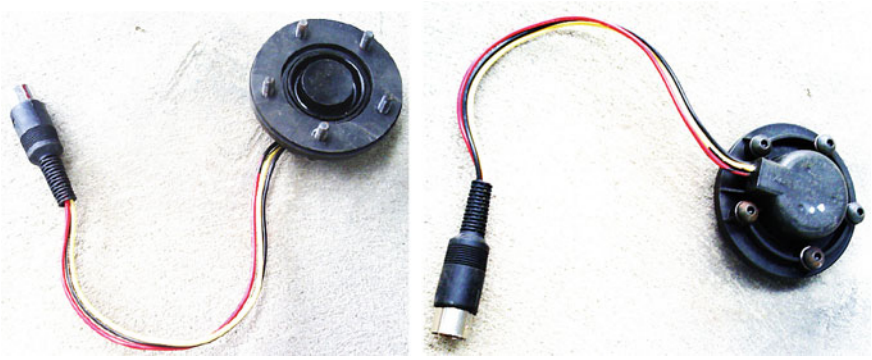

Fig. 5.3 Ultrasonic sensor used in the experiments

Table 5.2 Technical details of the ultrasonic transducer used in the experiments

Ultrasonic sensor specifications	
Accuracy	±0.32 cm
Output	0.5–4.5 V (min–max)
Resolution	0.18 cm
Operating temperature	−40 to 80 °C
Designed for gasoline and diesel liquids	

Fig. 5.4 Utility tank used in the experiments

The output of the sensor is a continuous voltage signal in the range of 0.5–4.5 V. The sensor uses the three wire connector, where two wires are used to power it and the third wire outputs the signal voltage.

5.4.2 Fuel Tank

The fuel tank used in all the experiments has a storage capacity of 70 L. The fuel tank originally belonged to the utility vehicle (Ute). The tank can be approximated as a rectangular cubicle with dimensions 34 × 34 × 81 cm. The ultrasonic sensor is mounted on top of the tank. Figure 5.4 shows the fuel tank properly fitted on linear actuator (refer to Sect. 5.4.3) (Fig. 5.5).

The fuel tank is filled with Exxsol D-40 Stoddard solvent. Exxsol is the brand name of Exxon Mobil Corporation. Exxsol solvents are a series of dearomatized

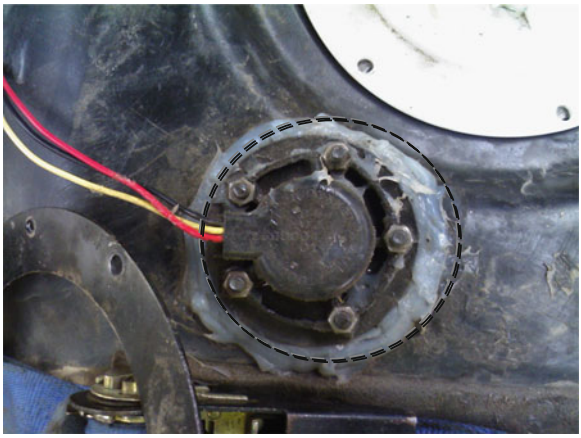

Fig. 5.5 A close view of ultrasonic sensor mounted on the fuel tank

aliphatic hydrocarbons [2], where typical Aromatic content is below 1 %. These fluids maintain good solvency characteristics for many applications. Exxon describes the Occupational Exposure Limit (OEL) of the Exxsol fluids as relatively high, because of this advantage they often serve as replacements for more conventional solvents that might not meet health or environmental regulations. Heavier Exxsol D grades have boiling ranges between 140° and 310° C [3]. The Exxsol D-40 has the same properties as gasoline fluids but it is relatively safe for industrial usage. Therefore, Exxsol D-40 fluid is used in the experimentations. The detailed specifications of the Exxsol D-40 solvent are provided in Appendix B.

5.4.3 Linear Actuator

The linear actuator used to run the slosh tests is shown in Figs. 5.6 and 5.7. The figures show the actuator and the frame body on which the fuel tank is mounted.

The pneumatic actuator is run by compressed air to slide the tank back and forth. The linear actuator is controlled by a Programmable Logic Controller (PLC) Timing Unit, which is shown in Fig. 5.7. As the linear actuator moved back and forth, slosh waves are created and observed in the fuel tank. The back and forward strike of the actuator can be controlled by setting the timer value of the PLC Timer. The PLC Timer actuates (fires) air pressure through the Actuator Controller Cables (highlighted in Fig. 5.7). The fire timing can be easily set by using the keypad located inside the PLC Timer Box.

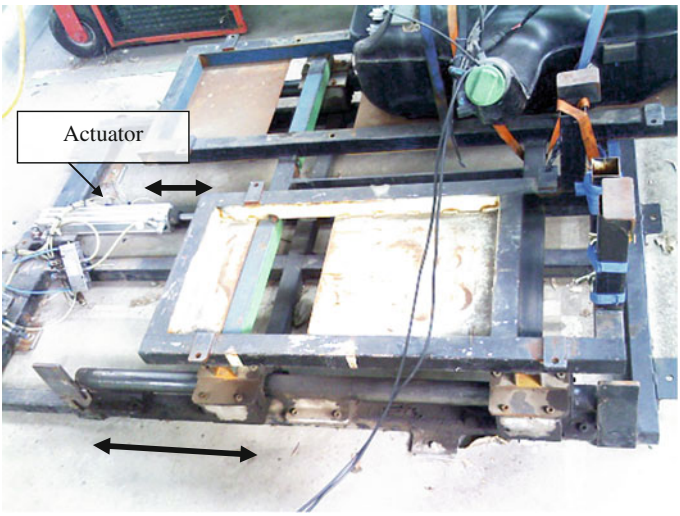

Fig. 5.6 Linear actuator used for creating slosh

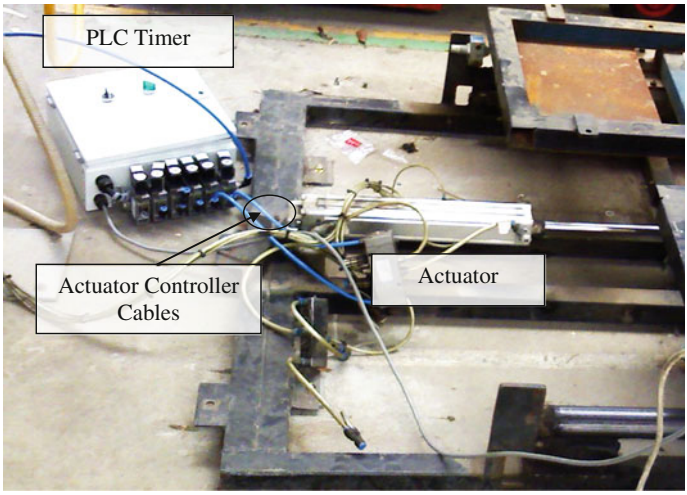

Fig. 5.7 Linear actuator showing PLC timer and linear actuator

5.4.4 Heater

To observe the effects of temperature variations on the sensor response, the heating chamber is used to heat up the fuel in some parts of the experiments.

5.4.5 Arizona Dust

Arizona dust is used as the impurity substance in experiments to test the performance of the ultrasonic sensor under the influence of small dust particles. The response of the ultrasonic sensor output is observed before and after the introduction of Arizona dust samples.

5.4.6 Signal Acquisition Card

All signals from the ultrasonic sensor are acquired and stored on the computer using the National Instruments Data Acquisition Card (DAQ card) and the LabVIEW software. The signal acquisition board and the power source are shown in the Figs. 5.8 and 5.9. The power supply box is sourced by the AC mains to provide the 12 V DC output for the ultrasonic sensor.

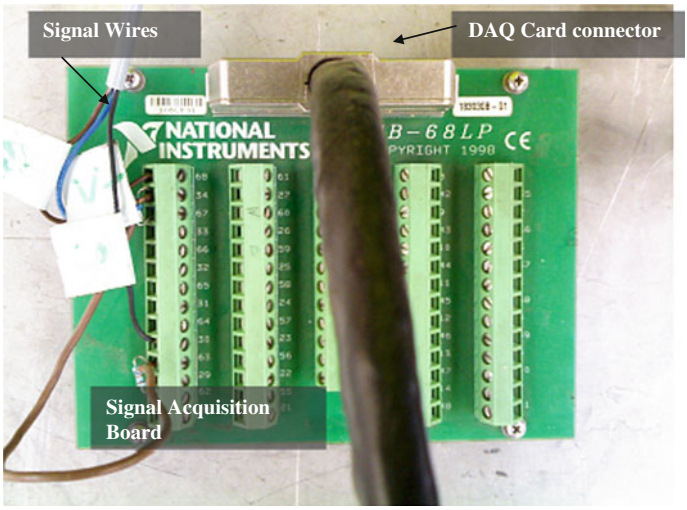

Fig. 5.8 Signal acquisition board

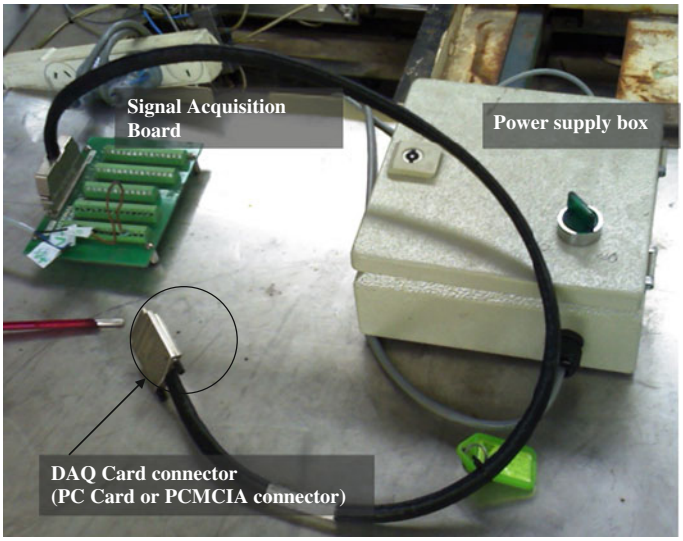

Fig. 5.9 Power supply used to power the ultrasonic sensor

5.5 Experiment Set A: Study of the Influential Factors

5.5.1 Overview

The purpose of running *Experiment Set A* is to study the magnitude of the interaction and the effects of the influential factors that were perceived in Chap. 2 to be: *Slosh frequency, Temperature, and Contamination.* In order to fully comprehend the behavior of the ultrasonic sensor in a dynamic environment, it is important to determine the magnitude of the influence that the environmental factors contribute to the response of the ultrasonic sensor in this environment.

5.5.2 Factorial Design

Experiment Set A is performed to understand the interactions between the three main influential factors and the magnitude of the effects that these factors have on the ultrasonic sensor output. The experiment is designed with the Design of Experiments (DOE) methodology. There are a wide variety of experimental designs for conducting factorial experiments [4]. Completely randomized design is one of the most straightforward designs to implement [4]. Mason et al. [5] described the randomization design method as: '*Randomization is a procedure whereby factor–level combinations are (a) assigned to experimental units or (b) assigned to a test sequence in such a way that every factor–level combination has an equal chance of being assigned to any experimental unit or position in the test sequence*'[4].

The factorial design is developed in the randomized way using Minitab software [6]. The high and low values of these factors are shown in Table 5.3. A full factorial matrix of 2^3 factors with one replicate is shown in Table 5.4.

The response variable in these designs is the fluid level, or the sensor output in voltage. Arizona dust is used as the contaminant in these experiments.

Table 5.3 High and low values of the influencing factors

Factors	Low value	High value	Unit
1-slosh frequency	0.5	2	Hz
2-temperature	10	50	°C
3-contamination	0	150	g

Table 5.4 Experiment A: full factorial matrix

Run order	Slosh frequency (Hz)	Temperature (°C)	Contamination (g)
1	2.0	10	0
2	0.5	50	150
3	0.5	50	0
4	2.0	10	150
5	2.0	50	0
6	0.5	10	150
7	0.5	10	0
8	2.0	50	150

5.5.3 Experimental Setup

Experiment Set A is setup to implement the aforementioned factorial design. A fuel tank with 50 L of Exxsol D-40 Stoddard solvent is firmly mounted on the linear actuator, as described in Sect. 5.4.2. The ultrasonic sensor described in Sect. 5.4.1 is mounted on top of the fuel tank. The sensor cable is connected to the Data Acquisition Card (DAQ Card). LabVIEW software is then run and the response of the sensor is obtained and stored. The ultrasonic sensor signal is sampled at 10 Hz sampling frequency. An overview of the experiment setup is illustrated in Fig. 5.10.

The experiment is run according to the run order shown in Table 5.4. The linear actuator is used to create slosh waves in the fuel tank. The frequency of the slosh is controlled by the Programmable Logic Controller (PLC) Timer described in 5.4.3. For heating the fluid up to 50 °C, a heating chamber is used (refer Sect. 5.4.4).

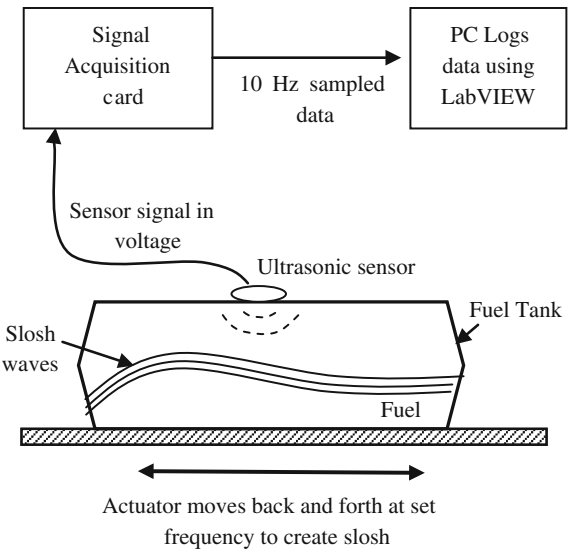

Fig. 5.10 Overview of the experimental setup for Experiment Set A

Each experiment order shown in Table 5.4 is run for 60 s and the response of the ultrasonic sensor is recorded throughout the run period.

5.6 Experiment Set B: Kernel Functions Examination

5.6.1 Overview

Experiment B is performed to compare the performance of four SVM kernel functions: linear, polynomial, RBF, and sigmoid. The data samples obtained from this experiment are used to develop four separate SVM models, where the kernel function of each model is one of the four investigated kernel functions. For simplicity, only four volume levels are used to run the experiment. The influence of contamination on the sensor output is observed in the results of Experiment Set A to be very small; therefore, the influence of the contamination factor was ignored in Experiment B. However, the effects of temperature changes indicate a significant effect on the ultrasonic output and hence the temperature readings is observed and recorded during this experiment (Fig. 5.11).

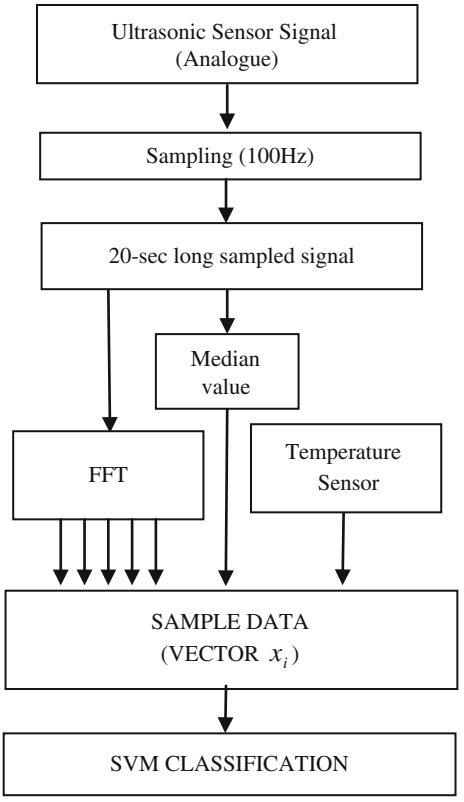

Fig. 5.11 System flow diagram for Experiment Set B

5.6.2 Experimental Setup

The setup for these experiments is similar to the setup described for Experiment Set A. The fuel tank is filled with Exxsol D-40 at four different tank volumes: 40, 45, 50, and 55 L. The ultrasonic sensor is fitted near the center of the tank. The tank is firmly mounted onto the linear actuator. The actuator is controlled by a pulse timer. The range of slosh frequency with very significant amplitude observed during a normal drive (refer Sect. 4.5) is 0.0–2.0 Hz. Hence in this experiment, the range of slosh frequency generated by the linear actuator is also fixed at 0.0–2.0 Hz. The slosh frequency or the cycle of linear actuator could be selected from 0.0 to 2.0 Hz at an interval of 0.2 Hz. The complete factorial matrix is shown in Table 5.5.

Figure 5.12 shows a block diagram of this experimental setup. The level signal from the ultrasonic sensor is acquired by LabVIEW using a Data Acquisition Card that is connected to the ultrasonic sensor. The ultrasonic signal indicating the fuel level is sampled and recorded at 100 Hz.

Table 5.5 Full factorial matrix for Experiment Set B

Run order	Slosh frequency (Hz)	Tank volume (L)	Run order	Slosh frequency (Hz)	Tank volume (L)
1	0	40	23	0	50
2	0.2	40	24	0.2	50
3	0.4	40	25	0.4	50
4	0.6	40	26	0.6	50
5	0.8	40	27	0.8	50
6	1	40	28	1	50
7	1.2	40	29	1.2	50
8	1.4	40	30	1.4	50
9	1.6	40	31	1.6	50
10	1.8	40	32	1.8	50
11	2	40	33	2	50
12	0	45	34	0	55
13	0.2	45	35	0.2	55
14	0.4	45	36	0.4	55
15	0.6	45	37	0.6	55
16	0.8	45	38	0.8	55
17	1	45	39	1	55
18	1.2	45	40	1.2	55
19	1.4	45	41	1.4	55
20	1.6	45	42	1.6	55
21	1.8	45	43	1.8	55
22	2	45	44	2.0	55

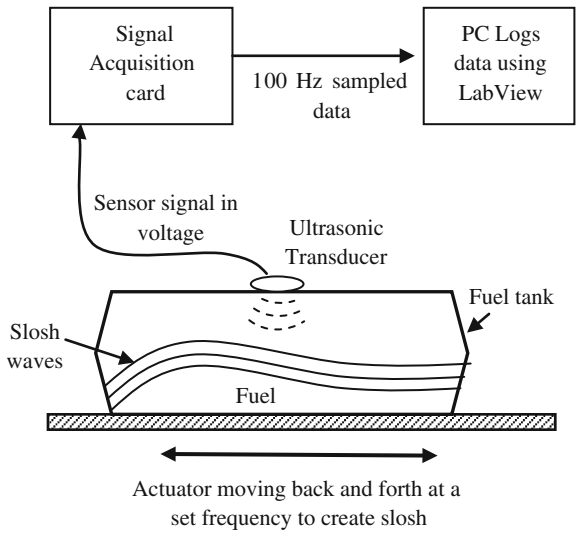

Fig. 5.12 Experimental setup for Experiment Set B

5.6.3 Parameters for the SVM Kernel Functions

5.6.3.1 Linear Kernel Parameters

The linear kernel function is given as [7]:

$$\kappa(\mathbf{x_i}, \mathbf{x_j}) = \mathbf{x_i} \cdot \mathbf{x_j} \tag{5.1}$$

Table 5.6 lists all the parameters and their values that are required by the LIBSVM [1] application to train the SVM-based signal processing system with Linear kernel function.

5.6.3.2 Polynomial Kernel Parameters

The polynomial kernel function is obtained by substituting the kernel parameters into Eq. (3.36) [7]:

$$\kappa(\mathbf{x_i}, \mathbf{x_j}) = (0.5(\mathbf{x_i} \cdot \mathbf{x_j}) + 0.3)^3 \tag{5.2}$$

Table 5.6 LIBSVM parameters for SVM model using linear kernel function

Parameter	Description	Value
-*s*	SVM type	1 (nu-SVM)
-t	Kernel function	0 (linear)
-n	ν Parameter	0.5
-e	ξ Epsilon (tolerance)	$1e^{-5}$

Table 5.7 LIBSVM parameters for SVM model using polynomial kernel function

Parameter	Description	Value
-*s*	SVM type	1 (nu-SVM)
-t	Kernel function	1 (polynomial)
-g	γ Parameter (gamma)	0.5
-n	ν Parameter (nu)	0.2
-d	d Parameter (degree)	3
-r	r Parameter (coef0)	0.3
-e	ξ Epsilon (tolerance)	1e-5

Table 5.7 lists all the parameters and their values that are required by the LIBSVM application to train the SVM-based signal processing system with polynomial kernel function.

5.6.3.3 Radial Basis Kernel Parameters

The RBF kernel function is obtained by substituting the kernel parameters into Eq. (3.37) [7]:

$$\kappa(\mathbf{x_i},\ \mathbf{x_j}) = \exp\left(-0.105\left\|\mathbf{x_i} - \mathbf{x_j}\right\|^2\right) \tag{5.3}$$

Table 5.8 lists all the parameters and their values that are required by the LIBSVM application to train the SVM-based signal processing system with RBF kernel function.

5.6.3.4 Sigmoid Kernel Parameters

The Sigmoid kernel function is obtained by substituting the kernel parameters into Eq. (3.38) [7]:

$$\kappa(\mathbf{x_i}, \mathbf{x_j}) = \tanh(0.05(\mathbf{x_i} \cdot \mathbf{x_j}) - 0.85) \tag{5.4}$$

Table 5.9 lists all the parameters and their values that are required by the LIBSVM application to train the SVM-based signal processing system with Sigmoid kernel function.

Table 5.8 LIBSVM parameters for SVM model using RBF

Parameter	Description	Value
-*s*	SVM type	1 (nu-SVM)
-t	Kernel function	2 (RBF)
-g	γ Parameter (gamma)	0.105
-n	ν Parameter (nu)	0.1
-e	ξ Epsilon (tolerance)	1e-5

Table 5.9 LIBSVM parameters for SVM model using Sigmoid kernel function

Parameter	Description	Value
-*s*	SVM type	1 (nu-SVM)
-t	Kernel function	3 (Sigmoid)
-g	γ Parameter (gamma)	0.05
-n	ν Parameter (nu)	0.70
-r	r Parameter (coef0)	−0.85
-e	ξ Epsilon (tolerance)	1e-5

5.7 Experiment Set C: Performance Estimation Using Filtration

5.7.1 Overview

Experiment Set C is carried out to understand the effectiveness of using the SVM-based approach in combination with selected signal smoothing methods on the driven vehicle data. Several consecutive field trials are carried out to obtain training and validation data from the ultrasonic sensor operating under the effects of sloshing. First, appropriate configurations of the feature extraction functions and the size of the input vector are determined by experimentation, which is coded as C1. Second, the optimal configurations of the signal smoothing functions (described in Sect. 4.6) and appropriate filter tap size are determined, which is coded as C2. Finally, the most appropriate configuration of the SVM-based system is used to compare the accuracy of the SVM-based measurement system with the currently used averaging methods, which is coded as C3. Figure 5.13 shows an overview of the experimental setup of Experiment C.

The level signal from the ultrasonic sensor is acquired using LabVIEW and a Data Acquisition Card, which is connected to the ultrasonic sensor in the vehicle. The ultrasonic sensor signal indicating the fuel level is sampled and recorded at 100 Hz. The sampled level signal is gathered over 20 s, which is the typical hold-on time used in automotive vehicles for averaging the fuel level signal. This collective signal over 20 s is then filtered through the three investigated filtration methods. After filtration, feature extraction is performed on the filtered signals using the MATLAB built-in Fast Fourier Transform (*fft*), Discrete Cosine Transform (*dct*), and Discrete Wavelet Transform (*dwt*) functions described in Sect. 3.2.4. The obtained coefficients (*coef*) from the transformation function, the median (*med*) value of the raw signal, and the value of the ambient temperature (*T*) in the tank, are stored in an input vector for training and classification of the SVM-based signal processing system.

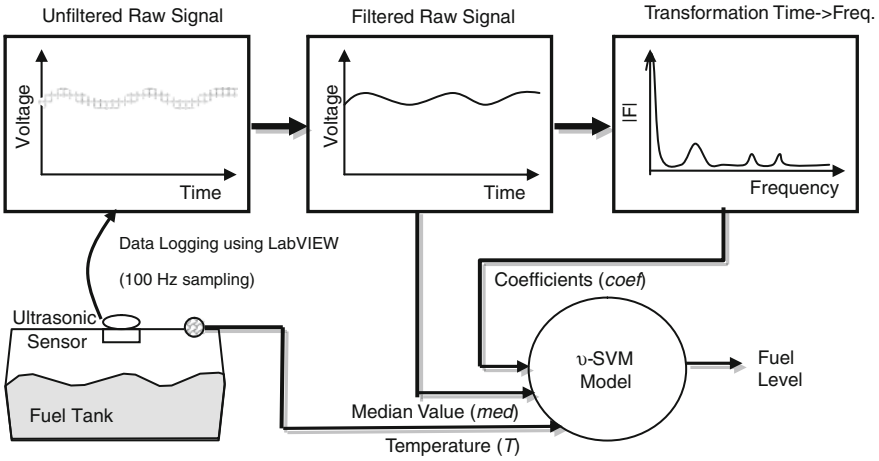

Fig. 5.13 Experimental setup for Experiment Set C

5.7.2 RBF Kernel Function

Each investigated SVM signal processing model had different preprocessing (input) configurations but they all share the same SVM parameters. The kernel function selected for this experiment is RBF, which was observed in Experiment B results to have a higher classification accuracy when compared with other kernel functions. RBF kernel function also has fewer kernel parameters, which can speed up the process to select the effective kernel parameter.

Table 5.10 lists all the parameters and their values that are required by the LIBSVM application to train the SVM signal processing models using the RBF kernel function. These parameters were originally based on the default parameters suggested by the LIBSVM software. However, after several quick tests, the values listed in Table 5.10 were found to be optimal for the training and classification of the slosh signals.

Table 5.10 Parameters of the SVM models using the RBF kernel function in Experiment Set C

Parameter	Description	Value
-*s*	SVM type	1 (nu-SVM)
-t	Kernel function	2 (RBF)
-g	γ Parameter (gamma)	0.105
-n	ν Parameter (nu)	0.1
-e	ξ Tolerance (epsilon)	1e-5

5.7.3 Experimental Setup

A fuel tank is fitted with an ultrasonic sensor near the center of the tank. The tank can be approximated as a rounded edge rectangle with dimensions 34 × 34 × 81 cm. The fuel tank is filled with fuel levels ranging from 5–50 L in the experiment, which corresponds to 6–70 % of the tank capacity. The fuel tank is mounted in latitudinal direction, where the longest length of the tank is in parallel to the direction of the vehicle. Table 5.11 lists all the fuel levels investigated in the experiment.

Each experiment is conducted by driving a vehicle containing the instrumented fuel tank for 3 km in a suburban residential area, where occasional stops are made at some road intersections. Figure 5.14 shows the typical speed and acceleration curves observed during the experiment.

The experiment labeled as C1 includes the selection of appropriate parameter values for the input window size ($\acute{\omega}$), feature extraction function, and the size of the input features, a factorial table (Table 5.13) of all feasible test values is generated according to the test conditions listed in Table 5.12. Each test in Table 5.13 is evaluated using the SVM-based signal processing model and the ultrasonic signal samples obtained from the field trials.

The coefficient sizes of 63 and 100 are chosen for the experiment because it was determined in the feature reduction section (Sect. 4.5) using Fig. 4.8 that the range of significant slosh frequency is 0–6.3 Hz. The range of slosh frequencies over 6.3–10 Hz has little magnitude but this range was also added in the section option to observe the performance of the ultrasonic sensor-based signal processing system over the whole 0–10 Hz range of slosh frequency. Coefficient size of 63 and 100 denote the slosh data that contain slosh frequencies of 0–6.3 and 0–10 Hz, respectively.

The experiment labeled as C2 includes the selection of appropriate parameter values for the smoothing function, feature extraction function, and the tap size of the smoothing filter, a factorial table (Table 5.15) of all feasible test values is generated according to the test conditions listed in Table 5.14. Each test in Table 5.15 is also evaluated using SVM-based signal processing model and the ultrasonic signal samples obtained from the field trials.

Table 5.11 List of tank volumes investigated in the experiment

Investigated tank levels
5 L, 6 L, 7 L, 8 L, 9 L, 15 L, 20 L, 25 L, 30 L, 35 L, 36 L, 37 L, 38 L, 39 L, 40 L, 45 L, 46 L, 47 L, 48 L, 49 L, 50 L

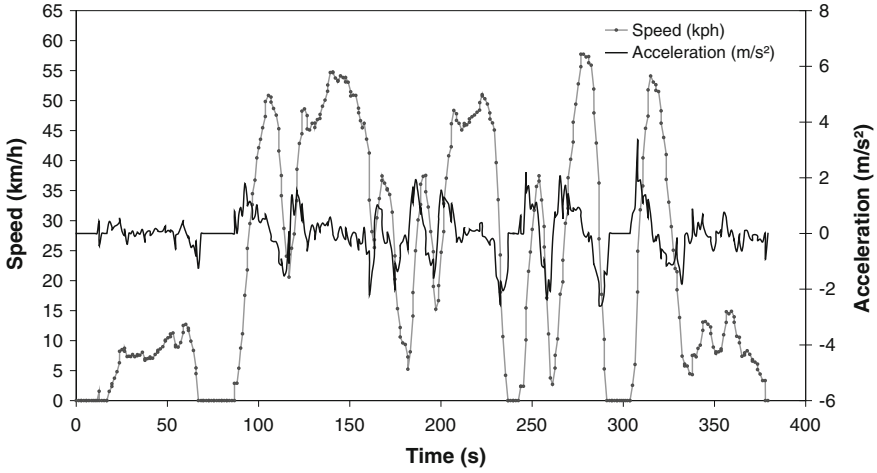

Fig. 5.14 Typical speed and acceleration observed during the experiment

Table 5.12 Test conditions for the evaluation of SVM input configuration

Window size $\acute{\omega}$ (sec)	Coefficient function	Coefficient size
5, 7, 10, 14, 20	FFT, DCT, WT	63, 100

Table 5.13 Complete factorial table for the evaluation of SVM input configuration

Test #	Window size $\acute{\omega}$ (sec)	Coefficient function	Coefficient size	Test #	Window size $\acute{\omega}$ (sec)	Coefficient function	Coefficient size
1	5	FFT	63	16	10	DCT	100
2	5	FFT	100	17	10	WT	63
3	5	DCT	63	18	10	WT	100
4	5	DCT	100	19	14	FFT	63
5	5	WT	63	20	14	FFT	100
6	5	WT	100	21	14	DCT	63
7	7	FFT	63	22	14	DCT	100
8	7	FFT	100	23	14	WT	63
9	7	DCT	63	24	14	WT	100
10	7	DCT	100	25	20	FFT	63
11	7	WT	63	26	20	FFT	100
12	7	WT	100	27	20	DCT	63
13	10	FFT	63	28	20	DCT	100
14	10	FFT	100	29	20	WT	63
15	10	DCT	63	30	20	WT	100

Table 5.14 Test conditions for the evaluation of optimal signal smoothing function configurations

Coefficient function	Signal smoothing function	Filter tap size
FFT, DCT, WT	Moving mean, moving median, wavelet filter	5, 10, 15

Table 5.15 Complete factorial table for the evaluation of optimal signal smoothing function configurations

Test #	Coefficient function	Filter function	Filter tap size	Test #	Coefficient function	Filter function	Filter tap size
1	FFT	Moving mean	5	15	DCT	Moving median	15
2	FFT	Moving mean	10	16	DCT	Wavelet	5
3	FFT	Moving mean	15	17	DCT	Wavelet	10
4	FFT	Moving median	5	18	DCT	Wavelet	15
5	FFT	Moving median	10	19	WT	Moving mean	5
6	FFT	Moving median	15	20	WT	Moving mean	10
7	FFT	Wavelet	5	21	WT	Moving mean	15
8	FFT	Wavelet	10	22	WT	Moving median	5
9	FFT	Wavelet	15	23	WT	Moving median	10
10	DCT	Moving mean	5	24	WT	Moving median	15
11	DCT	Moving mean	10	25	WT	Wavelet	5
12	DCT	Moving mean	15	26	WT	Wavelet	10
13	DCT	Moving median	5	27	WT	Wavelet	15
14	DCT	Moving median	10				

5.8 SVM Data Processing

Figure 5.15 shows the flowchart of the process used to train and validate the SVM models.

The raw signals acquired from the ultrasonic sensor during the experiments are stored in the LABVIEW file format. These raw signal files are then loaded up using the MATLAB software and the filtration and feature extraction is performed. The four investigated filtration functions, moving mean, moving median,

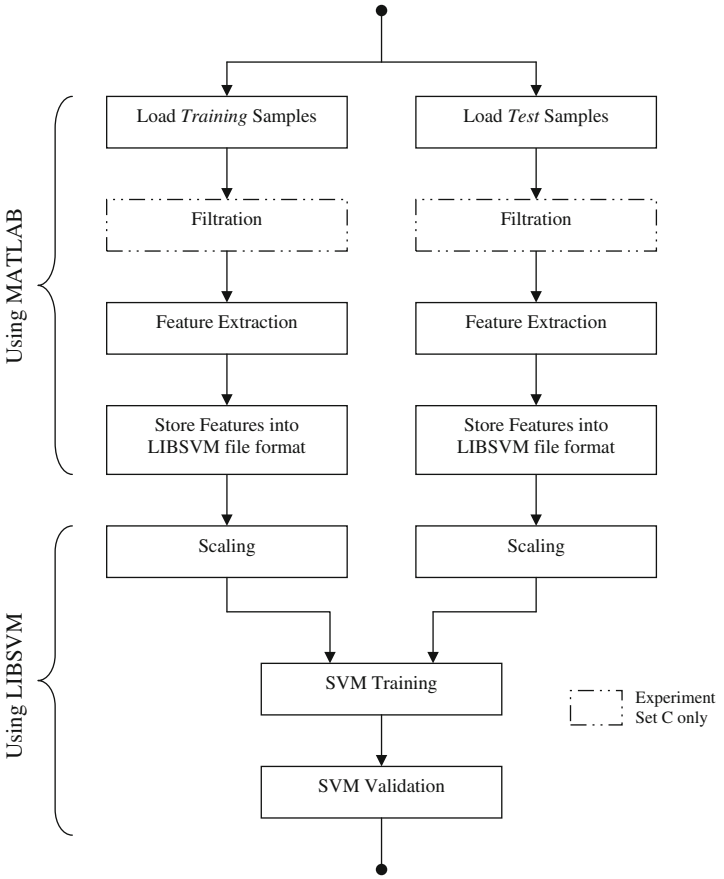

Fig. 5.15 Flowchart of the SVM model training and validation process

unfiltered, and wavelet filter, are applied on the raw signals using MATLAB. After filtration, the feature extraction is performed using the MATLAB's *fft*, *dct*, and *dwt* functions. The coefficients (coef) obtained from the feature extraction functions are stored in a vector array along with the median value (*med*) of the raw signals and the temperature value (*T*). The vector array is then exported into the SVM data file format.

Before the training of the SVM model, the feature vector stored in the SVM file format is scaled between 0 and 1 using the svm-scale tool in the LIBSVM. The scaling tool produces another file with the '.scale' file extension. Thereafter, an SVM model is created by using a *svm-train* tool. The svm-train tool is called with the SVM parameters, which describes the type of SVM, and the kernel function along with its variable values. After training, the SVM model is validated using the LIBSVM svm-predict tool. The training and validation process is repeated a number of times until the SVM parameters are close to the optimal values.

The complete program code for each experiment has been provided in Appendix D. The following lines shows the command used to scale, train, and predict an SVM model that used Linear kernel function using the LIBSVM software.

```
c:\test\> svm-scale.exe -l 0 -u 1 -s range traindata > traindata.scale
c:\test\> svm-scale.exe -r range testdata_LINEAR > testdata.scale
c:\test\> svm-train.exe -s 1 -t 0 -n 0.8 -e 1e-5 traindata.scale traindata.scale.model
c:\test\> svm-predict.exe testdata.scale traindata.scale.model RESULT.txt
```

5.8.1 Raw Signal File

The ultrasonic sensor readings are sampled and stored in the 'LabVIEW Measurement' file by the LabVIEW application. The raw signal file contained the raw sensor readings and the timestamp details of the instant when the sample readings are observed. Additionally, the LabVIEW Measurement file contains other details relating to the LabVIEW software, such as application version, time and date, username, and the details of the channel used to acquire the ultrasonic signal.

5.8.2 Signal Representation

The signal data is stored in files and folders that represent the conditions set in the experimental runs. The folders are named by the fluid volumes and the raw-data files are named by the slosh frequency or the set frequency of the linear actuator. Additionally, there is an extra file for each raw-data file that contained the experiment run configurations such as volume, slosh frequency, and temperature values.

The raw signals are loaded up and preprocessing performed. The feature coefficients (coef) are obtained using the investigated feature extraction functions (fft, dct, wt) on MATLAB software. The magnitude of the coefficients of the raw signal, the median value, and the temperature value are all bundled in a cell array having the structure format as shown in Table 5.16.

Table 5.16 Cell-array containing details of the training signal features

	Run		
Index	1	2	…
1	Raw signal filename	Raw signal filename	…
2	Slosh frequency	Slosh frequency	…
3	Actual volume	Actual volume	…
4	Temperature	Temperature	…
5	Average raw value	Average raw value	…
6	[Input vector **x**]	[Input vector **x**]	…

5.8.3 Filtration

The three investigated filters used in the analysis of the SVM system are developed as subroutine programs using MATLAB. The moving mean and moving median filters are developed using the equations (3.18) and (3.19), described in Sect. 4.6. Whereas, the wavelet filter used in the analysis was already contained in the Wavelet Toolbox [8] in MATLAB. The following commands are used in MATLAB to filter a signal $\boldsymbol{s}$ with the moving window size of w (Table 5.17).

The MATLAB code for these filtration functions is contained in Appendix D.

5.8.4 Feature Extraction

Feature extraction is performed by the MATLAB built-in FFT function. To obtain the magnitude of the frequency coefficients of the sampled signal $\boldsymbol{s}$ consisting of L number of sample points, the following MATLAB commands can be used:

```
% perform fft on the input signal s
fff_coefficients = abs(fft(s));

% remove symmetry due to the complex numbered values
Signal_Features = fff_coefficients (1:L/2 + 1)/L;

% reduce the number of coefficients to 63
Signal_Features = fff_coefficients (1:63);
```

Table 5.17 Call functions to smoothen the input signals

Filter	Filter call function
Moving mean	`AvgMean(s,w)`
Moving median	`avgMedian(s,w)`
Wavelet	`waveletfilter(s)`

References

1. Chang C-C, Lin C-J (2001) LIBSVM: a library for support vector machines. Software. http://www.csie.ntu.edu.tw/∼cjlin/libsvm
2. Cheremisinoff NP, Archer WL (2003) Properties and selection of organic solvents. Industrial solvents handbook. Marcel Dekker, New York, pp 81
3. Corporation, Exxon Mobil Aliphatics fluids (Exxsol Series)—grades and datasheets. Exxon Mobil Corporation. http://www.exxonmobilchemical.com/Public_Products/Fluids/Aliphatics/Worldwide/Grades_and_DataSheets/Fluids_Aliphatics_ExxsolSBP_Grades_WW.asp
4. Mason RL, Gunst RF, Hess JL (2003) Factorial experiments in completely randomized designs. Statistical design and analysis of experiments: with applications to engineering and science. Wiley-Interscience, Hoboken, pp 140–160
5. Mason RL, Gunst RF, Hess JL (2003) Statistical design and analysis of experiments: with applications to engineering and science. Wiley-Interscience, Hoboken
6. MINITAB (2000) User's guide 2: data analysis and quality tools. Minitab Inc., State College
7. Ivanciuc O (2007) Applications of support vector machines in chemistry. Rev Comput Chem 23:291–400
8. Michel M, Yves M, Georges O, Jean-Michel P (2009) Wavelet toolbox 4—users guide. MathWorks

Chapter 6
Results

6.1 Overview

This chapter provides the results obtained from the three sets of experiments described in Chap. 5. The results showing the response of the ultrasonic sensor in a dynamic environment without using the SVM-based signal processing system are provided in Sect. 6.2. The ultrasonic sensor signals, the training samples, and validation results for Experiment Sets B and C are given in Sects. 6.3 and 6.4, respectively.

6.2 Experiment Set A

6.2.1 Main Effects Plot

The results obtained from Experiment Set A were used to present main effects plots of the three factors that influence the accuracy of the level measurement system. The importance of main effects and interaction plots was discussed in Sect. 4.7.

The output of the ultrasonic sensor was recorded for each experiment trial described in Sect. 5.5. The ultrasonic sensor signal sampled at 10 Hz was averaged over 60 s to produce an averaged voltage that represented the fuel level. Table 6.1 shows the results obtained from Experiment Set A.

Figure 6.1 shows the cube plot for volume due to the effects of the three influencing factors. The single-order regression equation for volume is approximated using Minitab as:

$$\text{volume} = 52.6 - 4.25\,\text{slosh} + 0.148\text{temperature} + 0.0011\,\text{contamination} \tag{6.1}$$

J. Terzic et al., *Ultrasonic Fluid Quantity Measurement in Dynamic Vehicular Applications*, DOI: 10.1007/978-3-319-00633-8_6,
© Springer International Publishing Switzerland 2013

Table 6.1 Average volume readings obtained in Experiment Set A

Run order	Slosh frequency (Hz)	Temperature (°C)	Contamination (g)	Average volume (L)
1	0.5	50	0	58.94
2	0.5	10	150	49.97
3	2	10	150	45.64
4	0.5	10	0	52.27
5	2	50	0	48.17
6	2	10	0	47.71
7	0.5	50	150	58.99
8	2	50	150	53.16

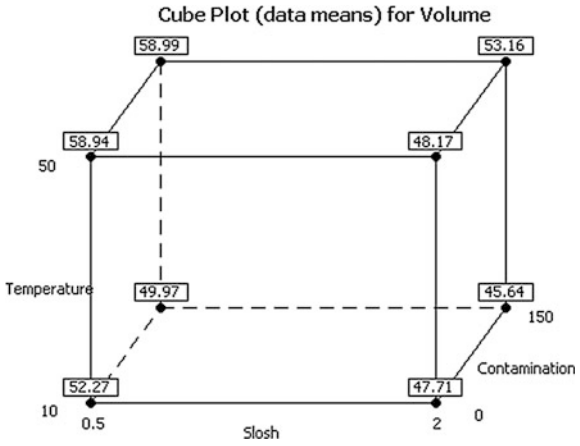

Fig. 6.1 Cube plot for volume in Experiment Set A

The main effects plots showing the degree of influence caused by the three influential factors: slosh, contamination, and temperature are shown in Figs. 6.2 and 6.3.

It can be observed that the fuel volume readings are influenced by the liquid slosh and the temperature changes. However, the effects plot of contamination

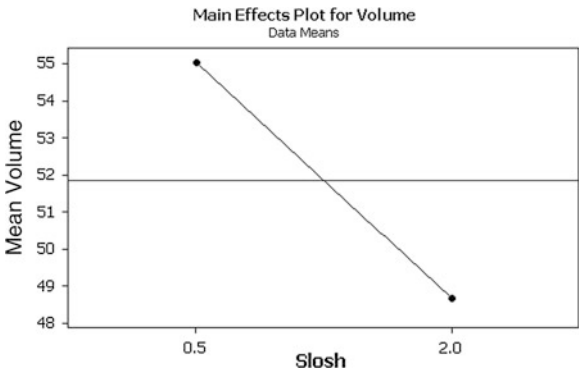

Fig. 6.2 Effects plot of the slosh factor

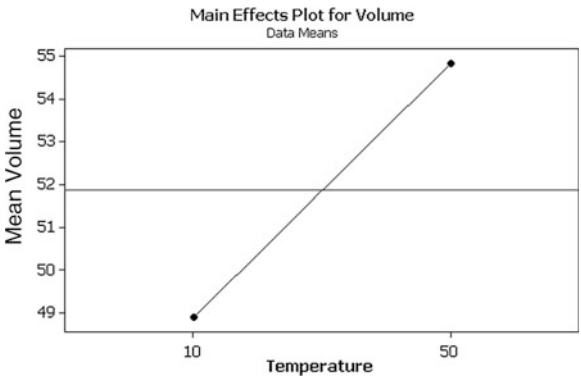

Fig. 6.3 Effects plot of the temperature factor

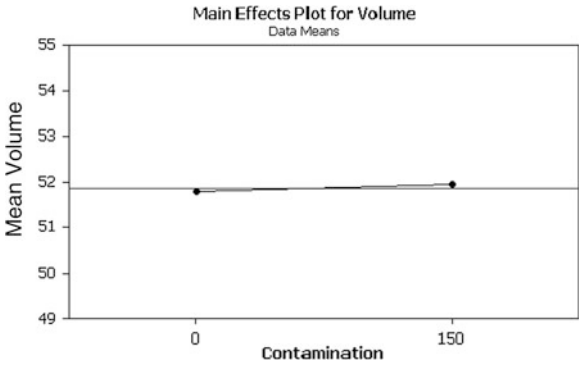

Fig. 6.4 Effects plot of the contamination factor

shown in Fig. 6.4, indicates that dust contaminants in the fluid did not significantly affect the ultrasonic sensor signal.

6.2.2 Interaction Plots

To observe the interaction between the influencing factors, results obtained from Experiment Set A were used to generate the interaction plot. The interaction plot shows that there is no interaction between contamination and the other two factors, namely, slosh and temperature. However, the interaction plot also reveals that there was some interaction between temperature and slosh.

6.2.3 Summary

The three influencing factors perceived to have influence on the level measurement were the following:

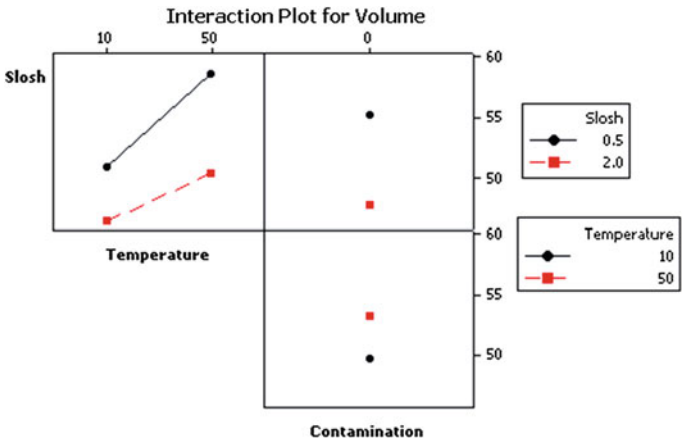

Fig. 6.5 Interaction plots of the influencing factors

- Liquid Slosh,
- Temperature, and
- Contamination.

It can be seen from the main effect plots that the effects of slosh and temperature were significant compared with the results for contamination. A reason for this little effect of contamination on level measurement could be that the Arizona Dust did not absorb or block the ultrasonic signals. Figure 6.5 showed the interaction plot of the influential factors. The interaction plot showed that there was no interaction between contamination and the other two factor being slosh and temperature. Hence, according to the observed results, the temperature and slosh factors are independent of contamination. But there was some interaction observed between temperature and slosh. As the temperature increased to 50 °C, the volume signal was also observed to have increased, which is in accordance with the Eq. 1.2 described in Chap. 1.

6.3 Experiment Set B

The training samples obtained from Experiment Set B at various tank volumes and slosh frequencies were loaded and classified in terms of their frequency response and their median value. Figure 6.6 shows the average fuel level data over 10 s obtained at various initial volume levels and generated slosh frequencies with the linear actuator. It can be seen that the average volume at various acceleration or slosh levels is not constant.

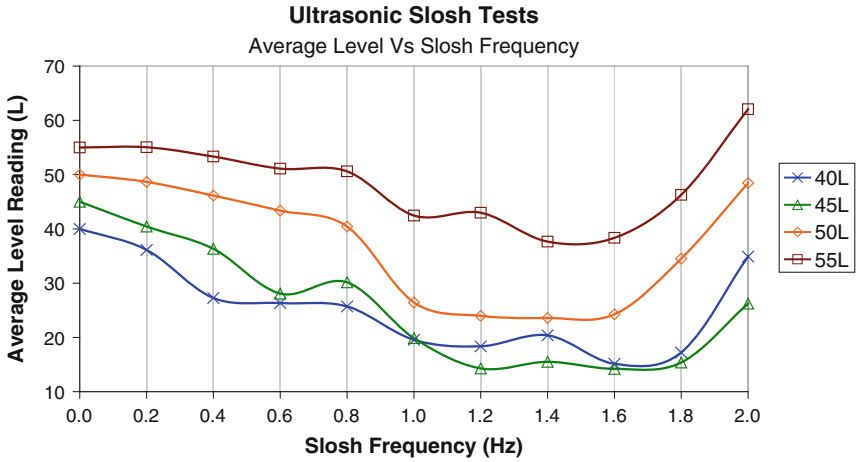

Fig. 6.6 Average volume of the tank measured over 10 s at selected slosh frequencies

6.3.1 Frequency Coefficients

The raw signals obtained from Experiment Set B were transformed into the frequency domain using the MATLAB built-in *fft* function. Figure 6.7 shows the frequency coefficients surface plot of the raw ultrasonic type fuel level sensor signals.

Four SVM-based signal processing models were investigated with four different kernel functions and parameters. After training the four SVM models, the

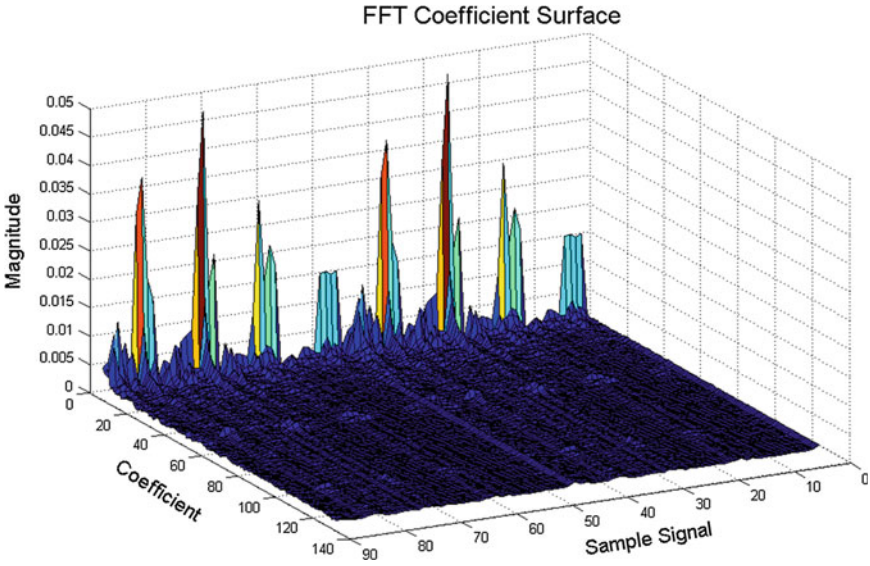

Fig. 6.7 Frequency coefficients surface plot

validation results for all SVM models exhibited more accurate level readings when compared with the simple averaging method. The validation results for each investigated kernel function using SVM are shown in the following figures. The circles shown in the following graphs illustrate misclassification of the sample signal at its particular slosh frequency.

6.3.2 Linear Kernel

Figure 6.8

6.3.3 Polynomial Kernel

Figure 6.9

6.3.4 RBF Kernel

Figure 6.10

6.3.5 Sigmoid Kernel

Figure 6.11

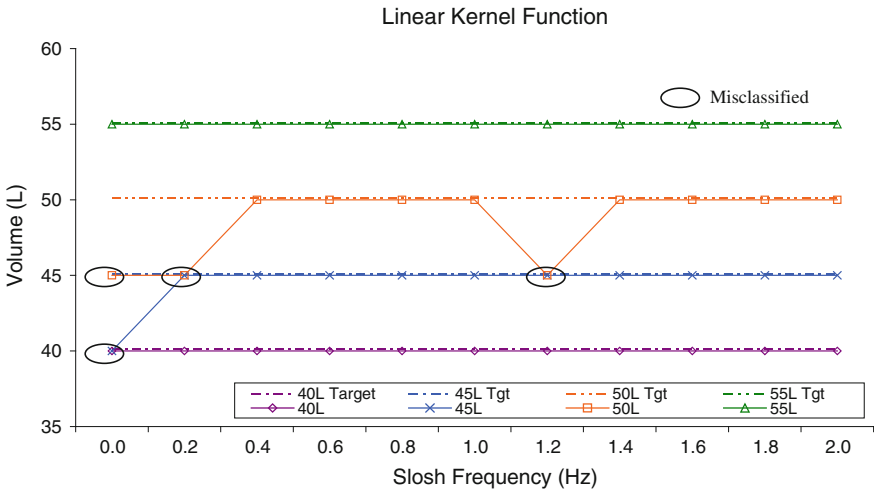

Fig. 6.8 Validation results using SVM with linear kernel function

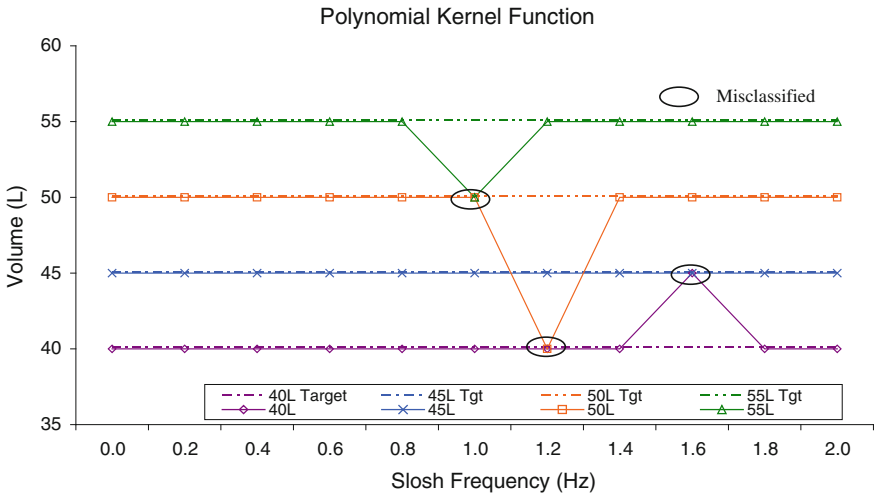

Fig. 6.9 Validation results using SVM with polynomial kernel function

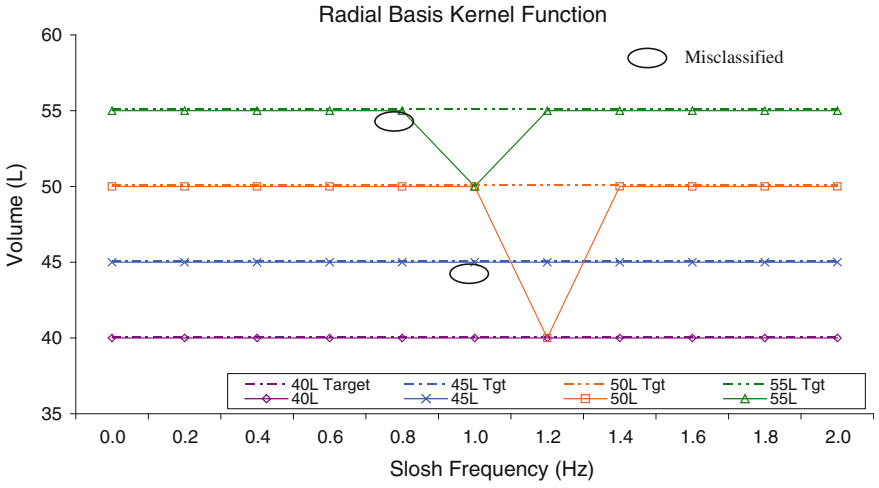

Fig. 6.10 Validation results using SVM with RBF kernel function

6.3.6 Summary

The comparison of performance of the four investigated SVM kernel functions is shown in the following tables. Table 6.2 shows the average volume calculated from the validation results for each investigated SVM model. Table 6.3 shows the error obtained at different fuel tank volumes.

Table 6.4 provides a summary of the performance of the four investigated SVM kernels based on the classification accuracy.

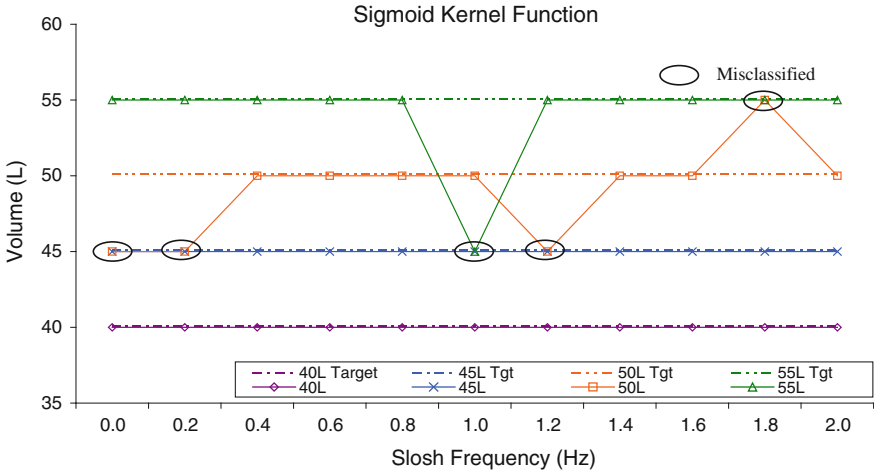

Fig. 6.11 Validation results using SVM with sigmoid kernel function

Table 6.2 Calculated average volume for each kernel function

Kernel	40 L	45 L	50 L	55 L
Linear	40.0	44.5	48.6	55.0
Polynomial	40.5	45.0	49.1	54.5
RBF	40.0	45.0	49.1	54.5
Sigmoid	40.0	45.0	49.1	54.1

Table 6.3 Calculated average error for each kernel function

Kernel	40 L	45 L	50 L	55 L	Average error (L)
Linear	0.0	0.5	1.4	0.0	0.5
Polynomial	0.5	0.0	0.9	0.5	0.5
RBF	0.0	0.0	0.9	0.5	0.3
Sigmoid	0.0	0.0	0.9	0.9	0.5

Table 6.4 Summary of overall classification for each kernel function

Kernel	Misclassified	Classification accuracy (%)
Linear	4	91
Polynomial	3	93
RBF	2	95
Sigmoid	5	89

The overall results obtained from the four SVM kernel functions have shown remarkable reduction in sloshing error, when compared with the results obtained by simple averaging. Both sigmoid and linear kernel functions could correctly

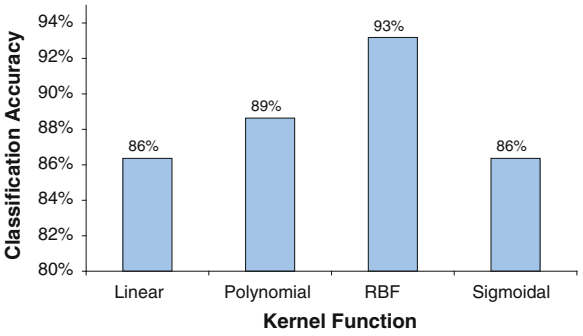

Fig. 6.12 Comparison of the classification accuracy of different kernel functions

classified 86 % of signals. Polynomial function produced better results with 89 % classification accuracy. The RBF function could correctly classify 93 % of signals, which indicates it to be the best performed of the kernel functions (Fig. 6.12).

6.4 Experiment Set C

The training samples obtained from Experiment Set C were processed with MATLAB using the methodology described in Sect. 5.3. The raw signals in this experiment were filtered through different filtration functions before the signals were trained by the SVM-based signal processing model. Twenty test drive trials at different fuel levels were carried out in this experiment, where each drive trial was conducted over a distance of 3 km. This section provides details on the raw signals obtained from the ultrasonic sensor during the course of this experiment. The frequency coefficients plot, the network weights coefficients, the validation results, and the validation error plots for all drive trials (at different fuel quantity) are contained in this section.

6.4.1 Raw Ultrasonic Sensor Signals

The ultrasonic sensor signals throughout each drive trial are shown in the figures below. Each graph shows the trial data run for 280 s over the same drive route. These graphs clearly show the slosh created in the fuel tank over the drive path. The magnitude of slosh can be seen as varying for different tank volumes (Figs. 6.13, 6.14, 6.15, 6.16, 6.17, 6.18, 6.19, 6.20, 6.21, 6.22).

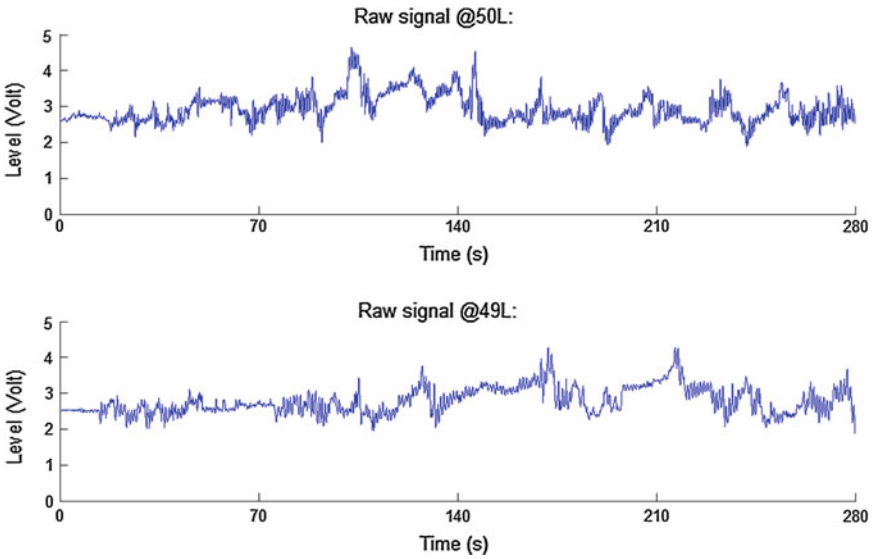

Fig. 6.13 Raw ultrasonic sensor signals (49 and 50 L)

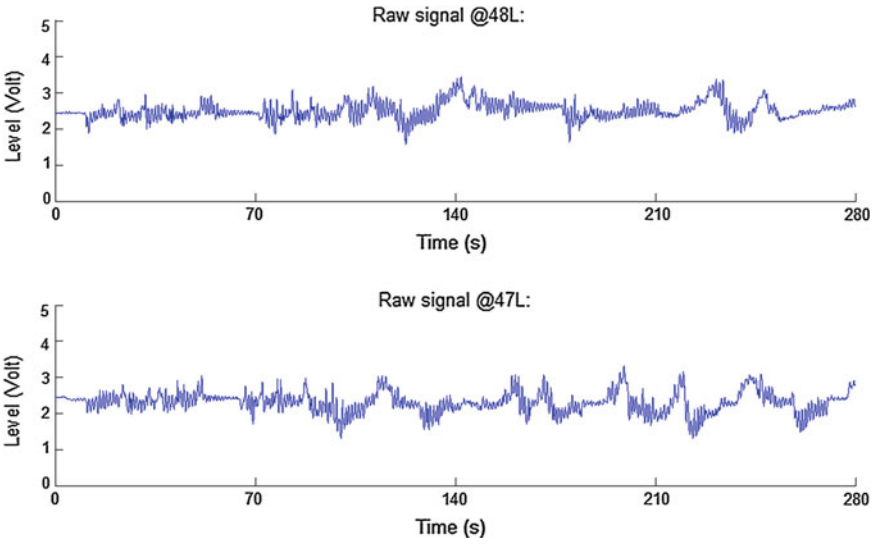

Fig. 6.14 Raw ultrasonic sensor signals (47 and 48 L)

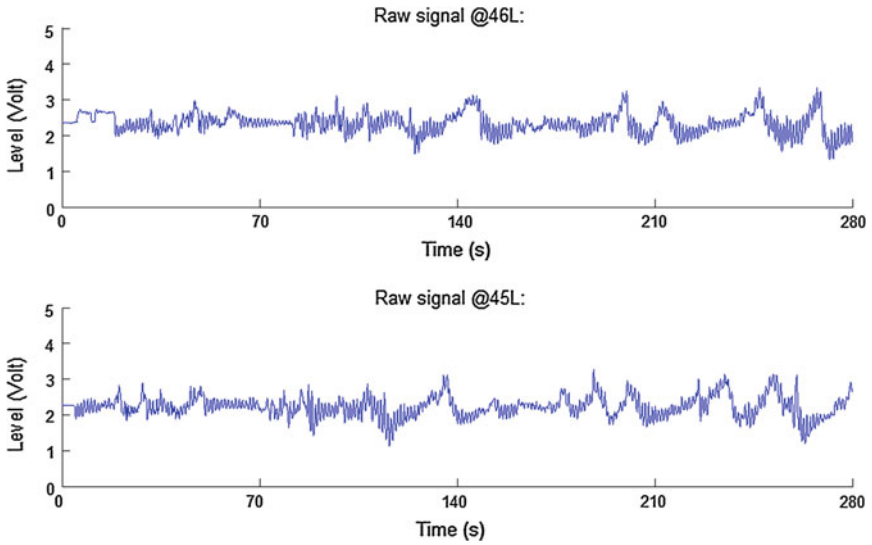

Fig. 6.15 Raw ultrasonic sensor signals (45 and 46 L)

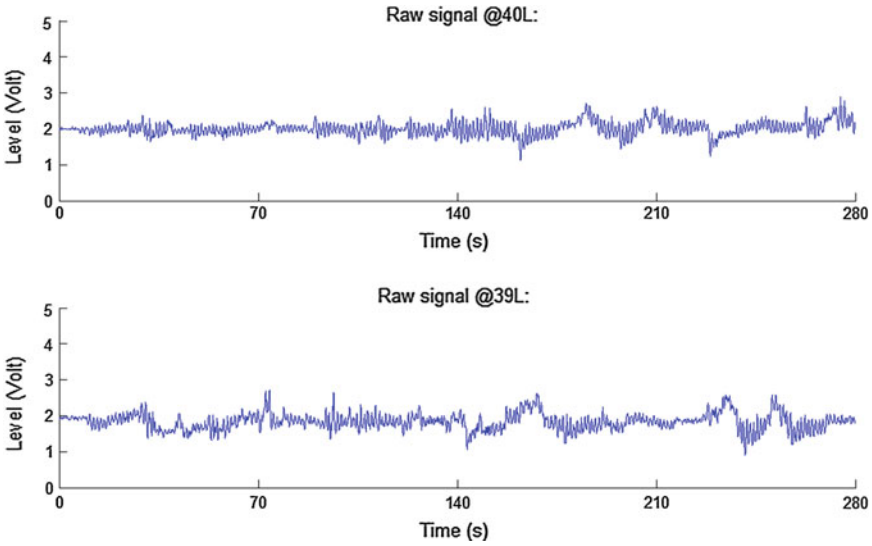

Fig. 6.16 Raw ultrasonic sensor signals (39 and 40 L)

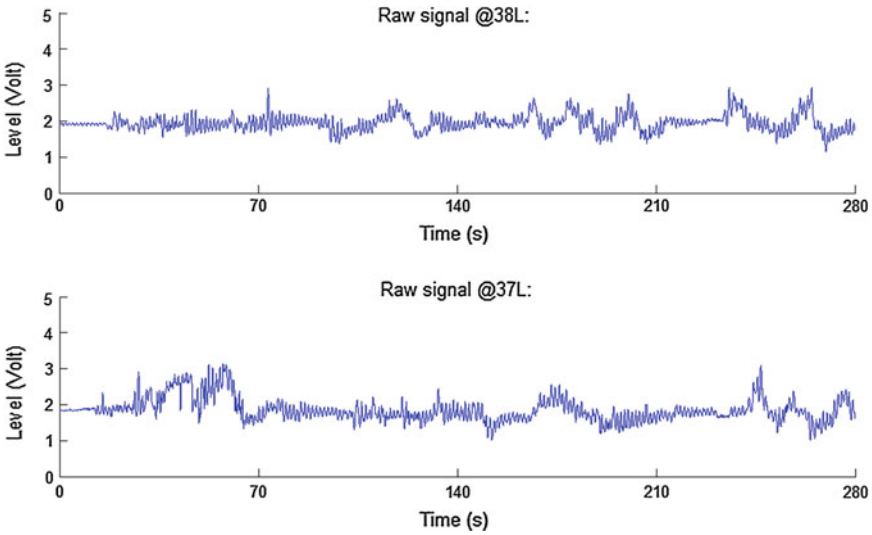

Fig. 6.17 Raw ultrasonic sensor signals (37 and 38 L)

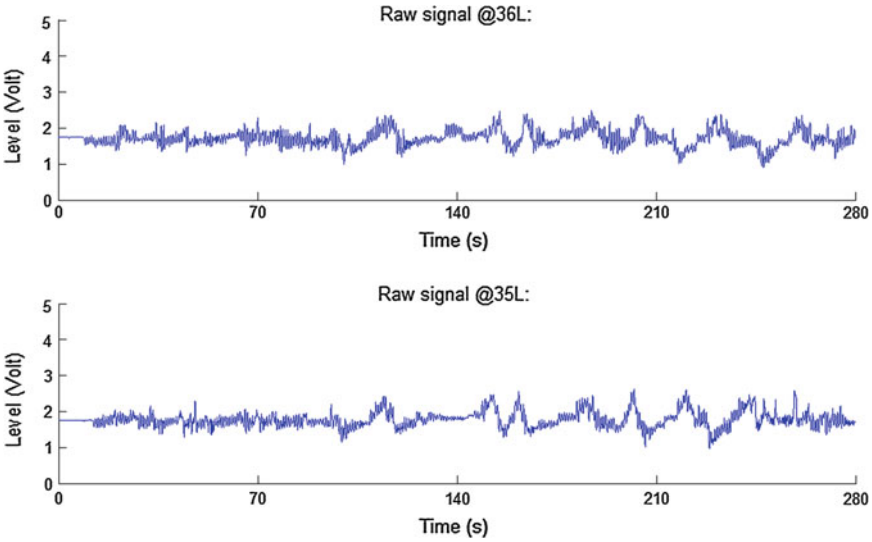

Fig. 6.18 Raw ultrasonic sensor signals (35 and 36 L)

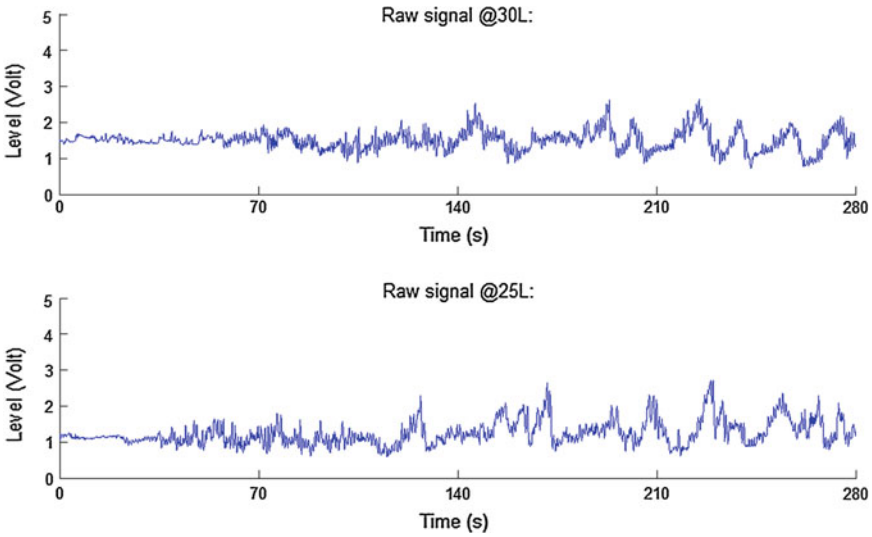

Fig. 6.19 Raw ultrasonic sensor signals (25 and 30 L)

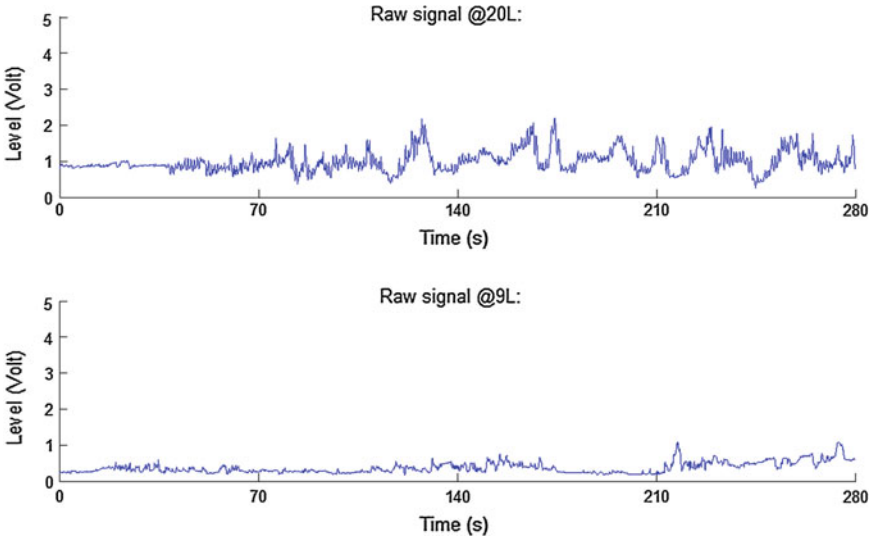

Fig. 6.20 Raw ultrasonic sensor signals (9 and 20 L)

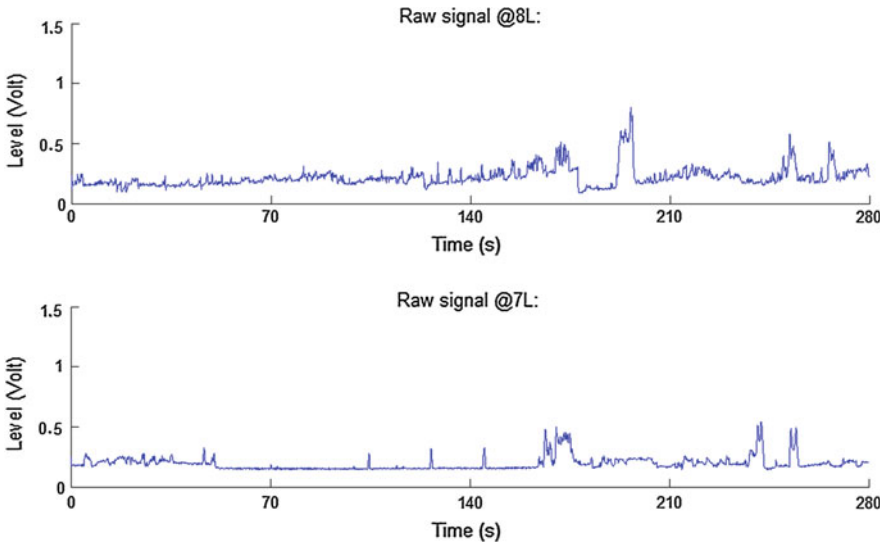

Fig. 6.21 Raw ultrasonic sensor signals (7 and 8 L)

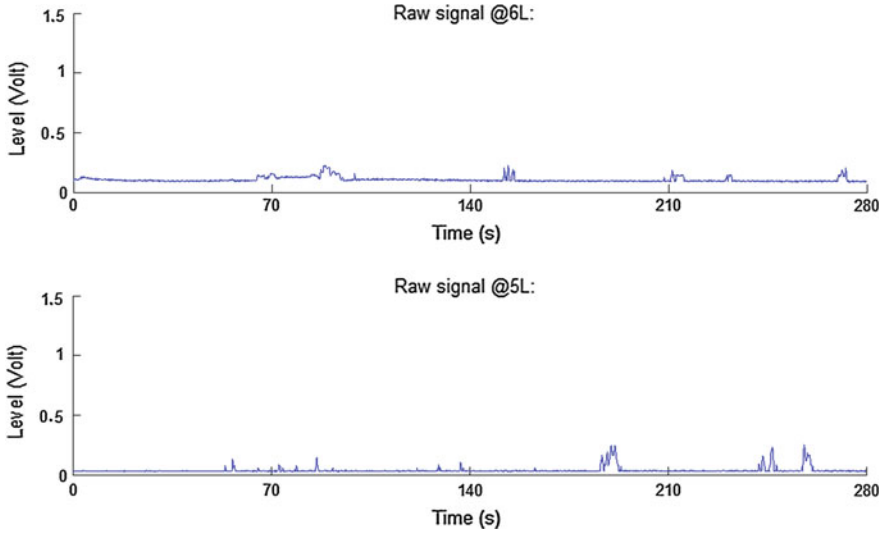

Fig. 6.22 Raw ultrasonic sensor signals (5 and 6 L)

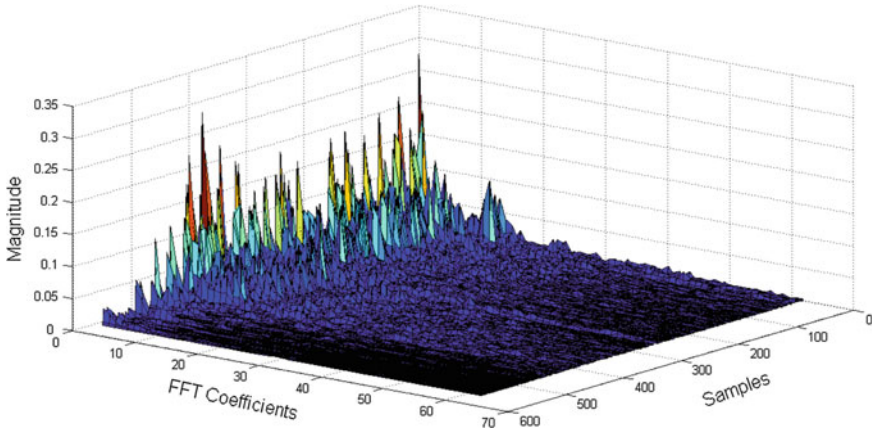

Fig. 6.23 Graph of the FFT coefficients obtained by using the training data

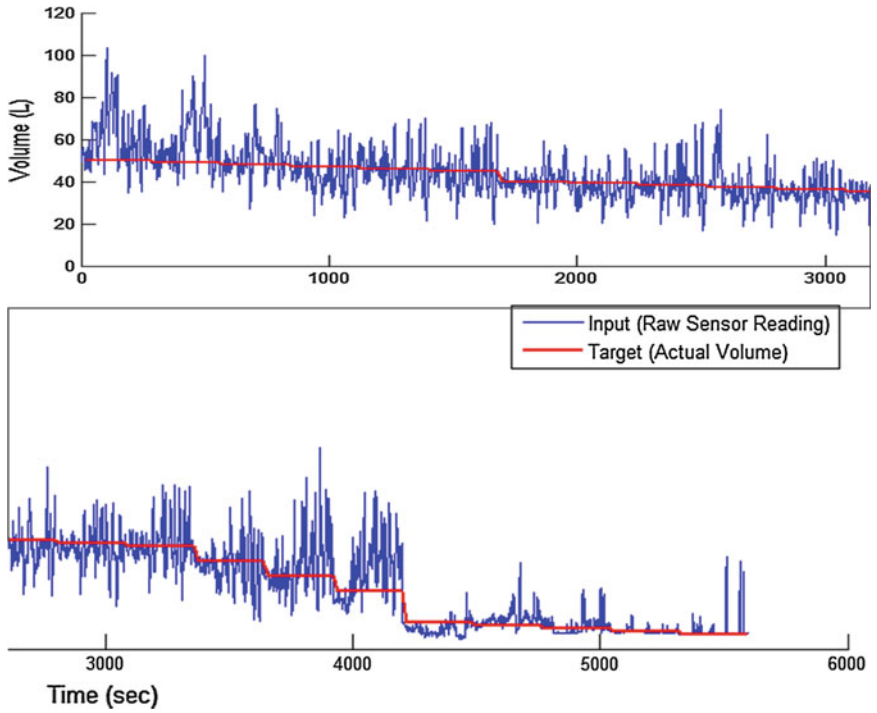

Fig. 6.24 Overall view of the observed raw signals and the actual fuel level

6.4.2 Frequency Coefficients

Figure 6.23 shows the frequency coefficients of the unfiltered signals obtained from the experiment using the MATLAB built-in *fft* function.

Feature reduction using filtration was described in Sect. 4.5. It was also described in Sect. 4.5 using Fig. 4.8 that the range of significant slosh frequency is 0–6.3 Hz. In this experiment, a low-pass filter was used to filter out slosh frequencies over 6.3 Hz. This was achieved to increase the network training speed without incurring a performance penalty. The frequency coefficients, the median value of the signals, and the temperature values were all bundled in an array of 64

Table 6.5 Results for the selection of optimal preprocessing configuration (Exp. C1)

Test #	Window size ($\acute{\omega}$)	Coefficient function	Coefficient size	Average error (L)			Standard deviation (L) error		
				Mean	Median	SVM	Mean	Median	SVM
1	5	FFT	63	2.89	2.92	0.81	1.53	1.53	0.62
2	5	FFT	100	2.89	2.92	0.99	1.53	1.53	0.70
3	5	DCT	63	2.89	2.92	0.90	1.53	1.53	0.66
4	5	DCT	100	2.89	2.92	0.98	1.53	1.53	0.80
5	5	WT	63	2.89	2.92	1.04	1.53	1.53	0.79
6	5	WT	100	2.89	2.92	1.04	1.53	1.53	0.79
7	7	FFT	63	2.75	2.76	0.78	1.50	1.50	0.64
8	7	FFT	100	2.75	2.76	0.95	1.50	1.50	0.72
9	7	DCT	63	2.75	2.76	0.83	1.50	1.50	0.63
10	7	DCT	100	2.75	2.76	1.02	1.50	1.50	0.83
11	7	WT	63	2.75	2.76	1.04	1.50	1.50	0.74
12	7	WT	100	2.75	2.76	0.93	1.50	1.50	0.73
13	10	FFT	63	2.59	2.60	0.75	1.51	1.51	0.62
14	10	FFT	100	2.59	2.60	0.93	1.51	1.51	0.61
15	10	DCT	63	2.59	2.60	0.89	1.51	1.51	0.56
16	10	DCT	100	2.59	2.60	0.84	1.51	1.51	0.59
17	10	WT	63	2.59	2.60	0.74	1.51	1.51	0.51
18	10	WT	100	2.59	2.60	0.74	1.51	1.51	0.51
19	14	FFT	63	2.36	2.26	0.65	1.45	1.37	0.64
20	14	FFT	100	2.36	2.26	0.79	1.45	1.37	0.63
21	14	DCT	63	2.36	2.26	1.08	1.45	1.37	0.84
22	14	DCT	100	2.36	2.26	1.02	1.45	1.37	0.71
23	14	WT	63	2.36	2.26	0.74	1.45	1.37	0.52
24	14	WT	100	2.36	2.26	0.71	1.45	1.37	0.52
25	20	FFT	63	2.17	2.04	0.75	1.51	1.40	0.74
26	20	FFT	100	2.17	2.04	0.86	1.51	1.40	0.80
27	20	DCT	63	2.17	2.04	1.21	1.51	1.40	1.39
28	20	DCT	100	2.17	2.04	0.85	1.51	1.40	0.76
29	20	WT	63	2.17	2.04	0.73	1.51	1.40	0.64
30	20	WT	100	2.17	2.04	0.68	1.51	1.40	0.59

elements, which were then used to train and validate the SVM-based signal processing system.

Figure 6.24 shows an overview of the slosh data in the vehicle over time. The training samples and the corresponding target value or the actual value of the initial fuel level in the tank are also shown in Fig. 6.24.

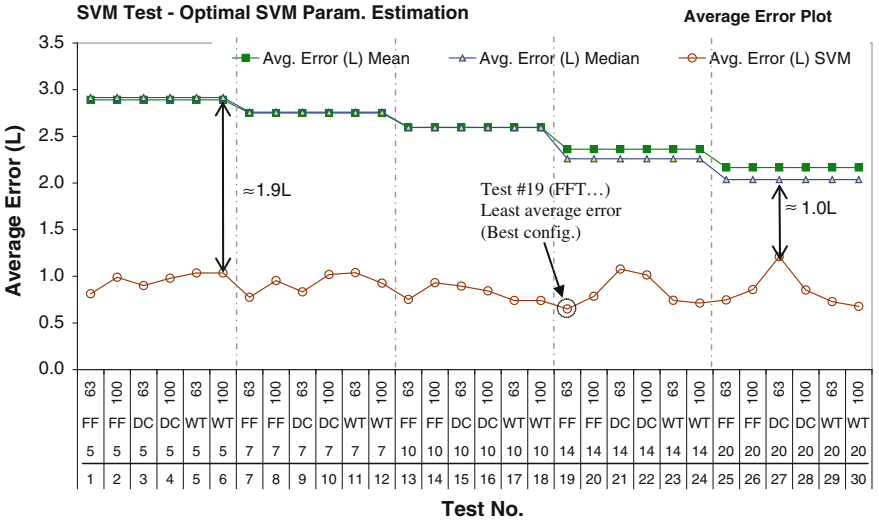

Fig. 6.25 Average error plot—optimal SVM preprocessing estimation

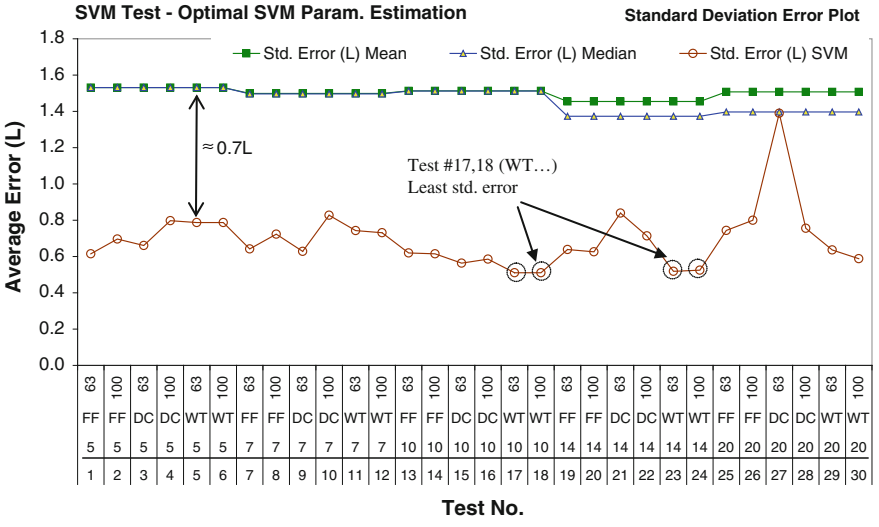

Fig. 6.26 Standard deviation error plot—optimal SVM preprocessing estimation

When the actual volume of fuel in the tank is compared with the volume obtained from the raw sensor signal, shown in Fig. 6.24, very large deviations in the calculated volume are observed due to the effects of sloshing. It is apparent that the amplitude of the sloshing is different at different initial volumes of fuel in the tank.

6.4.3 C1 Selection of Optimal Preprocessing Parameters

Table 6.5 shows the results for the optimal preprocessing parameters evaluation test. The preprocessing configuration list in the table for each test number was applied on the raw ultrasonic sensor signals and then processed through the *v*-SVM using LIBSVM software. The results obtained from each SVM test model are compared with the results obtained with standard statistical averaging methods.

Table 6.6 Results for the selection of optimal signal smoothing parameters (Exp. C2)

Test #	Coefficient function	Filter function	Filter tap size	Average error (L) [*v*-SVM]			
				Lower limit	Average	Upper limit	Standard deviation
1	FFT	Moving mean	5	0.08	0.63	1.18	0.55
2	FFT	Moving mean	10	0.11	0.66	1.21	0.55
3	FFT	Moving mean	15	0.13	0.73	1.33	0.60
4	FFT	Moving median	5	0.13	0.66	1.18	0.52
5	FFT	Moving median	10	0.14	0.69	1.24	0.55
6	FFT	Moving median	15	0.10	0.67	1.24	0.57
7	FFT	Wavelet	5	0.01	0.66	1.30	0.64
8	FFT	Wavelet	10	0.01	0.66	1.30	0.64
9	FFT	Wavelet	15	0.01	0.66	1.30	0.64
10	DCT	Moving mean	5	0.24	0.98	1.71	0.74
11	DCT	Moving mean	10	−0.07	0.95	1.97	1.02
12	DCT	Moving mean	15	−0.10	0.87	1.83	0.97
13	DCT	Moving median	5	0.28	0.93	1.58	0.65
14	DCT	Moving median	10	0.18	0.94	1.70	0.76
15	DCT	Moving median	15	−0.21	0.92	2.06	1.14
16	DCT	Wavelet	5	0.16	1.01	1.86	0.85
17	DCT	Wavelet	10	0.16	1.01	1.86	0.85
18	DCT	Wavelet	15	0.16	1.01	1.86	0.85
19	WT	Moving mean	5	0.20	0.74	1.27	0.54
20	WT	Moving mean	10	0.20	0.73	1.25	0.53
21	WT	Moving mean	15	0.20	0.73	1.26	0.53
22	WT	Moving median	5	0.20	0.74	1.27	0.54
23	WT	Moving median	10	0.19	0.72	1.26	0.53
24	WT	Moving median	15	0.21	0.75	1.29	0.54
25	WT	Wavelet	5	0.22	0.74	1.26	0.52
26	WT	Wavelet	10	0.22	0.74	1.26	0.52
27	WT	Wavelet	15	0.22	0.74	1.26	0.52

Figures 6.25 and 6.26 show plots of the average and standard deviation error results obtained from the optimal SVM preprocessing estimation test. In general, both plots show significantly low error results for the SVM-based signal

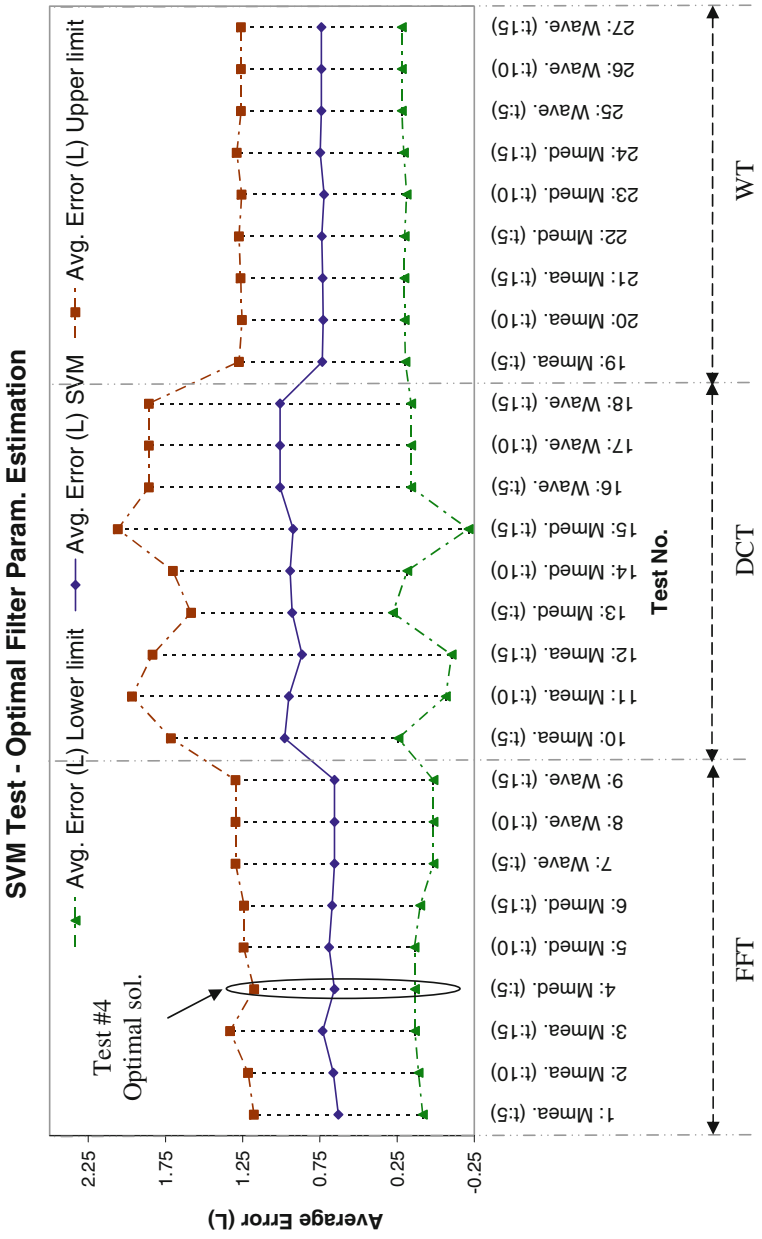

Fig. 6.27 Optimal SVM preprocessing filter parameter estimation

processing model when compared with the two currently used statistical averaging methods (*mean* and *median*). Figure 6.25 indicates that the optimal configuration for the SVM preprocessor is when it is configured with the parameters used in Test #19, which uses a window size of 14 s ($\acute{\omega} = 14$ s), Fast Fourier Transform Function (FFT) as the feature extraction function and 63 number of frequency coefficients. Figure 6.26 shows that the standard deviation error was the lowest for Test #17–18 and #23–24, where all these four tests used Wavelet Transformation (WT) as the feature extraction function. Based the on these observations, the optimal configurations for the SVM preprocessor system include: Fast Fourier Transform (FFT) and Wavelet Transform (WT) as the optimal feature extraction functions, 63 number of signal coefficients, and the window size ($\acute{\omega}$) of 14 s. The optimal configurations obtained in this test will be used to run the next test '*C2 Selection of Optimal Signal Smoothing Parameters*'. The results obtained using the Discrete Cosine Transform (DCT) function generally indicated a larger error when compared with the other two transformation functions (FFT and WT). However, by incorporating the signal smoothing technique with the DCT transformation function, the accuracy of the SVM-based signal processing system has the potential to improve. Hence, DCT will also be examined along with the FFT and WT functions in the next text '*C2 Selection of Optimal Signal Smoothing Parameters*'.

6.4.4 C2 Selection of Optimal Signal Smoothing Parameters

The selection of optimal signal smoothing parameter evaluation test was run to understand the significance and performance of signal smoothing technique in signal preprocessing. Table 6.6 lists the benchmark results of using different signal

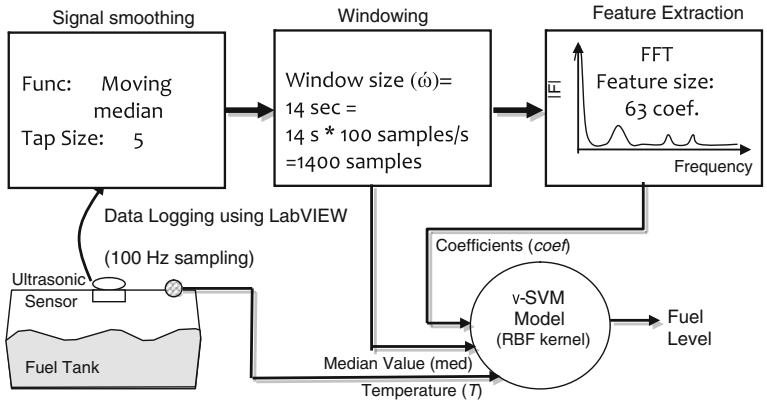

Fig. 6.28 Synthesized SVM-based measurement system model

preprocessing approaches to the SVM-based signal processing system. A graph of the figures list in this table is shown in Figure 6.27.

Figure 6.27 shows the influence of signal filtration on the SVM-based signal processing system. The results shown in Fig. 6.27 indicate that the SVM-based system provides the best results when it is configured with the configurations used in Test #4. Test #4 was configured with the window size of 14 s ($\acute{\omega} = 14$), FFT as the feature extraction function, 63 number of coefficients, and moving median function as the signal smoothing function with the filter tap size of 5. Figure 6.27 also indicates that the results obtained using FFT function generally had less errors than the other transformation functions (WT and DCT). The DCT function indicated a poor performance, when compared with FFT and WT. An interesting feature noticed in the Fig. 6.27 was that the signal smoothing function had little impact on the SVM-based system having the Wavelet Transform, as the results for

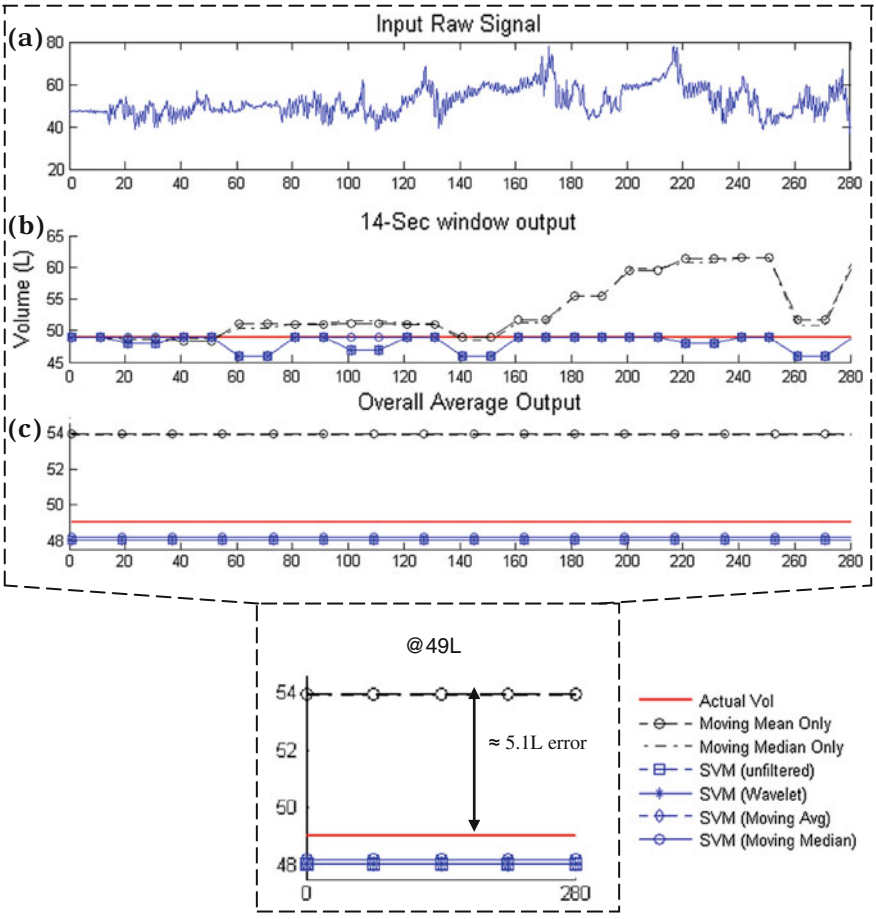

Fig. 6.29 Illustration of the evaluation of the SVM verification results

WT were mainly consistent for each filter test. The configurations used in Test #4 will be used in the next test to observe the performance of the SVM-based signal classification system at different tank volumes.

6.4.5 C3 Final Validation Results

A final model of the SVM-based signal process was synthesized based on the results observed in the previous experiments. The optimal selection values of the SVM preprocessor and the signal smoothing techniques were used to create a final version of the SVM-based signal processing and classification model. The configuration of the synthesised SVM model is shown in Fig. 6.28.

After training the final SVM model, the model was validated using the test samples obtained from the second field trial. Fig. 6.29 shows the output results obtained using different preprocessing filters. The output volume was calculated as the overall average of each investigated tank volume. Field trial results for each investigated tank volume are placed adjacent to each other. The time length of each trial is indicated as 280 s. A closer look at the 49 litre trial is also shown in Fig. 6.29. The raw signal illustrated in Fig. 6.29a was divided into 20 s long signals, as shown Fig. 6.29b, which were then filtered and processed through the

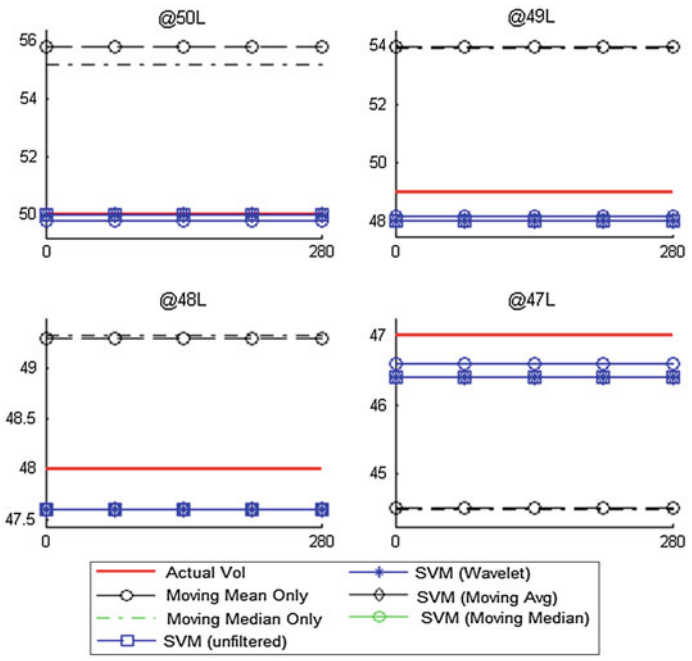

Fig. 6.30 Network verification results for volumes 47–50 L

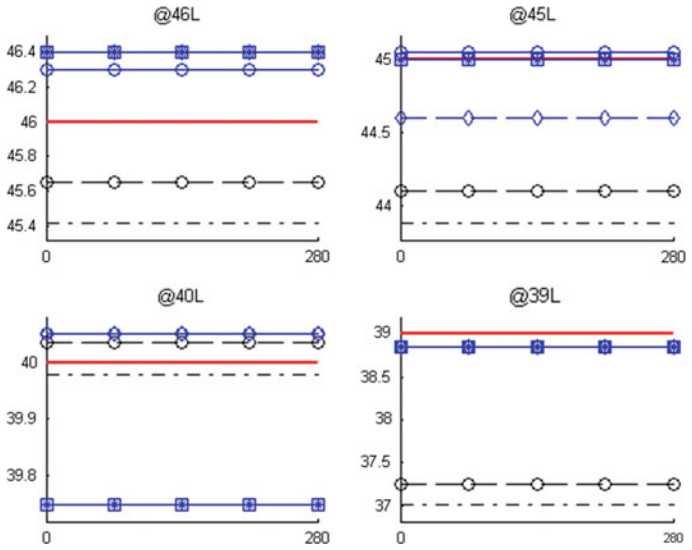

Fig. 6.31 Network verification results for volumes 39–46 L

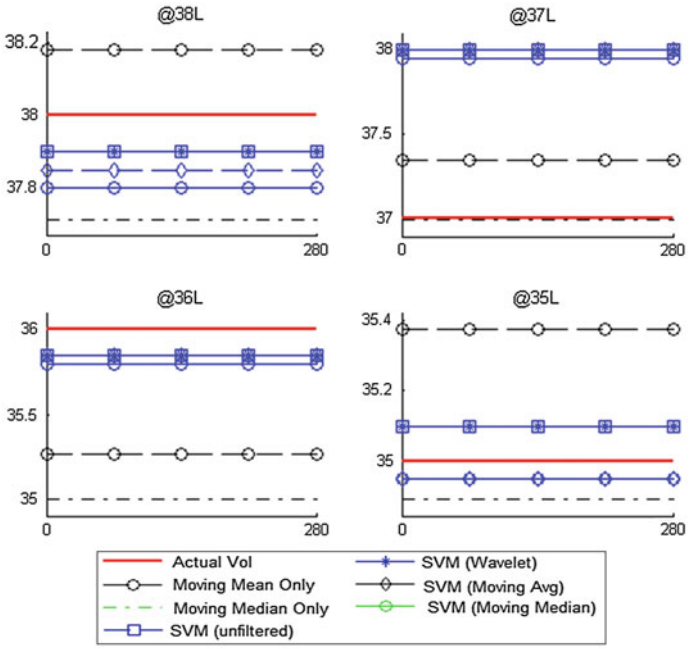

Fig. 6.32 Network verification results for volumes 35–38 L

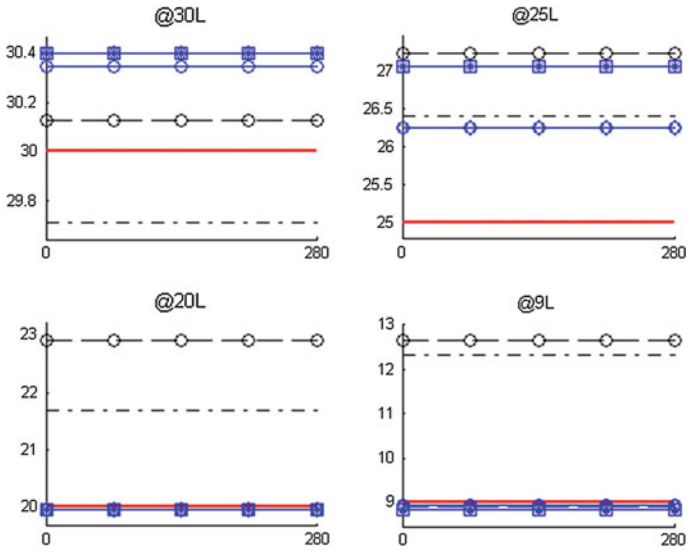

Fig. 6.33 Network verification results for volumes 9–30 L

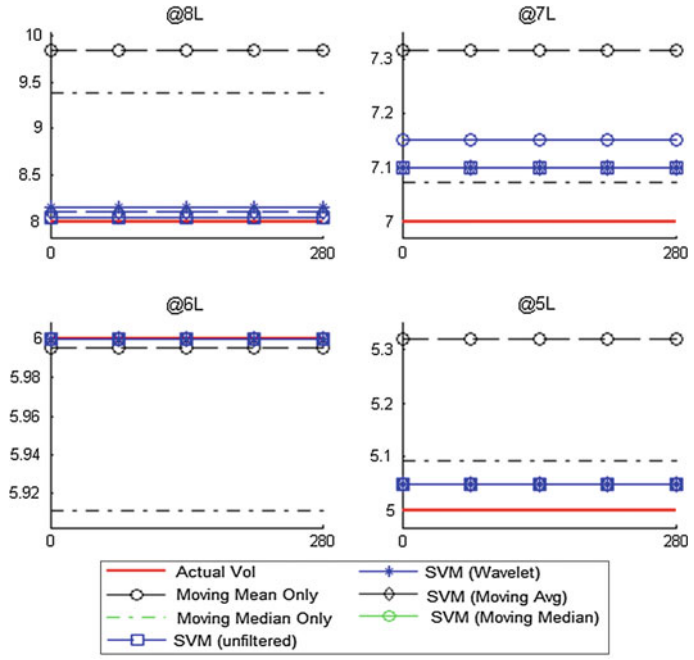

Fig. 6.34 Network verification results for volumes 5–8 L

SVM-based signal processing system. The overall averaged volume in Fig. 6.29c was calculated by averaging the SVM model outputs for each trial over 280 s (Figs. 6.30, 6.31, 6.32, 6.33, 6.34).

6.4.6 Validation Errors for Each Investigated Tank Volume

Table 6.7 shows the volume figures (in litres) obtained using the statistical mean and median functions, and the SVM predicted results using different preprocessing filters.

Table 6.8 shows the relative average error figures for all investigated volumes computed using the statistical averaging methods, and the SVM-based signal classification method having different preprocessing filters.

Table 6.7 Validation results using statistical averaging methods and the SVM approach with different preprocessing filters

Actual volume	Statistical averaging		Support vector machine			
	Moving mean* (without SVM)	Moving median* (without SVM)	*v*-SVM (Unfiltered)	*v*-SVM (Moving mean)	*v*-SVM (Moving median)	*v*-SVM (Wavelet filter)
50	55.77	55.18	50.02	50.03	49.80	50.01
49	53.93	53.87	48.05	48.05	48.20	48.05
48	49.29	49.32	47.60	47.60	47.60	47.60
47	44.51	44.49	46.40	46.40	46.60	46.40
46	45.65	45.42	46.40	46.40	46.30	46.40
45	44.10	43.88	45.02	44.60	45.05	45.03
40	40.04	39.98	39.75	40.05	40.05	39.75
39	37.26	37.02	38.85	38.85	38.85	38.85
38	38.18	37.71	37.90	37.85	37.80	37.90
37	37.34	36.99	38.03	38.01	37.95	38.02
36	35.27	35.00	35.85	35.85	35.80	35.85
35	35.37	34.89	35.10	34.95	34.95	35.10
30	30.13	29.71	30.40	30.40	30.35	30.40
25	27.23	26.40	27.05	26.25	26.25	27.05
20	22.91	21.69	19.95	19.95	19.95	19.95
9	12.65	12.32	8.85	8.90	8.95	8.85
8	9.84	9.38	8.05	8.10	8.05	8.15
7	7.31	7.07	7.10	7.10	7.15	7.10
6	6.00	5.91	6.01	6.03	6.01	6.03
5	5.32	5.09	5.05	5.05	5.05	5.05

*Standard statistical averaging method

Table 6.8 Relative average error using statistical averaging methods and SVM-based system

Actual volume	Statistical averaging		Support vector machines			
	Moving mean (without SVM) (%)	Moving median (without SVM) (%)	v SVM (Unfiltered)	v SVM (Moving mean) (%)	v SVM (Moving median)	v SVM (Wavelet filter)
50	+11.5	+10.4	+0.0	+0.1	−0.4	+0.0
49	+10.1	+9.9	−1.9	−1.9	−1.6	−1.9
48	+2.7	+2.8	−0.8	−0.8	−0.8	−0.8
47	−5.3	−5.3	−1.3	−1.3	−0.9	−1.3
46	−0.8	−1.3	+0.9	+0.9	+0.7	+0.9
45	−2.0	−2.5	+0.0	−0.9	+0.1	+0.1
40	+0.1	−0.1	−0.6	+0.1	+0.1	−0.6
39	−4.5	−5.1	−0.4	−0.4	−0.4	−0.4
38	+0.5	−0.8	−0.3	−0.4	−0.5	−0.3
37	+0.9	+0.0	+2.8	+2.7	+2.6	+2.8
36	−2.0	−2.8	−0.4	−0.4	−0.6	−0.4
35	+1.1	−0.3	+0.3	−0.1	−0.1	+0.3
30	+0.4	−1.0	+1.3	+1.3	+1.2	+1.3
25	+8.9	+5.6	+8.2	+5.0	+5.0	+8.2
20	+14.5	+8.5	−0.3	−0.3	−0.3	−0.3
9	+40.6	+36.9	−1.7	−1.1	−0.6	−1.7
8	+22.9	+17.2	+0.6	+1.3	+0.6	+1.9
7	+4.5	+1.0	+1.4	+1.4	+2.1	+1.4
6	−0.1	−1.5	+0.2	+0.5	+0.2	+0.5
5	+6.4	+1.9	+1.0	+1.0	+1.0	+1.0
Abs. Average Error	7.0 % (1.53 L)	5.7 % (1.37 L)	1.2 % (0.35 L)	1.1 % (0.32 L)	1.0 % (0.29 L)	1.3 % (0.36 L)
Max. Avg. Error	40.6 % (5.77 L)	36.9 % (5.18 L)	8.2 % (2.05 L)	5.0 % (1.25 L)	5.0 % (1.25 L)	8.2 % (2.05 L)

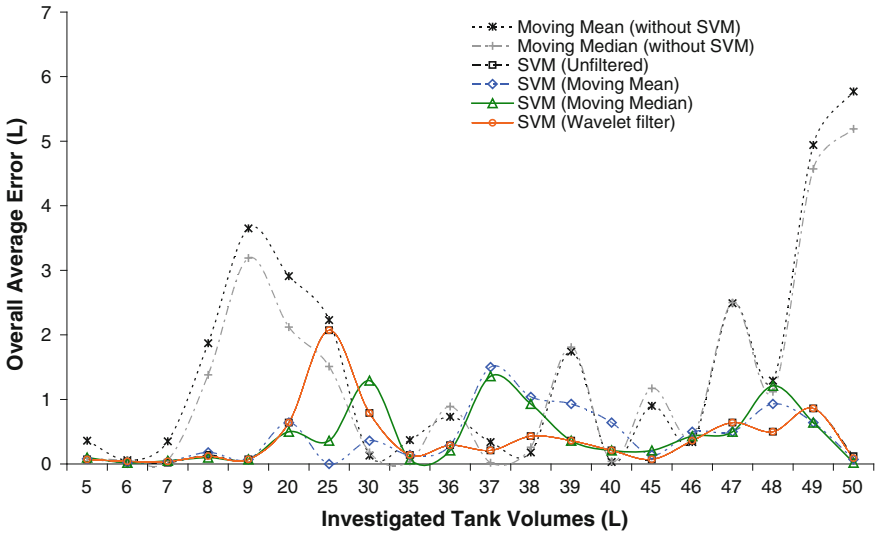

Fig. 6.35 Graph of the average error produced at different investigated tank volumes

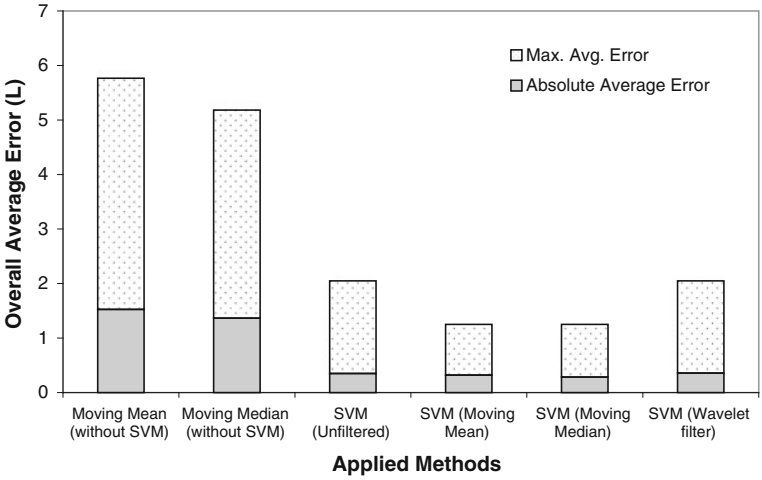

Fig. 6.36 Investigation summary results showing the maximum and average errors

6.4.7 Summary

A comparison of the accuracy of different processing techniques investigated in the experiment is shown in Figs. 6.35 and 6.36. The overall results obtained from the SVM-based signal processing system indicate significantly less error in fuel volume measurement compared with the simple averaging methods under dynamic conditions. The *v*-SVM model with the RBF kernel function and applied moving median filter produced the most accurate results compared with the other methods.

Figure 6.35 shows the overall average error plot using the investigated filters at different tank volumes. It shows that the SVM models with applied moving mean, unfiltered, and wavelet filters produced little error, especially near the lower and higher tank volumes, when compared with the simple statistical methods.

Figure 6.36 summarizes the errors obtained using the averaging method and the three investigated preprocessing techniques.

Chapter 7
Discussion

7.1 Overview

This chapter provides discussion on the selection and design of the SVM-based signal processing system. The selection parameters used for the SVM-based system and the results obtained from the experimentations, and the possible improvements to the design of the SVM-based system are all discussed in this section.

7.2 Support Vector Machine Configuration

The SVM-based fuel level measurement system designed and examined in this research uses v-SVM type of support vector machine. It was discussed in Sect. 3.3 that v-SVM was the improved form of the existing C-type SVM (C-SVM). The choice for selecting a particular kernel functions plays a crucial role in terms of the SVM performance [1–3]. Hence, four commonly used types of kernel functions were investigated using the samples obtained from the field trials (Exp. Set B). The parameters for the SVM models (i.e., v, ξ) and the kernel functions (i.e., γ, d, and r) (described in Sect. 5.6.3) were selected by first using the default parameters suggested by the LIBSVM software and then changing these parameters in several quick trials using the cross-validation function in LIBSVM. Parameters for which the classification accuracy was observed to be highest were used to conduct other investigation trials for determining optimal preprocessor configuration and optimal signal smoothing parameter. Results obtained from Experiment Set B indicated that the Radial Basis Function (RBF) (average error of 0.3 L) was the most feasible kernel function for the classification of the ultrasonic fuel level signals. However, the results obtained from other kernel functions such as linear kernel, polynomial kernel, and sigmoid kernel functions showed reasonably good classification results with average error of 0.5 L (see Sect. 6.3.6). These results using several SVM kernel functions showed good consistency in terms of the

J. Terzic et al., *Ultrasonic Fluid Quantity Measurement in Dynamic Vehicular Applications*, DOI: 10.1007/978-3-319-00633-8_7,
© Springer International Publishing Switzerland 2013

Table 7.1 Required parameters for different kernel functions

Kernel function	Nu (v)	Gamma (γ)	Coef0 (r)	Degree (d)
Polynomial	Uses	Uses	Uses	Uses
Sigmoid	Uses	Uses	Uses	–
RBF	Uses	Uses	–	–
Linear	Uses	–	–	–

response of the SVM-based system to the ultrasonic sensor-based fuel level measurement equipments.

Radial basis function (RBF) was observed to have an excellent classification rate. It is comparatively easier to obtain the optimal parameter values with the v-SVM models that use the RBF kernel function, since there are only a few parameters that need to be adjusted. The matrix of possible SVM parameters values is a lot smaller for the RBF kernel function compared with the polynomial and sigmoid functions. Table 7.1 shows a list of parameters that are used by the v-SVM for different kernel functions. To effectively train the v-SVM, the required parameters values need to be adjusted in factorial way. Since RBF function only requires two factors (v and γ), it is quicker to train with the near optimum parameter values.

7.3 Selection of Signal Preprocessing Parameters

To determine an appropriate configuration for the SVM-based fuel level measurement system, it was important to ascertain the optimal parameters for the signal preprocessing functional block. That is, to determine an appropriate feature extraction function out of the three functions (FFT, DCT, and WT) described in Sect. 3.2.4. Furthermore, the optimal size of the input window ($\acute{\omega}$), and the size of the feature vector was important to be determined experimentally. For this purpose, Experiment Sec C was conducted and the training and validation samples obtained from the field trials were used to investigate the performance of the SVM-based system based on the different types of feature extraction functions, different sizes of the input window ($\acute{\omega}$), and different sizes of the feature vector.

The results obtained from Experiment C1 indicated that the optimal solution for the signal preprocessor configuration is using the fast Fourier transform (FFT) function as the feature extraction function, with windows size ($\acute{\omega}$) of 14 s and feature vector size of 63 coefficients. The overall performance of each of these parameters is shown in the following figures. The parameters that were found to be most feasible are circled on the result figures below.

Figure 7.1 shows the average performance of several v-SVM models having different sizes of coefficients investigated in Experiment Set C1. It is interesting to note that the performance of the SVMs generally goes down as the size of the input coefficients increases [4]. This fact was discussed in Sect. 3.2.4 and it also confirms the findings of Trunk [5].

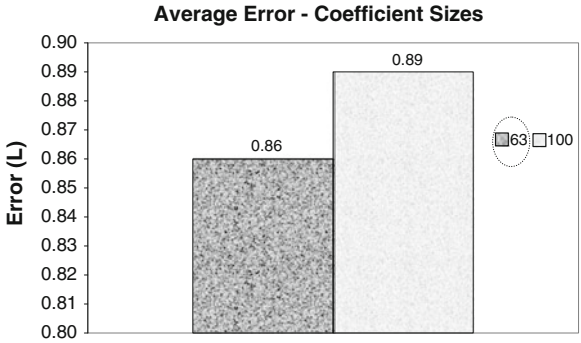

Fig. 7.1 Overall performance of the SVM-based measurement system using different input coefficient sizes

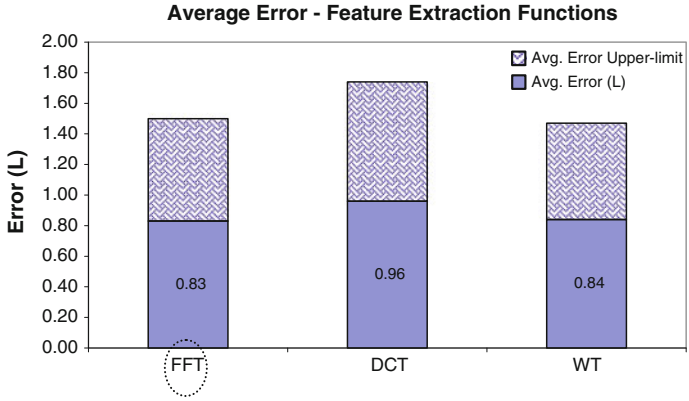

Fig. 7.2 Overall performance of the SVM-based measurement system using different feature extraction functions

Figure 7.2 shows the general performance of the three feature extraction functions used in the SVM-based measurement system. The overall performance of the SVM-based system using FFT, WT, and DCT has been observed to be competitive.

Figure 7.3 shows the performance of the SVM-based measurement system when implemented to have different window sizes (ω). A window size of 5 represents that the measurement system uses 5-s sampled data to process the output. Likewise, a window size of 14 means that the measurement system uses 14-s sampled data from the ultrasonic sensor to process and predict the output level. The graph shown in Fig. 7.3 describes that there were reasonable effects of using window size of different values. The performance of the SVM-based fuel level measurement system having different window sizes is generally seen as consistent

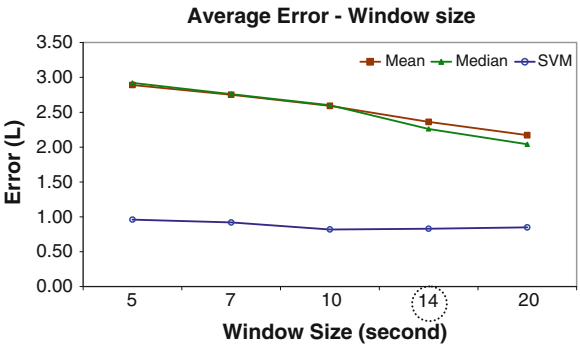

Fig. 7.3 Overall performance of the SVM-based measurement system using different window sizes compared with existing statistical averaging methods

and superior to the two statistical averaging methods (*mean* and *median*). The performance of the statistical averaging methods improves as the size of the input window increases, which conforms to the fact that a signal averaged over longer period will produce a more converged and accurate reading.

7.4 Selection of Signal Smoothing Parameters

To investigate the performance of the SVM-based measurement system, when used with the signal smoothing capability, it was important to determine appropriate parameters for the signal smoothing configuration. That is, to determine an appropriate signal smoothing (filter) function out of the three functions (moving mean, moving median, and wavelet filter) described in Sect. 4.6. Furthermore, the optimal size of the filter tap, and an appropriate feature extraction function was important to be determined experimentally. For this purpose, Experiment Set C2 was conducted and the training and validation samples obtained from the field trials were used to investigate the performance of the SVM-based system based on the different types of signal smoothing functions, different feature extraction functions, and different sizes of the filter tap.

The results obtained from Experiment Set C2 indicated that the optimal solution for the signal preprocessor configuration is using the FFT function as the feature extraction function, and moving median with tap size of 5 as the signal smoothing function. The overall performance of each of these parameters is shown in the following figures. The parameters that were found to be most suitable are circled on the result figures below (Figs. 7.4 and 7.5).

Figure 7.6 shows the overall performance of SVM-based measurement system incorporated with different feature extraction functions and signal smoothing technique. Figure 7.6 shows a general improvement in the SVM-based fuel level measurement system when incorporated with the signal smoothing technique. The average performance of the feature extraction functions is shown in Fig. 7.2 (without signal smoothing feature) Fig. 7.6 (with signal smoothing) indicate that

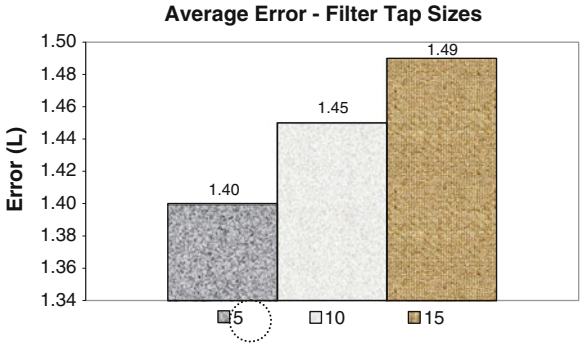

Fig. 7.4 Overall performance of the SVM-based measurement system using filter tap sizes

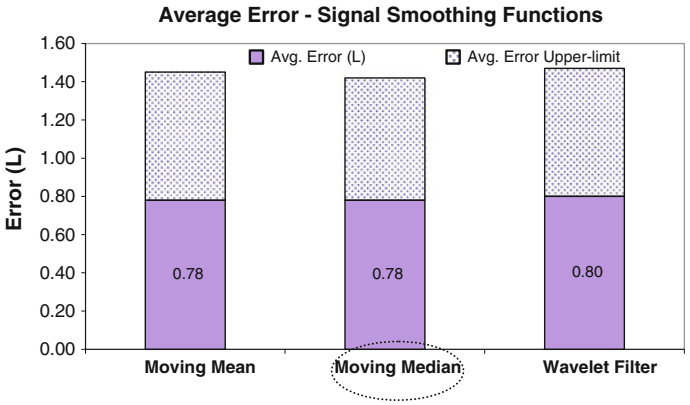

Fig. 7.5 Overall performance of the SVM-based measurement system using different signal smoothing functions

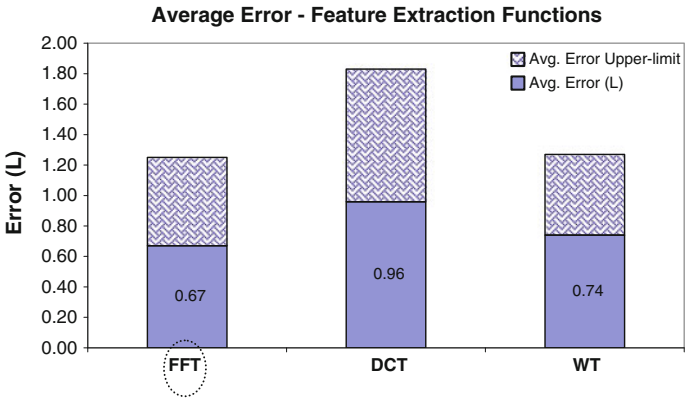

Fig. 7.6 Overall performance of the SVM-based measurement system incorporated with signal smoothing technique with different feature extraction functions

the performance of the SVM-based system has improved with the inclusion of the signal smoothing technique. The overall average error for the FFT function without the signal smoothing method was observed in Experiment C1 (Fig. 7.2) to be 0.83 L, but with the inclusion of the signal smoothing method, it has reduced to 0.67 L. However, there were no major improvements in the performance of the SVM-based system using the DCT function.

References

1. Hu Y, Hwang JN (2002) Handbook of neural network signal processing. CRC Press, Boca Raton
2. Tony J (2004) Multi-task feature and kernel selection for SVMs. In: Proceedings of the 21st international conference on machine learning
3. Fukunaga K (1990) Introduction to statistical pattern recognition. Academic Press, Boston
4. Bousquet O, Von Luxburg U, Rätsch G (2004) Machine Learning Summer School; Advanced lectures on machine learning: ML summer schools 2003, Canberra, Australia, Feb 2–14, 2003, Tübingen, Germany, Aug 4–16, 2003 : revised lectures. Bousquet O, Von Luxburg U, Rätsch G (eds). Springer, New York
5. Trunk GV (1979) A problem of dimensionality: a simple example. Pattern Anal Mach Intell (PAMI) 1(3):306–307

Chapter 8
Conclusion and Future Work

8.1 Conclusion

The support vector machine (SVM)-based signal processing and classification approach coupled with a single ultrasonic sensor have been used to accurately determine the fuel level in an automotive fuel tank under dynamic conditions. A thorough research review was conducted on the usage of ultrasonic sensors in dynamic environments and the effective use and properties of the support vector machines. Based on the findings of the research review, an ultrasonic sensor-based measurement system using the support vector machine (SVM)-based signal processing and classification was proposed to provide a robust and accurate fuel level measurement system in a dynamic environment.

Extensive experiments were performed to determine an optimal configuration for the proposed SVM-based fuel level measurement system. The selection of the SVM parameters, the kernel parameters, and the signal preprocessing configurations were all performed experimentally. To determine the performance of the SVM-based fluid level measurement system, many field trials were carried out to obtain a large amount of training and validation data for the training and validation of the system. The raw ultrasonic sensor signals obtained from the experiments data were observed to lead to large variations in the calculated fuel volume, when the actual fuel in the tank had remained constant. This variation in the ultrasonic output was caused by sloshing effects.

The overall results obtained from the SVM-based measurement system, when configured to have the optimal configurations obtained by experimentations, were observed to have remarkably higher accuracy in a dynamic environment when compared with the existing statistical averaging methods in similar applications. The SVM model applied with the moving median filter (with tap size of 5) produced a remarkably lower maximum average error of 1.25 l, when compared with the statistical averaging methods moving mean and moving median that produced a maximum average error of 5.8 and 5.2 l, respectively.

The increased accuracy in performance of the developed fuel level measurement system in dynamic environments will provide more confidence to drivers

J. Terzic et al., *Ultrasonic Fluid Quantity Measurement in Dynamic Vehicular Applications*, DOI: 10.1007/978-3-319-00633-8_8,
© Springer International Publishing Switzerland 2013

regarding the actual amount of fuel indicated by the instrument panel. With an accurate fuel level measurement system, the distance-to-empty figures can be accurately computed. In particular, the SVM-based method is suitable for use in a professional car racing where a vehicle is subjected to highly dynamic maneuvres. Drivers of cars equipped with this measurement method can confidently drive higher number of laps without fear of running out of fuel in situations where fuel level in the tank is low.

8.2 Future Work

An ultrasonic sensor coupled with the support vector machine (SVM) approach to signal processing will be used to address other influencing factors such as atmospheric pressure and the tilt that causes the liquid to shift to one side. With the rapid improvements in microprocessor technology, it will be possible to automatically train the SVM model in real time, which will further increase the effectiveness of the measurement system in dynamic environments.

Appendix A
Publications

Research Publications

The following references refer to the journal articles that were based on the work from this research.

- Terzic, J., Nagarajah, R., Alamgir, M., *"Accurate Fluid Level Measurement in Dynamic Environment Using Ultrasonic Sensor and v-SVM"*, Sensors & Transducers Journal, Vol. 109(10), pp. 76–91, 2009.
- Terzic, J., Nagarajah, R., Alamgir, M, *"Fluid level measurement in dynamic environments using a single ultrasonic sensor and Support Vector Machine (SVM)"*, Sensors and Actuators A: Physical; vol. 161, no. 1–2, pp. 278–287, 2010.

J. Terzic et al., *Ultrasonic Fluid Quantity Measurement in Dynamic Vehicular Applications*, DOI: 10.1007/978-3-319-00633-8,
© Springer International Publishing Switzerland 2013

Appendix B
Exxsol D-40 Fluid Specification

The Table B.1 provides detailed specifications for the Exxsol D-40 type Stoddard solvent used in the experimentations [127].

Table B.1 Exxsol D-40 fluid specifications

Property	Units	Typical values	Test method
Distillation range	°C		ASTM D 86
IBP		164	
DP		192	
Flash point	°C	48	ASTM D 56
Density @ 15 °C	kg/dm^3	0.772	ASTM D 4052
Viscosity @ 25 °C	mm^3/s	1.30	ASTM D 445
Evaporation rate (n-BuAc = 10Q)	–	15	EMC-AP-F01
KB value	–	32	ASTM D 1133
Aniline point	°C	70	ASTM D 611
Aromatic content	wt%	0.08	AM-S 140.31
Colour (Saybolt)	–	+30	ASTM D 156
Bromine index	mg/100g	15	ASTM D 2710
Surface tension @ 25 °C	mN/m	24.7	EC-M-F02 (Wilhelmy Plate)
Refractive index @ 20 °C	–	1.428	ASTM D 1218

J. Terzic et al., *Ultrasonic Fluid Quantity Measurement in Dynamic Vehicular Applications*, DOI: 10.1007/978-3-319-00633-8,
© Springer International Publishing Switzerland 2013

About the Authors

Dr. Jenny Terzic is the Director of Corporate Quality at Iveco Trucks Australia (Fiat Group). She holds a Bachelor of Mechanical Engineering (with honors), Master of Engineering in Computer Integrated Manufacturing, and PhD in Automotive Engineering from Swinburne University of Technology. She has published number of technical papers in the area of Engineering Applications of Artificial Intelligence. Areas of research include: support vector machines, artificial neural networks, advance signal processing, intelligent sensors, and non-contact inspection.

Dr. Edin Terzic is the Chief Manufacturing Engineer—Asia Pacific and Managing Director (CEO) of Powertrain at Delphi Automotive Systems Australia. He holds a Bachelor of Mechanical Engineering (with honors), Master of Engineering in Computer Integrated Manufacturing, and PhD in Automotive Engineering from Swinburne University of Technology. He has published a number of technical papers in the area of Engineering Applications of Artificial Intelligence. He also holds several international patents in the area of automotive engineering and had success in commercializing most of his research. Areas of research include: artificial neural networks, intelligent sensors, and non-contact inspection.

Prof. Romesh Nagarajah is the Professor of Mechanical Engineering at Swinburne University of Technology. He leads an internationally recognized research group working in the fields of Non-Contact Inspection and Intelligent Sensing. Professor Nagarajah has several international patents and has published over 150 international journal, conference, and technical papers in intelligent sensing and non-contact inspection. He has received several grants from the Australian Research Council and the automotive industry to develop intelligent sensing systems for process monitoring and non-contact inspection.

Muhammad Alamgir is a Software Engineer at Vipac Engineers and Scientists. He has graduated in Computer Systems Engineering from RMIT University. He has been developing microcontroller-based sensors and instruments, and has also been involved in smart-sensor-based projects, incorporating Artificial Intelligence-based techniques, at Delphi Automotive Systems, Australia.

J. Terzic et al., *Ultrasonic Fluid Quantity Measurement in Dynamic Vehicular Applications*, DOI: 10.1007/978-3-319-00633-8,
© Springer International Publishing Switzerland 2013